

คุณลักษณะและสมบัติการเป็นตัวเร่งปฏิกิริยาของตัวเร่งปฏิกิริยาโคบอลต์บนตัวรองรับอะลูมินา-ซีลิกา
ที่มีรูพรุนแบบไบโมดอลสำหรับคาร์บอนมอนอกไซด์ไฮโดรจิเนชัน



นางสาวจุฑาภรณ์ ศรีสวัสดิ์

สถาบันวิทยบริการ
จุฬาลงกรณ์มหาวิทยาลัย

วิทยานิพนธ์นี้เป็นส่วนหนึ่งของการศึกษาตามหลักสูตรปริญญาวิศวกรรมศาสตรมหาบัณฑิต

สาขาวิชาวิศวกรรมเคมี ภาควิชาวิศวกรรมเคมี
คณะวิศวกรรมศาสตร์ จุฬาลงกรณ์มหาวิทยาลัย

ปีการศึกษา 2550

ลิขสิทธิ์ของจุฬาลงกรณ์มหาวิทยาลัย

CHARACTERISTICS AND CATALYTIC PROPERTIES OF ALUMINA-SILICA BIMODAL PORE
SUPPORTED COBALT CATALYST FOR CARBON MONOXIDE HYDROGENATION



Miss. Jutakorn Srisawat

สถาบันวิทยบริการ
A Thesis Submitted in Partial Fulfillment of the Requirements
for the Degree of Master of Engineering Program in Chemical Engineering

Department of Chemical Engineering

Faculty of Engineering

Chulalongkorn University

Academic Year 2007

Copyright of Chulalongkorn University


Thesis Title CHARACTERISTICS AND CATALYTIC PROPERTIES OF
ALUMINA-SILICA BIMODAL PORE SUPPORTED COBALT
CATALYST FOR CARBON MONOXIDE HYDROGENATION

By Miss. Jutakorn Srisawat

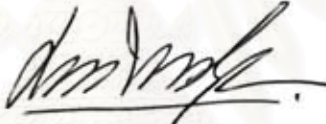
Field of Study Chemical Engineering

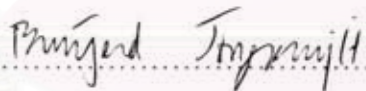
Thesis Advisor Assistant Professor Bunjerd Jongsomjit, Ph.D

Accepted by the Faculty of Engineering, Chulalongkorn University in Partial
Fulfillment of the Requirements for the Master's Degree


..... Dean of the Faculty of Engineering
(Professor Direk Lavansiri, Ph.D.)

THESIS COMMITTEE


..... Chairman
(Associate Professor ML Supakanok Thongyai)


..... Thesis Advisor
(Assistant Professor Bunjerd Jongsomjit, Ph.D.)


..... Member
(Assistant Professor Joongjai Panpranot, Ph.D.)


..... Member
(Assistant Professor Muenduen Phisalaphong, Ph.D.)


..... Member
(Assistant Professor Okorn Mekasuwandamrong, Ph.D.)

จุฬากรณ์ ศรีสวัสดิ์ : คุณสมบัติและสมบัติการเป็นตัวเร่งปฏิกิริยาของตัวเร่งปฏิกิริยา
โคบอลต์บนตัวรองรับอะลูมินา-ซิลิกาที่มีรูพรุนแบบไบ โมดอลสำหรับคาร์บอนมอนอก
ไซด์ไฮโดรจิเนชัน (CHARACTERISTICS AND CATALYTIC PROPERTIES
OF ALUMINA-SILICA BIMODAL PORE SUPPORTED COBALT
CATALYST FOR CARBON MONOXIDE HYDROGENATION) อ. ที่ปรึกษา :
ผศ. ดร. บรรเจิด จงสมจิตร, 95 หน้า

วิทยานิพนธ์นี้ศึกษาถึงคุณลักษณะและความว่องไวในการเร่งปฏิกิริยา ไฮโดรจิเนชันของ
คาร์บอนมอนอกไซด์ที่แตกต่างกันระหว่าง ตัวเร่งปฏิกิริยาโคบอลต์กระจายตัวอยู่บนตัวรองรับ อะลู
มินา-ซิลิกาที่มีรูพรุนแบบไบ โมดอลที่มีปริมาณของอะลูมินาในตัวรองรับอัตราส่วนต่างๆ โดย
อัตราส่วนระหว่างอะลูมินาต่อซิลิกาถูกเตรียมขึ้นที่อัตราส่วนต่างๆกัน โดยน้ำหนัก ด้วยวิธีฝังเคลือบ
ซิลิกาด้วยอะลูมินาแล้วนำไปเผาในอากาศ หลังจากนั้นนำไปฝังเคลือบอีกครั้งด้วยโคบอลต์ หลังจาก
การเผาในอากาศ ตัวอย่างต่างๆจะถูกนำไปตรวจสอบคุณลักษณะโดยใช้การดูดซับทางกายภาพด้วย
ไนโตรเจน การกระเจิงรังสีเอ็กซ์ การส่องผ่านด้วยกล้องจุลทรรศน์อิเล็กตรอน การวัดการกระจาย
ตัวของโลหะ การส่องกราดด้วยกล้องจุลทรรศน์อิเล็กตรอน การรีดักชันแบบโปรแกรมอุณหภูมิ
และการดูดซับด้วยไฮโดรเจน ปฏิกิริยาไฮโดรจิเนชันของคาร์บอนมอนอกไซด์ (มีอัตราส่วนของ
ไฮโดรเจนต่อคาร์บอนมอนอกไซด์=10/1) ถูกใช้เพื่อทดสอบความว่องไวของตัวเร่งปฏิกิริยาและ
การเลือกเกิดของผลิตภัณฑ์ ผลการศึกษาแสดงให้เห็นว่าขนาดของโคบอลต์ออกไซด์ขึ้นอยู่กับ
ปริมาณอะลูมินาของตัวรองรับและชนิดของโคบอลต์ที่นำมาใช้ ทั้งนี้ตัวแปรที่มีผลกระทบต่อ
กลไกของการรีดักชัน ได้แก่ ขนาดอนุภาค, อันตรกิริยาของตัวรองรับ และปริมาณของอะลูมินา
โดยพบว่าตัวเร่งปฏิกิริยาที่กระจายตัวอยู่บนตัวรองรับอะลูมินา-ซิลิกาที่มีรูพรุนแบบไบ โมดอลจะมี
ความว่องไวเพิ่มขึ้นเนื่องจากความสามารถในการรีดิวท์ที่เพิ่มขึ้นเมื่อปริมาณอะลูมินาสูงขึ้น และยัง
พบว่าความว่องไวของตัวเร่งปฏิกิริยามีค่าสูงเมื่อใช้โคบอลต์ในแคต และการใช้โคบอลต์คลอไรด์
พบว่า ความว่องไวของตัวเร่งปฏิกิริยามีค่าต่ำสุดเนื่องจากทำให้ความสามารถในการกระจายตัวของ
โคบอลต์ต่ำ

จุฬาลงกรณ์มหาวิทยาลัย

ภาควิชา.....วิศวกรรมเคมี..... ลายมือชื่อนิสิต.....จุฬากรณ์ ศรีสวัสดิ์.....
สาขาวิชา.....วิศวกรรมเคมี..... ลายมือชื่ออาจารย์ที่ปรึกษา.....
ปีการศึกษา.....2550.....

##4970262521: MAJOR CHEMICAL ENGINEERING

KEY WORD: COBALT CATALYST/ COBALT PRECURSOR/ BIMODAL/
SUPPORT/ ALUMINA/ SILICA/ CO HYDROGENATION

JUTAKORN SRISAWAT: CHARACTERISTICS AND CATALYTIC
PROPERTIES OF ALUMINA-SILICA BIMODAL PORE SUPPORTED
COBALT CATALYST FOR CARBON MONOXIDE HYDROGENATION.

THESIS ADVISOR: BUNJERD JONGSOMJIT, Ph.D., 95 pp.

In the present study, differences in characteristics and catalytic activity towards CO hydrogenation of Co catalysts dispersed on alumina-silica bimodal pore supports were investigated. The various amounts of alumina were prepared by incipient wetness impregnation method, then calcined them in air. Then, consequently impregnated with the cobalt precursors. After calcination, the various samples were characterized using N_2 physisorption, XRD, SEM/EDX, TEM, TPR and H_2 chemisorption. CO hydrogenation ($H_2/CO = 10/1$) was also performed to determine the overall activity and selectivity. It revealed that the size of Co oxide species depends on the amount of alumina in support and type of Co precursor. A wide range of variables including particle size, support interaction, and the alumina content can affect the kinetics of reduction. It was found that for the alumina-silica bimodal pore catalyst, the catalyst dispersed on the high alumina content support exhibited high activities due to high reducibility. The use of cobalt nitrate as Co precursor exhibited highest activities. The use of cobalt chloride as Co precursor exhibited lowest activities due to decrease in cobalt dispersion.

สถาบันวิทยบริการ
จุฬาลงกรณ์มหาวิทยาลัย

Department.....Chemical Engineering... Student's signature... *Jutakorn Srisawat*...
Field of study...Chemical Engineering... Advisor's signature... *Bunjerd Jongsomjit*...
Academic year.....2007.....

ACKNOWLEDGEMENTS

The author would like to express her greatest gratitude and appreciation to her advisor, Dr, Bunjerd Jongsomjit for his invaluable guidance, providing value suggestions and his kind supervision throughout this study. In addition, she is also grateful to Associate Professor ML Suppakanok Thongyai, as the chairman, Assistant Professor Muenduen Phisalaphong, Assistant Professor Joongjai Panpranot and Assistant Professor Okorn Mekasuwandamrong as the members of the thesis committee. The financial supports from the Thailand Research Fund (TRF) is also gratefully acknowledged.

Many thanks for kind suggestions and useful help to Mr. Pimchanok Tupabut, Miss Nitinart Chitpong, and many friends in the petrochemical laboratory who always provide the encouragement and co-operate along the thesis study.

Most of all, the author would like to express her greatest gratitude to her parents and her family who always pay attention to her all the times for suggestions, support and encouragement.

สถาบันวิทยบริการ
จุฬาลงกรณ์มหาวิทยาลัย

CONTENTS

	page
ABSTRACT (IN THAI).....	iv
ABSTRACT (IN ENGLISH).....	v
ACKNOWLEDGMENTS.....	vi
CONTENTS.....	vii
LIST OF TABLES.....	x
LIST OF FIGURES.....	xi
CHAPTER	
I INTRODUCTION.....	1
II LITERATER REVIEWS.....	3
2.1 Silica supported cobalt catalysts.....	3
2.2 Bimodal pore supported cobalt catalysts	9
2.3 Effect of cobalt precursors on cobalt catalyst.....	11
III THEORY.....	15
3.1 Fischer-Tropsch synthesis (FTS)	15
3.1.1 The surface carbide mechanism.....	18
3.1.2 The hydroxycarbene mechanism.....	20
3.1.3 The CO insertion mechanism.....	22
3.2 Cobalt.....	24
3.2.1 General.....	24
3.2.2 Physical properties.....	24
3.2.3 Cobalt oxides.....	27
3.3 Cobalt-based catalysts.....	27
3.4 Cobalt-support compound formation (Co-SCF).....	28
3.4.1 Co-Aluminate Formation	28
3.4.2 Co-Silicate Formation.....	28
3.5 Silicon dioxide	29
3.5.1 General feature of silica.....	29
3.6 Bimodal pore structure	32
3.6.1 General feature of Bimodal pore structure	33

	page
IV EXPERIMENTS.....	34
4.1 Catalyst preparation.....	34
4.1.1 Chemicals.....	34
4.1.2 Preparation of alumina-silica bimodal pore supports.....	35
4.1.3 Preparation of the supported Co samples	35
4.1.5 Sample nomenclature	35
4.2 Catalyst characterization.....	36
4.2.1 N ₂ physisorption.....	36
4.2.2 X-ray diffraction (XRD).....	36
4.2.3 Temperature programmed reduction (TPR).....	36
4.2.4 Electron Microscopy.....	37
4.2.5 Transmission Electron Microscopy (TEM).....	37
4.2.6 Hydrogen chemisorption	37
4.3 Reaction study in CO hydrogenation.....	38
4.3.1 Materials.....	38
4.3.2 Apparatus.....	38
4.3.3 Procedures.....	40
V RESULTS AND DISCUSSION	43
5.1 Various alumina loading of 20 wt% cobalt on alumina-silica bimodal pore supported catalyst.....	43
5.2 Various Co precursors of silica and 15% Al-Si bimodal pore supported catalyst.....	61
VI CONCLUSIONS AND RECOMMENDATIONS.....	79
6.1 Conclusions.....	79
6.2 Recommendations.....	80
REFERENCES.....	81
APPENDICES.....	85
APPENDIX A: CALCULATION FOR CATALYST PREPARATION.....	86
APPENDIX B: CALCULATION FOR TOTAL H ₂ CHEMISORPTION AND DISPERSION.....	88
APPENDIX C: CALIBRATION CURVES.....	90

	page
APPENDIX D: CALCULATION OF CO CONVERSION, REACTION RATE AND SELECTIVITY.....	93
APPENDIX E: LIST OF PUBLICATIONS.....	94
VITA	95



สถาบันวิทยบริการ
จุฬาลงกรณ์มหาวิทยาลัย

LIST OF TABLES

Table	page
3.1 Physical properties of cobalt	25
3.2 Physical properties of silica	29
4.1 Chemicals used in the preparation of catalysts.....	34
4.2 Operating condition for gas chromatograph.....	39
5.1 BET surface area, average pore diameter and pore volume of various supports	43
5.2 BET surface area, average pore diameter and pore volume of various catalysts	45
5.3 Results of H ₂ chemisorption, Cobalt dispersion, steady state rate and selectivity to products	60
5.4 BET surface area, average pore diameter and pore volume of various Co precursors.....	61
5.5 Results of steady-state rate and selectivity to products.....	78
B.1 H ₂ chemisorption results for various alumina-silica bimodal pore supported Co catalysts samples.....	89
C.1 Conditions use in Shimadzu modal GC-8A and GC-14B.....	90

LIST OF FIGURES

Figure	page
3.1 Formation scheme of the bimodal pore support.....	33
4.1 Flow diagram of CO hydrogenation system.....	41
5.1 The pore distributions of various supports	44
5.2 XRD pattern for various alumina loading of Al-Si bimodal pore supports....	46
5.3 XRD pattern of cobalt based catalysts on various alumina loading of Al-Si bimodal pore supports.....	47
5.4 SEM micrograph and EDX mapping for silica (Q50) support granule.....	49
5.5 SEM micrograph and EDX mapping for 15% Al-Si bimodal pore support granule.....	50
5.6 SEM micrograph and EDX mapping for Co/Silica catalyst granule.....	51
5.7 SEM micrograph and EDX mapping for Co/15% Al-Si catalyst granule.....	52
5.8 TEM micrographs of silica (Q-50), 5% Al-Si, 10% Al-Si and 15% Al-Si bimodal pore supports.....	54
5.9 TEM micrographs of 20% Al-Si bimodal pore supports, silica supported Co catalyst , 5% Al-Si bimodal pore supported Co catalyst and 10% Al-Si bimodal pore supported Co catalyst structure.....	55
5.10 TEM micrographs of 15% Al-Si bimodal pore supported Co catalyst and 20% Al-Si bimodal pore supported Co catalyst structure.....	56
5.11 TPR profiles for Co catalysts with various alumina loading of Al-Si bimodal pore supports used.....	58
5.12 XRD pattern of cobalt based catalysts on various cobalt precursors.....	63
5.13 SEM micrograph and EDX mapping for CoN/SiO ₂ catalyst granule.....	65
5.14 SEM micrograph and EDX mapping for CoAT/SiO ₂ catalyst granule.....	66
5.15 SEM micrograph and EDX mapping for CoAA/SiO ₂ catalyst granule.....	67
5.16 SEM micrograph and EDX mapping for CoCl/SiO ₂ catalyst granule.....	68
5.17 SEM micrograph and EDX mapping for CoN/15% Al-Si catalyst granule....	69
5.18 SEM micrograph and EDX mapping for CoAT/15% Al-Si catalyst granule...	70
5.19 SEM micrograph and EDX mapping for CoAA/15% Al-Si catalyst granule..	71
5.20 SEM micrograph and EDX mapping for CoCl/15% Al-Si catalyst granule....	72

Figure	page
5.21 TEM micrographs of all cobalt dispersed on silica supports.....	74
5.22 TEM micrographs of all cobalt dispersed on 15% Al-Si bimodal pore supports.....	75
5.23 TPR profiles for Co catalysts with various Co precursors.....	77
C.1 The calibration curve of methane.....	91
C.2 The calibration curve of ethylene.....	91
C.3 The chromatograms of catalyst sample from thermal conductivity detector, gas chromatography Shimadzu model 8A (Molecular sieve 5A column).....	92
C.4 The chromatograms of catalyst sample from flame ionization detector, gas chromatography Shimadzu model 14B (VZ10 column).....	92

CHAPTER I

INTRODUCTION

It is expected that in the near future the feedstock for the chemical industry will shift from crude oil to natural gas due to the limited reserves of crude oil and the increasing environmental constraints. To enable its chemical conversion, natural gas is first transformed into synthesis gas, which is a mixture of carbon monoxide and hydrogen. This synthesis gas is the basis for a number of large-scale industrial processes. Fischer-Tropsch synthesis (FTS) is one of the routes for the chemical liquefaction of natural gas. As such, it allows the economic exploitation of remote natural gas resources and constitutes an alternative route for the production of clean transportation fuels and petrochemical feedstock in relation to the classic refining of crude oil.

Fischer-Tropsch synthesis (FTS) is known as a carbon monoxide (CO) hydrogenation which is added hydrogen to carbon monoxide. In general, the process is most widely used for synthesis of hydrocarbon waxes which are further cracked into gasoline and diesel fuel. Many transition metals of Group VIII can be used as catalysts for FTS such as iron (Fe), cobalt (Co), nickel (Ni) and ruthenium (Ru). However, supported cobalt catalysts are preferred for Fischer-Tropsch synthesis (FTS) for years. This is because of their high activity for FTS, high selectivity for linear hydrocarbons and low activity for the competitive water-gas shift reaction. Since the activity of Co catalyst apparently depends on the number of reduced Co metal dispersed on the support used, thus the nature of support can play important roles on such the phenomenon. The activity of supported cobalt catalyst in the FTS should be proportional to the area of the exposed metallic cobalt atoms (Iglesia., 1997). The high dispersion of the cobalt metal is usually done by deposition of a cobalt salt on high surface area supports, such as silica and alumina, and subsequent reduction. The support with large surface area, however, usually contains small pore size, which results in poor intra-pellet diffusion efficiency of reactants and products. Slow transportation of reactants to and products from catalytic sites often controls the rate of primary and secondary reactions even on small catalyst pellet. Meanwhile, the pore size of catalyst also affects product selectivities, due to the spatial effect of support. In

contrast, the bimodal pore structure support, which contains large pores and small pores at the same time, contributes to higher dispersion of supported cobalt crystallites by the small pores, which enlarged the surface area of the support. Furthermore, it is able to diminish the diffusion resistance by its large pores (Iglesia *et al.*,1997). A support with a distinct bimodal pore structure has excellent advantages in solid catalysis reaction because the large pores provide pathways for rapid molecular transportation and small pores serve a large area of active surface, contributing to high diffusion efficiency and dispersion of supported metal simultaneously, as theoretically expressed by Levenspiel (Levenspiel, 1972).

This thesis focuses on investigation of characteristics and catalytic properties for alumina–silica bimodal pore supported cobalt catalysts. Bimodal pore supported cobalt catalysts can be identified as alumina–silica bimodal pore supported cobalt catalysts consisting of various alumina loading in alumina-silica bimodal pore supports and different cobalt precursors. The study was scoped as follows:

1. Preparation of alumina-silica bimodal pore supports (0,5,10,15 and 20 wt% Al) by the incipient wetness impregnation method.
2. Characterization of the alumina-silica bimodal pore supports samples using BET surface area, pore volume, X-ray diffraction (XRD), scanning electron microscopy (SEM) and energy dispersive X-ray spectroscopy (EDX) and transmission electron spectroscopy (TEM).
3. Preparation of alumina-silica bimodal pore supported Co catalyst (20 wt% Co and various Co precursors) using the incipient wetness impregnation method.
4. Characterization of the catalyst samples using BET surface area, X-ray diffraction (XRD), temperature programmed reduction (TPR), hydrogen chemisorption, scanning electron microscopy (SEM) and energy dispersive X-ray spectroscopy (EDX) and transmission electron spectroscopy (TEM).
5. Reaction study of the catalyst samples in carbon monoxide (CO) hydrogenation at 220°C , 1 atm and a H₂/CO ratio of 10 in order to measure catalytic activity and selectivity.

CHAPTER II

LITERATURE REVIEWS

There are several studies of silica, bimodal pore supported catalysts and cobalt precursors of cobalt catalysts. Many researchers have been found better knowledge about silica especially supported cobalt catalyst in Fischer-Tropsch synthesis. These reports are very useful and will use to develop works for the future.

2.1 Silica supported cobalt catalysts

A. Feller *et al.* (1995) studied the addition of zirconium oxide chloride to the catalyst formulation of Co/SiO₂. It leads to a higher reducibility of cobalt, due to the formation of a cobalt zirconium species, which can be reduced at lower temperatures than cobalt silicate. Furthermore, the metal particle size of cobalt is increased, but the size of cobalt clusters is reduced. The Co-Zr/SiO₂ catalysts were tested for their activity in the Fischer-Tropsch synthesis. The steady-state activity increased with increasing zirconium loading, which was attributed to the resistance against reoxidation of the larger cobalt particles and thus to the larger amounts of surface cobalt metal present at steady-state in the zirconium promote catalysts. Based on the assumption that the intrinsic activity of cobalt in these catalysts remains unchanged, the observed changes in selectivity could be explained on the basis of secondary reactions in the Fischer-Tropsch system. With increasing zirconium content the number of surface metal atoms at steady-state conditions increases, leading to a higher extent of secondary reactions, but the size of the cobalt clusters decreases, leading to a decrease in the extent of secondary reactions. With increasing zirconium content the extent of secondary hydrogenation of olefins (e.g., ethene) passes a minimum, and the C₅₊-selectivity passes a maximum due to readsorption of small, reactive organic product compounds, which can be incorporated in larger product compounds. Double bond isomerization increases with increasing zirconium content. This might be attributed to the catalytic activity of zirconia.

A. Kogelbauer *et al.* (1995) studied the formation of cobalt silicates on Co/SiO₂ under hydrothermal conditions. Hydrothermal treatment at 220°C led to a catalyst with lower reducibility due to the formation of both reducible and nonreducible (at temperatures < 900°C) Co silicates. They also showed that silicate was formed in catalysts which had been used for FT synthesis. No significant change occurred upon hydrothermal treatment of calcined catalyst. The presence of air during the hydrothermal treatment inhibited the formation of silicate and they proposed that the formation of silicate was linked to the presence of metallic cobalt.

J. Choi *et al.* (1995) investigated the reduction of cobalt catalysts supported on Al₂O₃, SiO₂ and TiO₂ and the effect of metal loading on the reduction. He reported that the activation energy of reduction increased in the following order: Co/SiO₂ > Co/Al₂O₃ > Co/TiO₂. For different metal loading, the catalyst with the higher loading is more readily reducible than with the lower metal loading.

S.Ali *et al.* (1995) investigated the influence of Zr promotion of 20 wt% Co/SiO₂ on Fischer-Tropsch synthesis using catalysts prepared in different ways and having different loadings of Zr (up to 8.5 wt%). The catalysts were investigated using FTS (H₂/CO=2), H₂-D₂ exchange, and CO dissociation to provide insight into how Zr modifies the Co properties. The Zr-promoted exhibited higher overall rates of FTS compared to unpromoted Co/SiO₂. The sequentially impregnated Co/Zr/SiO₂ catalysts appeared to be the most active. However, the co-impregnation method of preparation appeared to result in higher cobalt dispersion. While Zr promotion did not appear to promote or inhibit H₂ activation, hydrogen spillover may have been partly responsible for enhancing the activity of the sequentially impregnated Zr/Co/SiO₂ catalysts. Zr also possibly created an active interface with Co that increased catalyst activity by facilitating Co dissociation. Although high levels of promotion tended to increase the selectivity for higher hydrocarbon, Zr appears to be primarily an excellent rate promoter for Co/SiO₂.

R. Oukaci *et al.* (1999) studied the catalyst support in both promoted and non-promoted cobalt catalysts was found to play a major role in influencing the overall hydrocarbon production rate with little or no effect on catalyst selectivity (except for titania) in both the fixed-bed and the slurry bubble column reactor. Zr oxide had a similar effect on the activity of Co/silica. Addition of ZrO_2 to the support prior to the impregnation of cobalt probably serves somewhat to hinder the formation of cobalt silicates. ZrO_2 was found, thus, to be an excellent F–T synthesis rate promoter for SiO_2 -supported Co catalysts without any effect, negative or positive, on catalyst selectivity. However, the long-term protecting effect of the zirconia remains to be determined. It is also important to note the differences observed in the two reaction systems, i.e. fixed-bed versus slurry bubble column reactors.

V. Curtis *et al.* (1999) synthesized TiO_2 - and SiO_2 -supported cobalt Fischer-Tropsch catalysts load with low concentration of sulfur (100-2000 ppm) from different sources ($(NH_4)_2S$, $(NH_4)_2SO_4$, and $(NH_4)_2SO_3$) and characterized using diffuse reflectance infrared fourier transform spectroscopy (DRIFTS) and TPR. They reported that, for the IR data, sulfur inhibits CO adsorption onto the surface of Co catalysts for a sulfur concentration studied possibly due to (i) site blockage and (ii) inhibited reduction of the catalysts. They also found that sulfur also affects the TiO_2 - and SiO_2 -supported cobalt catalysts during the Fischer-Tropsch reaction. The *in situ* F-T reactions, monitored by DRIFTS, further suggest that lower concentrations of sulfur (100 ppm) on TiO_2 -supported cobalt catalysts improves catalysts activity. Besides, the surface of the silica supported catalysts decreased the intensity of the TPR peak related to reducible silicate.

R. Riva *et al.* (2000) studied the interaction of cobalt with two different kinds of support: silica and titania and their effect on the dispersion and reducibility by XPS, TPR, TPO, XRD and TEM. They also showed that the interaction is much stronger in the case of titania. The different reactivity of cobalt with silics and titania explains why reducing and reoxidizing treatments have opposite effects on the dispersion of cobalt depending on whether it is supported on SiO_2 or TiO_2 . The low reactivity of cobalt with silica favours sintering effects. Conversely, due to the high reactivity of cobalt with titania, the coverage of TiO_2 by cobalt tends to increase after the same treatments.

S.L. Sun *et al.* (2000) prepared by mixed impregnation of cobalt(II) nitrate and cobalt(II) acetate displayed higher activity than the catalysts prepared from either mono-precursor at mild reaction conditions (1MPa total pressure, $H_2/CO=2$, $TD513$ K) of Fischer–Tropsch synthesis (FTS). X-ray diffraction (XRD) indicated that highly dispersed cobalt metal provided the main active sites on the catalyst prepared by mixed impregnation method. Through the mixed impregnation, different cobalt species were formed and their reduction performances were detected by the temperature-programmed reduction (TPR) and thermal gravimetric analysis. Transmission electronic microscopy (TEM) and FT-IR spectroscopy of adsorbed CO as probe molecule revealed that the presence of different sites associated with cobalt after the reduction of the catalysts with hydrogen at 673 K. It was assumed that the metal readily reduced from cobalt nitrate promoted the reduction of Co^{2+} to metallic state in cobalt acetate by H_2 spillover mechanism during catalyst reduction process. The reduced cobalt from cobalt acetate was highly dispersed and remarkably enhanced the catalytic activity.

G. Jacobs *et al.* (2002) investigated the effect of support, loading and promoter on the reducibility of cobalt catalysts. They have reported that significant support interactions on the reduction of cobalt oxide species were observed in the order $Al_2O_3 > TiO_2 > SiO_2$. Addition of Ru and Pt exhibited a similar catalytic effect by decreasing the reduction temperature of cobalt oxide species, and for Co species where a significant surface interaction with the support was present, while Re impacted mainly the reduction of Co species interaction with the support. They also suggested that, for catalysts prepared with a noble metal promoter and reduced at the same temperature, the increase in the number of active sites was due mainly to improvements in the percentage reduction rather than the actual dispersion (cluster size). Increasing the cobalt loading, and therefore the average Co cluster size, was found to exhibit improved reducibility by decreasing interactions with the support.

M. Voß *et al.* (2002) investigated the structural, chemical and electronic properties of Co and Co/Mn catalysts supported on Al_2O_3 , SiO_2 and TiO_2 by a combination of different methods such as TEM, XRD, XPS, TPR and TPO. They reported that temperature-programmed reduction and oxidation reveal the formation of

various oxides in dependence on temperature. In case of the alumina- and titania-supported cobalt catalysts, the formation of high-temperature compounds CoAl_2O_4 and CoTiO_3 , respectively. Moreover, these compounds are not reducible under the applied conditions, the degrees of reduction are only 18-20% ($\text{Co}/\text{Al}_2\text{O}_3$) and 77% (Co/TiO_2).

G.R. Moradi *et al.* (2003) studied the effect of zirconia addition at various loading ratios on the performance of 10 wt% Co/SiO_2 catalysts for the so-called reaction of Fischer–Tropsch synthesis. The catalysts were prepared through a new pseudo sol–gel method which permits a uniform distribution of the incorporated components and a low deviation from theoretical composition. By increasing zirconia, Co–SiO_2 interaction decreases and is replaced by Co–Zr interaction which favours reduction of the catalysts at lower temperatures. The activity and selectivity toward higher hydrocarbons of the promoted catalysts increase with increasing zirconium loading ratios. No appreciable decrease in activity was observed when all catalysts were employed under H_2/CO at 230 °C and 8 bar for 240 h.

L.S. Sales *et al.* (2003) prepared silica embedded with transition metals exhibits adequate properties for applications in catalysis, sensors and optics. Cobalt–silica (Co–SiO_2) nanocomposites were prepared by the sol–gel method and thermally treated at 700, 900, 1100 and 1250 °C. Characterization of the samples was performed by XRD and BET nitrogen adsorption. The performance of the nanocomposites was investigated by catalysis reactions of oxidation. These catalysts were found to be recyclable showing a catalytic activity even after a third recovering. The results indicate that thermal treatment of sol–gel nanocomposites at temperatures higher than 900 °C is essential for the preparation of active heterogeneous catalysts.

K. Okabe *et al.* (2004) investigated Fischer–Tropsch synthesis was carried out in slurry phase over uniformly dispersed Co–SiO_2 catalysts prepared by the sol–gel method. When 0.01–1 wt.% of noble metals were added to the Co–SiO_2 catalysts, a high and stable catalytic activity was obtained over 60 h of the reaction at 503 K and 1 MPa. The addition of noble metals increased the reducibility of surface Co on the catalysts, without changing the particle size of Co metal significantly. High dispersion of metallic Co species stabilized on SiO_2 was responsible for stable activity. The uniform pore size of the catalysts was enlarged by varying the preparation conditions

and by adding organic compounds such as *N,N*-dimethylformamide and formamide. Increased pore size resulted in decrease in CO conversion and selectivity for CO₂, a byproduct, and an increase in the olefin/paraffin ratio of the products. By modifying the surface of wide pore silica with Co–SiO₂ prepared by the sol–gel method, a bimodal pore structured catalyst was prepared. The bimodal catalyst showed high catalytic performance with reducing the amounts of the expensive

A. K. Dalai *et al.* (2005) studied The effect of water on the performance of narrow and wide-pore silica-supported cobalt catalysts was investigated during Fischer–Tropsch synthesis in a continuously stirred tank reactor (CSTR). In these studies the added water replaced an equivalent amounts of inert gas so that all other reaction conditions remained the same before, during and after water addition. A low cobalt loading of 12.4 wt.% on wide-pore silica exhibited a beneficial effect on CO conversion with the addition of water up to 25 vol.% of the total feed. In contrast, the addition of up to 20 vol.% water to a 20 wt.% Co on narrow- or wide-pore silica did not significantly alter the CO conversion. It appears that the CO conversion mainly increases when cobalt clusters are small enough to fit inside the silica pores.

D. Song *et al.* (2006) prepared cobalt catalysts supported on silica with different pore size by incipient wetness impregnation method. N₂ physisorption, XRD, H₂-TPR, H₂-TPD, DRIFTS and O₂ pulse reoxidation were used to characterize the catalysts. The results showed that the pore size of the support had a significant influence on the Co₃O₄ crystallite diameter, catalyst reducibility and Fischer–Tropsch activity. The larger pore could cause the Co/SiO₂ to form larger Co₃O₄ crystallite and decreased its dispersion. Catalysts with different pore size showed different CO adsorption property. The catalysts with pore size of 6–10 nm displayed higher Fischer–Tropsch activity and higher C₅⁺ selectivity, due to the moderate particle size and moderate CO adsorption on the catalysts.

2.2 Bimodal pore supported cobalt catalysts

N. Tsubaki *et al.* (2001) developed the method of bimodal silica by introducing SiO_2 sol into large pores of SiO_2 gel pellet directly. It was found that cobalt supported on this kind of bimodal silica support, exhibited remarkably high activity in liquid-phase Fischer-Tropsch synthesis, which was attributed to its bimodal structure having not only a higher surface area but also a larger pore size. The support with a large surface area allowed highly dispersed cobalt particle and its large pore size improved the diffusion of reactants and products.

S. Sun *et al.* (2003) studied the activity and the selectivity of silica-supported cobalt (20 wt%) catalysts. The catalysts were prepared by incipient wetness impregnation of silica with different cobalt nitrate solution. The catalyst prepared from dehydrated ethanol solution exhibited highest activity and very low methane selectivity. The catalyst prepared from cyclohexanol had the lowest activity and highest methane selectivity. The catalyst prepared from aqueous solution, a most conventional catalyst, exhibited moderate reaction behavior. The catalyst prepared from dehydrated ethanol had cobalt particles with two different size where the large particles showed low bulk density with cluster-like structure.

M. Shinoda *et al.* (2003) prepared bimodal pore supports by introducing SiO_2 or ZrO_2 sols into large pores of SiO_2 gel pellets directly. The pores of the obtained bimodal pore supports distributed distinctly as two kinds of main pores. The increased BET surface area and decreased pore volume, compared to those of original silica gel, indicated that the obtained bimodal pore supports formed according to the designed route. The obtained bimodal pore supports were applied in liquid-phase Fischer-Tropsch synthesis (FTS) where cobalt was supported. The bimodal pore catalysts presented the best reaction performance in liquid-phase Fischer-Tropsch synthesis (FTS) as higher reaction rate and lower methane selectivities, because the spatial promotional effect of bimodal pore structure and chemical effect of the porous zirconia behaved inside the large pores of original silica gel.

Y. Zhang *et al.*(2004) prepared nano-sized silica-silica or zirconia-silica bimodal pore catalyst support by direct introduction of silica or zirconia sols into silica gel. The pores of the obtained bimodal pore supports distributed distinctly at two kinds of main pores. On the other hand, the increased BET surface area and decreased pore volume, compared to those of original silica gel, indicated that the obtained bimodal pore supports formed according to the designed route, and it is found that the zirconia-silica bimodal support improved catalyst activity significantly via not only spatial effect, the intrinsic property of the bimodal structure, but also chemically promotional effect of zirconia, when this kind of support was applied in the liquid-phase Fischer-Tropsch synthesis as a cobalt-loading catalyst.

Y. Zhang *et al.*(2005) studied a multi-functional bimodal pore catalyst support, alumina-silica bimodal pore support, was prepared from a polymer complex solution and silica gel. The obtained bimodal pore support had two kinds of main pores; the pore volume was decreased and the specific surface area was enlarged, comparing with the original silica gel. This kind of bimodal pore support was applied in slurry phase Fischer-Tropsch synthesis, where cobalt was supported as active metal. Alumina-silica bimodal pore catalyst exhibited high catalytic activity and favorite selectivity, due to the spatial effects of bimodal pore structure and chemical effects of coexisting alumina, which formed the new small pores inside SiO₂ large pores. Alumina-silica bimodal pore catalyst showed higher activity than silica-silica bimodal pore catalyst with similar pore structure, proving that hetero-atom bond between alumina and silica was important to promote the performance of the dispersed cobalt. The various catalysts were characterized by XRD, chemisorption, in situ DRIFT, TPR, and TPSR. It was found that alumina in alumina-silica bimodal structure improved cobalt dispersion significantly while keeping the reduction degree almost the same. TOF of alumina-silica bimodal catalysts was the highest, supported by the largest bridge-type adsorbed CO peak in DRIFT observation of this catalyst, as bridge-type adsorbed CO was the active intermediate in FTS.

Y. Zhang *et al.*(2007) prepared silica-supported cobalt (20 wt%) catalysts by incipient-wetness impregnation of silica with different cobalt nitrate solutions. The catalyst prepared from dehydration ethanol solution exhibited stable and the highest activity, as well as significantly low methane selectivity. Cobalt crystalline size of the

catalyst prepared from dehydrated ethanol was smaller than that of the catalyst prepared from aqueous solution, and existed two different size where the large particles showed low bulk density with cluster-like structure. But only larger clusters existed in the catalyst prepared from aqueous solution. The increased amount of active sites and more reactive adsorbed CO on the surface determined the highest activity of the catalyst prepared from dehydrated ethanol solution in FTS.

2.3 Effect of cobalt precursors on cobalt catalyst

A. Martínez *et al.* (2003) investigated the influence of cobalt loading (10–40 wt%Co), cobalt precursor, and promoters (Re,Mn) on the physico-chemical and catalytic properties of mesoporous Co/SBA-15 catalysts for the Fischer–Tropsch Synthesis (FTS) reaction ($T = 493$ K, $P = 20$ bar, $H_2/CO = 2$). Catalysts were characterized by N₂ and Ar adsorption, X-ray diffraction (XRD), transmission electron microscopy (TEM), X-ray photoelectron spectroscopy (XPS), and temperature-programmed reduction (TPR). For Co/SBA-15 catalysts prepared from Co(II) nitrate the dispersion decreased and the extent of cobalt reduction increased with cobalt loading. A maximum CO conversion was found for the sample with ca. 30 wt% Co loading, though the intrinsic activity of Co remained constant in the range of Co loading studied. More methane and less C₅⁺*n*-paraffins were produced over the less reducible 10 wt% Co loading sample. The addition of ca. 1 wt% Re enhanced the reducibility of cobalt oxides and increased the catalyst activity, though the intrinsic activity of cobalt sites was not altered. Rhenium also favored the formation of long-chain *n*-paraffins (C₁₀⁺) while decreasing methane selectivity. Promotion of cobalt with ca. 2 wt% Mn significantly improved cobalt dispersion but decreased its reducibility, producing catalysts that were less active than the unpromoted one. At similar cobalt loading (ca. 20 wt%), a much better dispersion and a stronger cobalt–support interaction leading to the formation of lowreducible cobalt silicates was observed for oxidized samples prepared from acetate and acetylacetonate precursors as compared to that derived from cobalt(II) nitrate, as evidenced by TEM, XPS, and TPR. The former catalysts were characterized by a low FTS activity and a product distribution shifted toward the formation of lighter products. Finally, at comparable Co loading Co/SBA-15 catalysts (nitrate precursor) were about 1.5 times more active per weight of total Co than a Co/SiO₂ sample, with only minor differences in product selectivity.

J. Panpranot *et al.* (2003) prepared Co/MCM-41 catalysts using the incipient wetness impregnation technique with aqueous solutions of different cobalt compounds such as cobalt nitrate, cobalt chloride, cobalt acetate, and cobalt acetylacetonate. MCM-41 is known to have a restricted pore structure; however, using organic precursors such as cobalt acetate and cobalt acetylacetonate resulted in very small cobalt oxide particles that could not be detected by XRD even for a cobalt loading as high as 8wt%. These cobalt particles were small enough to fit into the pores of MCM-41. However, they were found to chemisorb CO in only relatively small amounts and to have low activities for CO hydrogenation—probably due to the formation of cobalt silicates. The use of cobalt chloride resulted in very large cobalt particles/clusters and/or residual Cl₂-blocking active sites, and, consequently, very small active surface area was measurable. The use of cobalt nitrate resulted in a number of small cobalt particles dispersed throughout MCM-41 and some larger particles located on the external surface of MCM-41. Cobalt nitrate appeared to be the best precursor for preparing high-activity MCM-41-supported cobalt Fischer–Tropsch synthesis catalysts.

Y. Ohtsuka *et al.* (2004) studied mesoporous molecular sieves (MCM-41 and SBA-15) with different pore diameters as supports of high loading of Co catalysts, and the performances in FT synthesis have been examined with a fixed bed stainless steel reactor at 2.0MPa for the purpose of efficient production of C₁₀–C₂₀ fraction as the main component of diesel fuel. The method of exchanging template ions in uncalcined MCM-41 with Co²⁺ ions is effective for holding 10–20% Co within the mesopores while keeping the structure regularity of MCM-41 to some extent, compared with the conventional impregnation method using calcined MCM-41. At 523 K, CO conversion and selectivity to C₁₀–C₂₀ hydrocarbons are both higher at larger loading of 20% Co for the exchanged catalysts with pore diameters of 2.7–2.9 nm. When four kinds of 20% Co/SBA-15 with the diameters of 3.5–13 nm, prepared by the impregnation method using an ethanol solution of Co acetate, are used in FT synthesis at 523 K, the catalyst with the diameter of 8.3 nm shows the largest CO conversion, which is higher than those over MCM-41 supported Co catalysts. At a lower temperature of 503 K, however, the acetate-derived Co is almost inactive. In contrast, the use of Co nitrate alone or an equimolar mixture of the acetate and nitrate as Co precursor drastically enhances the reaction rate and consequently provides high space–time yield (260–270 g C/kgcat h) of C₁₀–C₂₀ hydrocarbons. The X-ray diffraction and temperature-programmed

reduction measurements show that the dependency of the catalytic performance of 20% Co/SBA-15 on its precursor originates probably from the differences in not only the reducibility of the calcined catalyst but also the dispersion of metallic Co. Catalyst characterization after FT synthesis strongly suggests the high stability of the most effective Co/SBA-15 in the dispersion and reducibility of the oxide species and in the mesoporous structure.

J. Girardon *et al.* (2005) studied the effect of cobalt precursor and pretreatment conditions on the structure of cobalt species in silica-supported Fischer–Tropsch (FT) catalysts was studied with a combination of characterization techniques (X-ray diffraction, UV–visible, X-ray absorption, X-ray photoelectron spectroscopies, DSC-TGA thermal analysis, propene chemisorption, and temperature-programmed reduction combined with in situ magnetic measurements). The catalysts were prepared via aqueous impregnation of silica with solutions of cobalt nitrate or acetate followed by oxidative pretreatment in air and reduction in hydrogen. It was found that after impregnation and drying cobalt exists in octahedrally coordinated complexes in catalysts prepared from cobalt nitrate or cobalt acetate. Decomposition of the octahedral complexes results in the appearance of Co_3O_4 crystallites and cobalt silicate species. Cobalt repartition between crystalline Co_3O_4 and the cobalt silicate phase in the oxidized samples depends on the exothermicity of salt decomposition in air and the temperature of the oxidative pretreatment. Co_3O_4 crystallite is the dominant phase in the samples prepared via endothermic decomposition of supported cobalt nitrate. Significantly higher cobalt dispersion is found in the catalyst prepared via low-temperature cobalt nitrate decomposition. The uncovered enhanced cobalt dispersion is associated with lower cobalt reducibility. The high exothermicity of cobalt acetate decomposition leads primarily to amorphous, barely reducible cobalt silicate. A more efficient heat flow control at the stage of cobalt acetate decomposition significantly increases the concentration of easy reducible Co_3O_4 in the oxidized catalysts and the number of cobalt metal active sites after reduction. The catalytic measurements show that FT reaction rates depend on the number of cobalt surface metal sites; a higher concentration of cobalt metal sites in the catalysts prepared from cobalt nitrate or with the use of soft cobalt acetate decomposition results in higher catalytic activity in FT synthesis.

N. Nobuntu *et al.* (2005) prepared a series of Co (10%)/Zn ($x\%$)/TiO₂ ($x = 0, 5$) catalysts from different nitrate and acetate precursors. TPR and chemisorption techniques revealed that a mixture of cobalt precursors (cobalt acetate and cobalt nitrate) on titania were more easily reduced when compared to Co (10%)/TiO₂ catalysts prepared from either cobalt acetate or cobalt nitrate alone. By contrast, after addition of zinc, catalysts prepared from zinc acetate and cobalt nitrate had the most highly dispersed cobalt species when compared to catalysts prepared from the other combinations of nitrate and acetate precursors of zinc and cobalt.

Mixed precursors of zinc and cobalt were also more active and had higher CO conversion in Fischer–Tropsch synthesis (FTS) when compared to catalysts prepared from: (i) both nitrate precursors or (ii) both acetate precursors of zinc and cobalt. However, the catalyst prepared from zinc nitrate and cobalt nitrate produced more wax (>C₁₆) when compared to the other catalysts studied (50% versus 12–32% wax). Data suggest that larger Co particles correlate with wax production as well as reduced CO conversion. CO chemisorption data correlated better with the FT activity data than did Co XPS data.

CHAPTER III

THEORY

In the previous chapter, reviews of recent research on silica supported cobalt catalysts, and bimodal pore supported cobalt catalysts for CO hydrogenation have been reviewed. They present knowledge and understanding of influencing parameters on the performance of Co-based catalysts for CO hydrogenation system. This chapter focuses on the fundamental theory of the Fischer-Tropsch Synthesis (FTS) which is well known as one type of carbon monoxide (CO) hydrogenation using Co-based catalysts. The chapter consists of five main sections. Basic details of Fischer-Tropsch Synthesis (FTS) are discussed in section 3.1. Cobalt properties are explained in section 3.2. Details of Co-based catalysts are described in section 3.3. Cobalt-support compound formation (Co-SCF) is discussed in section 3.4. Silicon dioxide which used as a support is detailed in section 3.5. Details of bimodal pore support are described in section 3.6.

3.1 Fischer-Tropsch synthesis (FTS)

Fischer-Tropsch synthesis (FTS) that discovered by Fischer and Tropsch over 80 years ago, as an alternate process, can convert the synthesis gas (H_2/CO) derived from carbon sources such as coal, peat, biomass and natural gas, into hydrocarbons and oxygenates. During the past decades, FTS has been developed continuously by many researchers, although the rise and fall in research intensity on this process has been highly related to the demands for liquid fuels and relative economics. This synthesis is basically the reductive polymerization (oligomerization) of carbon monoxide by hydrogen to form organic products containing mainly hydrocarbons and some oxygenated products in lesser amounts.

By manipulation of the reaction conditions, the process may be designed to produce heavier saturated hydrocarbons or lower olefins or oxygenated hydrocarbons as we shall see in the following discussion.

Metals that have significant activity for Fischer-Tropsch synthesis include iron, cobalt, nickel and ruthenium. Iron has proved so far to be the best. It is superior to

cobalt with respect to conversion rate, selectivity and flexibility. Nickel has disadvantage of producing appreciable amounts of methane. Ruthenium enhance the formation of high molecular weight alkanes and catalyzes polymerization to polymethane. Other group VIII metals are of low activity. Copper does not catalyze Fisher-Tropsch synthesis.

The catalyst is usually prepared by fusion or precipitation over a silica, alumina or kieselguhr support. Small amounts of promoters such as alkali metal or copper salts are included in the catalytic mix. Copper is believed to facilitate the reduction of the catalyst, alkali metal salt, particularly K_2O_2 enhance activity and olefins selectivity. The support increased the surface area of the catalyst metal thus extremely increasing in dispersion.

Sulfur compounds generally poison the catalyst and they must be removed from the synthesis gas feed stream. However, partial sulfur poisoning may have favorable effects. Thus, it has been found that deliberate slight sulfur poisoning of the iron/manganese catalyst enhances selectivity to short chain olefins.

Three main types of reactors are currently in use in the Fischer-Tropsch processes: Fixed-bed, fluidized-bed and slurry bed reactors. Fixed-bed reactors are usually tubular, each tube having 50 mm ID and 12 m length. A single reactor may contain as many as 2000 such tubes. Fluidized-bed reactors provide for better heat transfer and continuous regeneration of the catalyst. The catalyst used in fluidized-bed reactors must have high physical stability. SASOL (in South Africa), uses fluidized-bed reactors 46 m high, 230 cm in diameter with reaction temperature of 320-360°C and pressure. In the slurry-bed reactors the feed gas is bubbled through a suspension of finely divided catalyst particles. It has the advantage of good temperature control thus providing greater flexibility of reaction conditions.

Each type of reactor is better suited for certain product composition. Fixed-bed reactors, for example, produce high boiling straight-chain hydrocarbons consisting, typically, of 33% gasoline hydrocarbons (C_5-C_{11}), 17% diesel and 40% heavy paraffins and higher waxes. The gasoline fraction is of low octane value and requires further treatment (isomerization or blending) before use. Fluidized-bed reactors are the best

when lighter hydrocarbons are desired. A typical product composition is 72% lower molecular weight gasoline-range hydrocarbons rich in olefins and 14% oxygenated hydrocarbons. However, the product is low in diesel. Thus two or more different reactors may be operated in parallel to provide an integrated fuel plant.

The demands on selectivity of Fischer-Tropsch reactions are ever-increasing. In the earlier days of the process the concern was to improve selectivity with respect to better gasoline grade and/or diesel oil chemicals. With the realization of feasible route of converting synthesis gas to industrial intermediates, more stringent conditions are being imposed on the reaction parameters to make the process more selective.

Selectivity improvement is sought with respect to product properties such as chain length, chain branching, olefin content, alcohol content and methane content. Reaction conditions that particularly eliminate or minimize carbon deposition are desirable. In order to achieve and improve product selectivity the optimization of the following reaction parameters has been investigated: reaction temperature and pressure, H_2/CO ratio, conversion, space velocity, amount and type of promoters, nature of the catalyst, size of catalyst particles and mode of its deposition, type of support, and type of reactor.

We have already seen examples of how the choice of the metal catalyst and support affects the product distribution. The effect of the choice of the reactor type on the nature of the reaction products has also been demonstrated.

Selectivity to olefins may be enhanced by addition of promoters such as K_2O , Ti, Mn or V. Selectivity of greater than 70% to C_2-C_4 olefins at high conversion rate has been achieved.

The search for selectivity to lower olefins by controlling the chain growth and inhibiting hydrogenation has been followed in three directions:

- (a) The use of highly dispersed catalyst either by improving the method of deposition or using special dispersing supports.

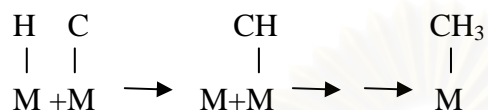
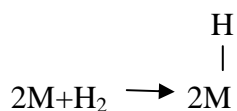
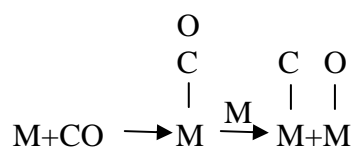
- (b) The use of bimetallic catalyst eg. With Mn/Fe ratio of 9:1 at 330 °C up to 90% olefin selectivity has been achieved. However, the activity of the catalyst and its life-time are low.
- (c) The use of shape-selective catalyst.

Since the Fischer-Tropsch process was originally intended for the production of hydrocarbons, little attention was paid in the early phases of the application of the process to the oxygenated products obtained as co-products. With the search for more economical sources of the oxygenated hydrocarbons, the possibility of tuning the Fischer-Tropsch process for the production such as oxygenates has been investigated. It has been found that with a nitrated iron catalyst, selectivity for alcohols may exceed 80%. A Rh/Hg/SiO₂ catalyst system gave 75% selectivity with respect to ethanol. The major side products are olefins.

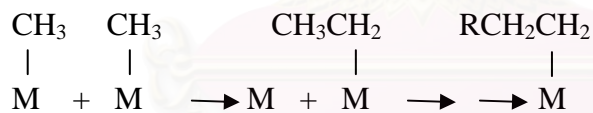
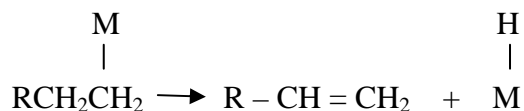
The Fischer-Tropsch process may be defined as being the hydrogenative oligomerization of CO over heterogeneous catalyst to produce alkanes, alkenes oxygenated hydrocarbons and water. A complete mechanism must account for the formation of all products observed. The first attempt at elucidating the mechanism of the process was made by the inventors of the process themselves, Fischer and Tropsch.

3.1.1 The surface carbide mechanism

Fischer and Tropsch apparently were trying to explain the formation of alkanes and alkenes rather than introduce a mechanism for whole line of the products that could be formed from the process. They observed that hydrocarbon formation occurred with heterogeneous metal catalysts (Ni, Fe, Co, Ru) that tend to absorb CO dissociatively to form surface carbide species. Their mechanism consists of the following steps:

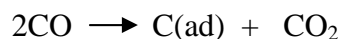
(i) Initiation:

Note: M-X means species X chemisorbed on the metal surface atom M. The hyphen has no implication with respect to the strength of the M-X interaction or the order of the bond. More recently it has been suggested, based spectroscopic evidence, that in order to for an absorbed CO to undergo dissociation it must be bonded side-on to the metal, not end-on.

(ii) Propagation:**(iii) Termination:**

The carbide mechanism has survived the several decades since its introduction. Several items of evidence arising from recent investigation support this mechanism e.g.

(a) In the hydrogenation of CO over clean Ni surface it has been observed that CO₂ evolution precedes that CH₄ thus



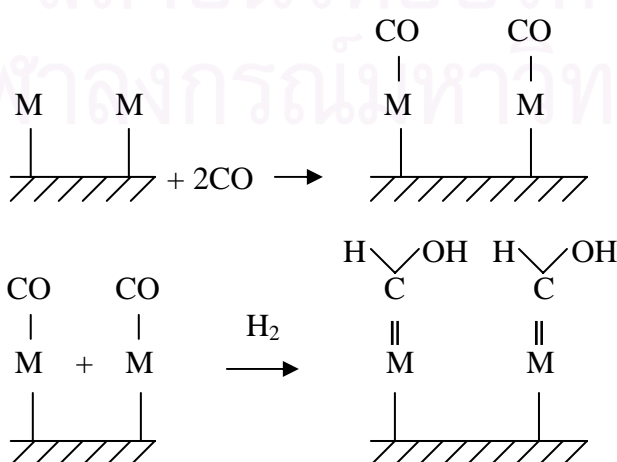
(b) Decomposition of diazomethane(CH₂N₂) at 200°C in the presence of H₂ over Co, Fe and Ru catalysts gives linear alkanes and olefins with distribution similar to that obtained from CO/H₂ reaction over the same catalyst.

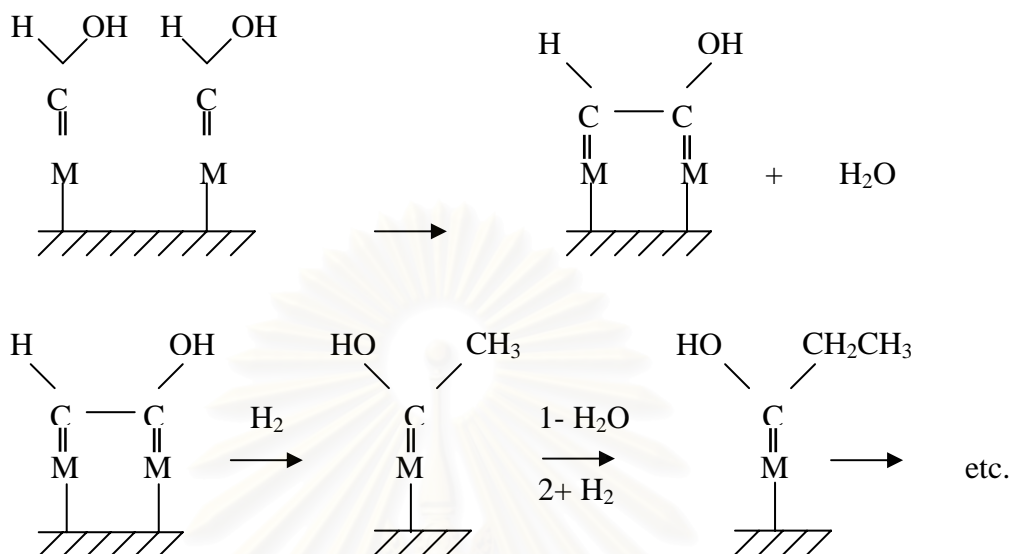
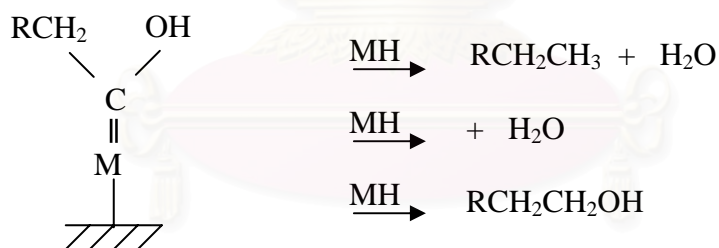
(c) Distribution of ¹³C in CH₂=CH formed when ¹³CO, H₂- and ¹²CH₂N₂ were reacted under Fischer-Tropsch conditions is consistent with the distribution predicted based on the carbided mechanism and inconsistent with other proposed mechanism.

However, a drawback of this mechanism is that it does not explain the formation of oxygenated products.

3.1.2 The hydroxycarbene mechanism

(i) Initiation:



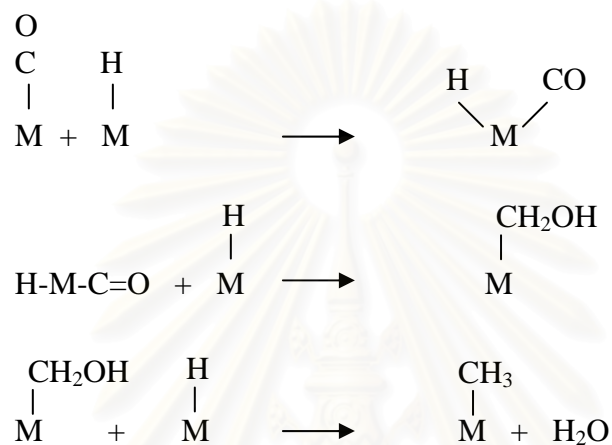
(ii) Propagation:**(iii) Termination:**

This mechanism explains the formation of alkanes, and olefins as well as oxygenated hydrocarbons. However, it precludes the dissociation of CO, which is not consistent with many experimental observations.

3.1.3 The CO insertion mechanism.

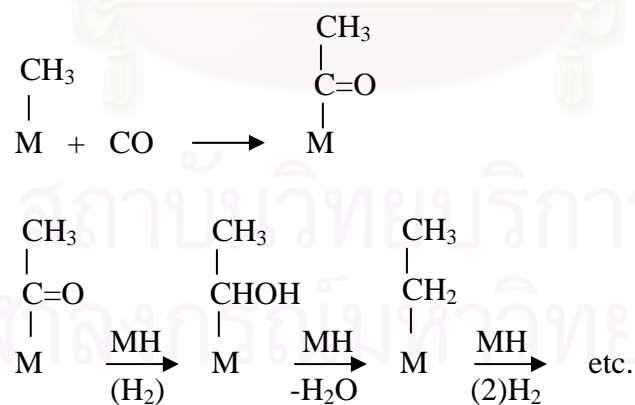
(i) initiation :

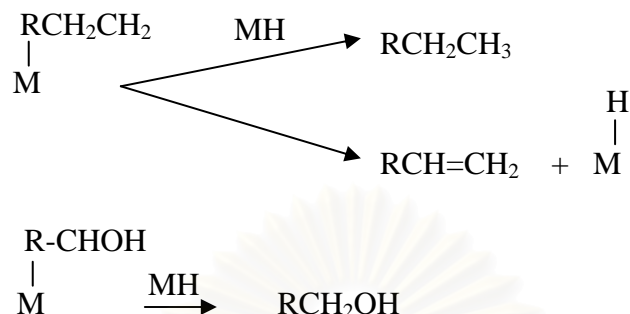
The initiation of active species is similar to that of the carbide mechanism although the mechanism of its formation is different.



(ii) Propagation:

propagation proceeds via CO insertion rather than $-\text{CH}_2-$ insertion.



(iii) Termination:

Normally, catalysts used for FTS are group VIII metals. By nature, the hydrogenation activity increases in order of $\text{Fe} < \text{Co} < \text{Ni} < \text{Ru}$. Ru is the most active. Ni forms predominantly methane, while Co yields much higher ratios of paraffins to olefins and much less oxygenated products such as alcohols and aldehydes than Fe does.

The current main goal in FTS is to obtain high molecular weight, straight chain hydrocarbons. However, methane and other light hydrocarbons are always present as less desirable products from the synthesis. According to the Anderson-Schulz-Flory (ASF) product distribution, typically 10 to 20% of products from the synthesis are usually light hydrocarbon ($\text{C}_1\text{-C}_4$). These light alkanes have low boiling points and exist in the gas phase at room temperature, which is inconvenient for transportation. Many attempts have been made to minimize these by-products and increase the yield of long chain liquid hydrocarbons by improving chain growth probability. It would be more efficient to be able to convert these less desirable products into more useful forms, rather than re-reforming them into syngas and recycling them (Farrauto and Bartholomew, 1997). Depending upon the type of catalyst used, promoters, reaction conditions (pressure, temperature and H_2/CO ratios), and type of reactors, the distribution of the molecular weight of the hydrocarbon products can be noticeably varied.

3.2 Cobalt (Young 1960; Othmer, 1991)

3.2.1 General

Cobalt, a transition series metallic element having atomic number 27, is similar to silver in appearance.

Cobalt and cobalt compounds have expanded from use colorants in glasses and ground coat frits for pottery to drying agents in paints and lacquers, animal and human nutrients, electroplating materials, high temperature alloys, hard facing alloys, high speed tools, magnetic alloys, alloys used for prosthetics, and used in radiology. Cobalt is also as a catalyst for hydrocarbon refining from crude oil for the synthesis of heating fuel.

3.2.2 Physical Properties

The electronic structure of cobalt is $[\text{Ar}] 3d^7 4s^2$. At room temperature the crystalline structure of the α (or ϵ) form, is close-packed hexagonal (cph) and lattice parameters are $a = 0.2501$ nm and $c = 0.4066$ nm. Above approximately 417°C , a face-centered cubic (fcc) allotrope, the γ (or β) form, having a lattice parameter $a = 0.3544$ nm, becomes the stable crystalline form.

The scale formed on unalloyed cobalt during exposure to air or oxygen at high temperature is double-layered. In the range of 300 to 900°C , the scale consists of a thin layer of mixed cobalt oxide, Co_3O_4 , on the outside and cobalt (II) oxide, CoO , layer next to metal. Cobalt (III) oxide, Co_2O_3 , may be formed at temperatures below 300°C . Above 900°C , Co_3O_4 decomposes and both layers, although of different appearance, are composed of CoO only. Scales formed below 600°C and above 750°C appear to be stable to cracking on cooling, whereas those produced at 600 - 750°C crack and flake off the surface.

Cobalt forms numerous compounds and complexes of industrial importance. Cobalt, atomic weight 58.933, is one of the three members of the first transition series of Group 9 (VIII B). There are thirteen known isotopes, but only three are significant: ^{59}Co is the only stable and naturally occurring isotope; ^{60}Co has a half-

life of 5.3 years and is a common source of γ -radioactivity; and ^{57}Co has a 270-d half-life and provides the γ -source for Mössbauer spectroscopy.

Cobalt exists in the +2 or +3 valance states for the major of its compounds and complexes. A multitude of complexes of the cobalt (III) ion exists, but few stable simple salt are known. Octahedral stereochemistries are the most common for cobalt (II) ion as well as for cobalt (III). Cobalt (II) forms numerous simple compounds and complexes, most of which are octahedral or tetrahedral in nature; cobalt (II) forms more tetrahedral complex than other transition-metal ions. Because of the small stability difference between octahedral and tetrahedral complexes of cobalt (II), both can be found equilibrium for a number of complexes. Typically, octahedral cobalt (II) salts and complexes are pink to brownish red; most of the tetrahedral Co (II) species are blue.

Table 3.1 Physical properties of cobalt (Othmer, 1991)

Property	Value
atomic number	27
atomic weight	58.93
transformation temperature, °C	417
heat of transformation, J/g ^a	251
melting point, °C	1493
latent heat of fusion, ΔH_{fus} J/g ^a	395
boiling point, °C	3100
latent heat of vaporization at bp, ΔH_{vap} kJ/g ^a	6276
specific heat, J/(g·°C) ^a	
15-100°C	0.442
molten metal	0.560
coefficient of thermalexpansion, °C ⁻¹	
cph at room temperature	12.5
fcc at 417°C	14.2
thermal conductivity at 25 °C, W/(m·K)	69.16
thermal neutron absorption, Bohr atom	34.8

Table 3.1 Physical properties of cobalt (cont.)

Property	Value		
resistivity, at 20 °C ^b , 10 ⁻⁸ Ω·m	6.24		
Curie temperature, °C	1121		
saturation induction, 4πI _s , T ^c	1.870		
permeability, μ			
initial	68		
max	245		
residual induction, T ^c	0.490		
coercive force, A/m	708		
Young's modulus, Gpac	211		
Poisson's ratio	0.32		
Hardness ^f , diamond pyramid, of %Co	99.9	99.98 ^e	
At 20 °C	225	253	
At 300 °C	141	145	
At 600 °C	62	43	
At 900 °C	22	17	
strength of 99.99 %cobalt, MPa ^g	as cast	annealed	sintered
tensile	237	588	679
tensile yield	138	193	302
compressive	841	808	
compressive yield	291	387	

^aTo convert J to cal, divided by 4.184.

^bconductivity = 27.6 % of International Annealed Copper Standard.

^cTo convert T to gauss, multiply by 10⁴.

^dTo convert GPa to psi , multiply by 145,000.

^eZone refined.

^fVickers.

^gTo convert MPa to psi , multiply by 145.

3.2.3 Cobalt Oxides

Cobalt has three well-known oxides:

Cobalt (II) oxide, CoO , is an olive green, cubic crystalline material. Cobalt (II) oxide is the final product formed when the carbonate or the other oxides are calcined to a sufficiently high temperature, preferably in a neutral or slightly reducing atmosphere. Pure cobalt (II) oxide is a difficult substance to prepare, since it readily takes up oxygen even at room temperature to re-form a higher oxide. Above about 850°C , cobalt (II) oxide form is the stable oxide. The product of commerce is usually dark gray and contains 75-78 wt % cobalt. Cobalt (II) oxide is soluble in water, ammonia solution, and organic solvents, but dissolves in strong mineral acids. It is used in glass decorating and coloring and is a precursor for the production of cobalt chemical.

Cobalt (III) oxide, Co_2O_3 , is formed when cobalt compounds are heated at a low temperature in the presence of an excess of air. Some authorities told that cobalt (III) oxide exists only in the hydrate form. The lower hydrate may be made as a black powder by oxidizing neutral cobalt solutions with substances like sodium hypochlorite. Co_2O_3 or $\text{Co}_2\text{O}_3 \cdot \text{H}_2\text{O}$ is completely converted to Co_3O_4 at temperatures above 265°C . Co_3O_4 will absorb oxygen in a sufficient quantity to correspond to the higher oxide Co_2O_3 .

Cobalt oxide, Co_3O_4 , is formed when cobalt compounds, such as the carbonate or the hydrated sesquioxide, are heated in air at temperatures above approximately 265°C and not exceeding 800°C .

3.3 Co-based Catalysts

Supported cobalt (CO) catalysts are the preferred catalysts for the synthesis of heavy hydrocarbons from natural gas based syngas (CO and H_2) because of their high Fischer-Tropsch (FT) activity, high selectivity for linear hydrocarbons and low activity for the water-gas shift reaction. It is known that reduced cobalt metal, rather than its oxides or carbides, is the most active phase for CO hydrogenation in such catalysts. Investigations have been done to determine the nature of cobalt species on various

supports such as alumina, silica, titania, magnesia, carbon, and zeolites. The influence of various types of cobalt precursors used was also investigated. It was found that the used of organic precursors such as CO (III) acetyl acetate resulting in an increase of CO conversion compared to that of cobalt nitrate. (Kraum and Baerns, 1999).

3.4 Cobalt-Support Compound Formation (Co-SCF)

Compound formation between cobalt metal and the support can occur under pretreatment and/or reaction conditions, leading to catalyst deactivation. The compound formation of cobalt metal with support materials, however, is difficult to predict because of the lack of sufficient thermodynamic data. Co-support compound formation can be detected evidentially.

3.4.1 Co-Aluminate Formation

Interaction of cobalt with its alumina support has been observed by many authors using various techniques including TPR, XRD, EXAFS, and XPS (ESCA). The migration of cobalt ions into alumina lattice sites of octahedral or tetrahedral symmetry is limited to the first few layers of the support under normal calcination conditions. The reaction of Co with γ -Al₂O₃ can form a surface spinel in Co/ γ -Al₂O₃ catalysts. The surface spinel structure can not be observed by X-ray diffraction because it does not have long range, three dimensional order. It has been suggested that cobalt ions occupying surface octahedral site of γ -Al₂O₃ are reducible while cobalt ions occupying tetrahedral sites are non-reducible, at least at temperatures $\leq 900^\circ\text{C}$. At lower calcination temperatures, filling of the octahedral sites is more favorable. Filling of the tetrahedral site of γ -Al₂O₃ may be enhanced by an increase in calcination temperature.

3.4.2 Co-Silicate Formation

The formation of cobalt silicates on Co/SiO₂ under hydrothermal conditions has been extensively studied by Kogelbauer *et al.* (1995). Hydrothermal treatment at 200°C led to a catalyst with lower reducibility due to the formation of both

reducible and non-reducible (at temperatures $\leq 900^{\circ}\text{C}$) cobalt silicates. It was found that hydrothermal treatment of the reduced catalyst or hydrothermal treatment of the calcination catalyst in the presence of hydrogen produces cobalt silicates, while hydrothermal treatment of the calcined catalyst in air does not result in their formation. Hydrothermal treatment of the calcined catalyst in inert gas also has little effect.

3.5 Silicon dioxide (Patnaik,2002)

3.5.1 General feature of silica

Table 3.2 Physical properties of silica

Properties	
Other names	Silica
Molecular formula	SiO_2
Molar mass	60.1 g/mol
Appearance	white or colourless solid (when pure)
Density and phase	2.6 g/cm ³ , solid
Solubility in water	insoluble
Melting point	1610 °C
Boiling point	2230 °C

In its many forms, silica has been used in all stages of civilization, from the ancient flints of the Stone Age to the modern silica laboratory ware. Because of its many uses, and of the many varied forms in which it occurs, silica has been called by more names than any other mineral. Many of the older names of flint are now so obsolete that repetition is needless, but many of the present-day names for quartz gems are unknown save to a few jewellers. Then, too, the exact research of the modern

laboratory has shown several distinct crystallographic varieties of silica; some of which are closely connected with the temperatures experienced in their life-history.

The many different names, and their different connotations, which are now in use for silica minerals, call for a classification and arrangement in a more ample, yet more concise manner than is to be found in the usual discussion of the varieties of silica. This article is written with the hope of making a scientific classification of these names, so that the use of the different terms will no longer be a cause for tedious searching for definitions.

These varieties are named in the order formed with descending temperatures. Recrystallization changes occur at the temperatures noted when ample time is allowed for the action, often in the laboratory only in the presence of catalysts. Besides the changes at these critical temperatures, there are probably similar changes from unstable forms towards quartz at atmospheric temperatures, especially after long time intervals. With fairly rapid cooling or heating intermediate forms may not occur in their stable zone, but a direct change from one to another without the intermediate product may take place. Most of the recrystallization changes noted are found to occur at both ascending and descending temperatures.

(A) SILICA GLASS - amorphous, a true non-crystalline glass, stable below the melting point and above the "gc" temperature. Quartz Glass, Fused Silica, Fused Quartz, are other names for this supercooled liquid. In most forms at atmospheric temperatures there are traces of cristobalite.

(B) CRISTOBALITE - isometric, or pseudo-isometric, "gc" range is at 1710° where Cristobalite changes to glass as temperatures rise, or glass to cristobalite as they fall. Cristobalite, an alternate spelling. Beta Cristobalite, also called High Cristobalite, is the high temperature product, forming in the "gc" range in cooling. It is isometric, and in cooling recrystallizes to Alpha Cristobalite, or Low Cristobalite, at 200-275°, providing cooling through the "ct" and "tq" ranges has been too rapid for recrystallization. It is tetragonal.

(C) TRIDYMITE - hexagonal, bipyramidal. "ct" range is at 1470°, where cristobalite

changes to tridymite on cooling. Glass may crystallize as tridymite at 1670° if the cooling was too rapid through the "gc" range. Beta Second Tridymite, or Upper High Tridymite, is the high temperature product, forming in the "ct" range in cooling, and which recrystallizes to Beta First Tridymite, also called Lower High Tridymite, at 163° if cooling was too rapid for the "tq" transformation. This in turn alters to Alpha Tridymite, or Low Tridymite, at 117°, which is the usual tridymite of nature.

- Asmanite - a meteoric tridymite, related to the above series.
- Vestan - a doubtful silica mineral, probably to be ascribed to tridymite.
- Granuline - a doubtful pulverescent mineral which seems allied to tridymite on optical grounds.

(D) QUARTZ - hexagonal, forms from tridymite in the "tq" range at 870° in cooling. Glass may change to crystalline quartz at about 1400° providing cooling was too rapid for the "gc", "gt" and "ct" transformations. Beta Quartz, or High Quartz, is the high temperature product, forming at the "tq" point. It is hemihedral. On cooling it recrystallizes to Alpha Quartz, also called Low Quartz, at 573°, yielding the stable low temperature mineral. It is tetartohedral, showing polarity along the c axis and is divisible into Right Hand Quartz and Left Hand Quartz

(E) CHALCEDONY - a cryptocrystalline, or very finely fibrous mineral, which has not been successfully located in the thermal equilibrium diagram. Heating to 725-850° usually results in an alteration to tridymite, which thereafter acts as normal tridymite. Chalcedony is usually found as a deposit from solutions, and may be a mixture of glass and quartz, or more probably an intermediate product in the dehydration of the opal colloid. Various subdivisions of chalcedony have been made on optical grounds.

- Chalcedony - biaxial, positive, elongation positive.
- Chalcedonite - biaxial, negative.
- Lussatite - biaxial, positive, parallel elongation.
- Quartzine - biaxial, positive, negative elongation
- pseudochalcedonite, Lutecite.
- Jenzschite - differently soluble, but of same S. G. as chalcedony.

- Melanophlogite - possibly impure chalcedony.
 Sulfuricin - probably a chalcedony rich in sulphur.

(F) COLLOIDAL SILICA - is usually hydrous, and is commonly described under opal. Silicon occurs in nature combined with oxygen in various forms of silica and silicates. Silicates have complex structures consisting of SiO_4 tetrahedral structural units incorporated to a number of metals. Silicon is never found in nature in free elemental form. Among all elements silicon forms the third largest number of compounds after hydrogen and carbon. There are well over 1000 natural silicates including clay, mica, feldspar, granite, asbestos, and hornblende. Such natural silicates have structural units containing orthosilicates, SiO_4^{4-} , pyrosilicates $\text{Si}_2\text{O}_7^{6-}$, and other complex structural units, such as, $(\text{SiO}_3)_n^{2n-}$ that have hexagonal rings arranged in chains or pyroxene $(\text{SiO}_3^{2-})^n$ and amphiboles, $(\text{Si}_4\text{O}_{11})^{6-}$ in infinite chains. Such natural silicates include common minerals such as tremolite, $\text{Ca}_2\text{Mg}_5(\text{OH})_2\text{Si}_8\text{O}_{22}$; diopside, $\text{CaMg}(\text{SiO}_3)_2$; kaolin, $\text{H}_8\text{Al}_4\text{Si}_4\text{O}_{18}$; montmorillonite, $\text{H}_2\text{Al}_2\text{Si}_4\text{O}_{12}$; tale, $\text{Mg}_3[(\text{OH})_2\text{SiO}_{10}]$; muscovite (a colorless form of mica), $\text{H}_2\text{KAl}_3(\text{SiO}_4)_3$; hemimorphite, $\text{Zn}_4(\text{OH})_2\text{Si}_2\text{O}_7 \cdot \text{H}_2\text{O}$; beryl, $\text{Be}_3\text{Al}_2\text{Si}_6\text{O}_{18}$; zircon, ZrSiO_4 ; benitoite, $\text{BaTiSi}_3\text{O}_9$; feldspars, KAlSi_3O_8 ; zeolites, $\text{Na}_2\text{O} \cdot 2\text{Al}_2\text{O}_3 \cdot 5\text{SiO}_2 \cdot 5\text{H}_2\text{O}$; nephrite, $\text{Ca}(\text{Mg,Fe})_3(\text{SiO}_3)_4$; enstatite, $(\text{MgSiO}_3)_n$; serpentine, $\text{H}_4\text{Mg}_3\text{Si}_2\text{O}_{10}$, jadeite, $\text{NaAl}(\text{SiO}_3)_2$; topaz, $\text{Al}_2\text{SiO}_4\text{F}_2$; and tourmaline, $(\text{H,Li,K,Na})\text{Al}_3(\text{BOH})_2\text{SiO}_{19}$. silica, the other most important class of silicon compounds, exists as sand, quartz, flint, amethyst, agate, opal, jasper, and rock crystal.

3.6 Bimodal pore structure

3.6.1 General feature of Bimodal pore structure

The support with large surface area, usually contains small pore size, which results in poor intra-pellet diffusion efficiency of reactants and products. Slow transportation of reactants to and products from catalytic sites often controls the rate of primary and secondary reactions even on small catalyst pellet (Iglesia et al.,1997). the pore size of catalyst also affects product selectivities, due to the spatial effect of support.

The bimodal pore structure support, which contains large pores and small pores at the same time, contributes to higher dispersion of supported cobalt crystallites by the small pores, which enlarged the surface area of the support. Furthermore, it is able to diminish the diffusion resistance by its large pores. A support with a distinct bimodal pore structure has excellent advantages in solid catalysis reaction because the large pores provide pathways for rapid molecular transportation and small pores serve a large area of active surface, contributing to high diffusion efficiency and dispersion of supported metal simultaneously.

Several preparation methods were reported to form bimodal pore catalyst support. But these methods used very corrosive reagents such as aqua regia, and the size of large pores of the obtained bimodal structure was as high as several hundred nanometer that the effect of bimodal structure was not obvious (R. Takahashi *et. al.*, 2001; T. Inui *et. al.*, 1979). The formation scheme of bimodal pore support show in Figure3.1. Furthermore, the reported methods are only effective for one specific oxide support, such as Al₂O₃ or SiO₂. A general method to prepare bimodal structure, especially containing hetero-atom structure, is expected. For example of bimodal pore catalyst support, silica-silica and silica-zirconia bimodal pore supports were obtained by building up nano-particles from silica or zirconia sol to form small pores, inside tailor-made large silica pores (Y. Zhang *et. al.*, 2004).

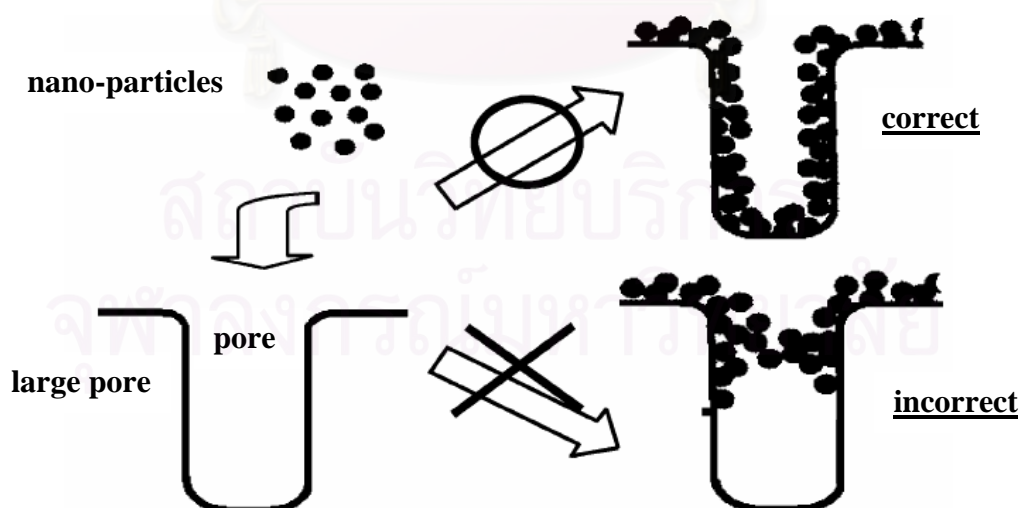


Figure 3.1 Formation scheme of the bimodal pore support.

CHAPTER IV

EXPERIMENTAL

This chapter consists of experimental systems and procedures used in this work which is divided into three parts including catalyst preparation, catalyst characterization and reaction study in CO hydrogenation.

The first part (section 4.1) is described catalyst preparation such as alumina-silica bimodal pore supports consisting of various alumina loadings, bimodal pore supported cobalt catalysts consisting various cobalt precursors and catalyst nomenclature. The second part (section 4.2) is explained catalyst characterization by various techniques including of BET surface area, pore volume, TPR, hydrogen chemisorption, XRD, TEM and Electron microscopy. Finally, the last part (section 4.3) is illustrated catalyst activity measurement in CO hydrogenation.

4.1 Catalyst preparation

4.1.1 Chemicals

The details of chemicals used in this experiment are shown in Table 4.1.

Table 4.1 Chemicals used in the preparation of catalysts.

Chemical	Supplier
Silica gel (Cariact Q-50)	Fuji Silysia Chemicals Ltd.,
Aluminium nitrate	Aldrich
Cobalt (II) nitrate hexahydrate	Aldrich
Cobalt (II) acetate tetrahydrate	Aldrich
Cobalt (II) acetylacetonate	Aldrich
Cobalt(II) chloride	Carlo erba
Polyethylene glycol (PEG)	Aldrich

4.1.2 Preparation of alumina-silica bimodal pore support

A alumina-silica bimodal pore support was prepared by incipient wetness impregnation method. The Aluminium nitrate was dissolved in a 0.3 mol/l polyethylene glycol aqueous solution to prepare the polymer complex solution. After stirring at 80°C for 1 hour, the solution was impregnated into silica gel (Cariact Q-50). After impregnation, the support was dried at 110°C for 12 hours and calcined in air at 400°C for 2 hours.

4.1.3 Preparation of the supported Co samples

The catalysts were prepared by the incipient wetness impregnation with aqueous solution of different cobalt precursors such as cobalt (II) nitrate hexahydrate, cobalt (II) acetate tetrahydrate, cobalt (II) acetylacetonate and cobalt (II) chloride. Cobalt loading was approximately 20 % by weight of catalyst (see Appendix A). The catalysts were dried at 110°C for 12 hours and calcined in air at 500°C for 4 hours.

4.1.4 Sample nomenclature

The nomenclature used for the samples in this study is following:

- i %Al-Si** refers to the alumina-silica bimodal pore support where:
i is the weight percents of alumina
- Co/SiO₂** refers to the silica supported cobalt catalyst
- Co/i %Al-Si** refers to the alumina-silica bimodal pore supported cobalt catalyst where:
i is the weight percents of alumina
- CoN** refers to the cobalt (II) nitrate hexahydrate
- CoAT** refers to the cobalt (II) acetate tetrahydrate
- CoAA** refers to the cobalt (II) acetylacetonate
- CoCl** refers to the cobalt (II) chloride
- CoAT/SiO₂** refers to the silica supported cobalt catalyst (type of the cobalt precursor is cobalt acetate tetrahydrate)

CoAT/i %Al-Si refers to the alumina-silica bimodal pore supported cobalt catalyst (type of the cobalt precursor is cobalt acetate tetrahydrate)

4.2 Catalyst characterization

Various characterization techniques were used in this studied in order to clarify the catalyst structure and morphology, surface composition of various alumina-silica bimodal pore supported cobalt catalyst.

4.2.1 N₂ physisorption

Surface area, pore volume and average pore diameter of catalysts were measured by the BET method, with nitrogen as the adsorbate using a micrometric model ASAP 2000 at liquid-nitrogen point temperature (77 K) at the Analysis Center of Department of Chemical Engineering, Faculty of Engineering, Chulalongkorn University.

4.2.2 X-ray diffraction (XRD)

XRD were performed to determine the bulk phase of catalysts by SIEMENS D 5000 X-ray diffractometer connected with a computer with Diffract ZT version 3.3 program for fully control of the XRD analyzer. The experiments were carried out by using $\text{CuK}\alpha$ ($\lambda = 1.54439 \text{ \AA}$) radiation with Ni filter in the 2θ range of 20-80 degrees resolution 0.04° . The crystallite size was estimated from line broadening according to the Scherrer equation and $\alpha\text{-Al}_2\text{O}_3$ was used as standard.

4.2.3 Temperature programmed reduction (TPR)

TPR was used to determine the reducibility of catalysts using a Micrometric Chemisorb 2750:

1. The catalyst sample 0.2 g used in the sample cell.
2. Prior to operation, the catalysts were heated up to 200°C in flowing nitrogen and held at this temperature for 1 h.

3. After the catalyst sample was cooled down to room temperature, carrier gas (10 % H₂ in Ar) were ramping from 35°C to 800°C.
4. During reduction, a cold trap was placed to before the detector to remove water produced.

4.2.4 Electron microscopy

Scanning electron microscopy (SEM) and Energy dispersive X-ray spectroscopy (EDX) was used to determine the morphology and elemental distribution of the catalyst particles. Model of SEM: JEOL mode JSM-5800LV and EDX was performed using Link Isis Series 300 program at the Scientific and Technological Research Equipment Center, Chulalongkorn University (STREC).

4.2.5 Transmission Electron Microscopy (TEM)

The dispersion of cobalt oxide supports was determined using JEM-2100 transmission electron spectroscopy operated at 100 kV with 25 k magnification. The sample was dispersed in ethanol prior to the TEM measurement.

4.2.6 Hydrogen Chemisorption

Static H₂ chemisorption at 100°C on the reduced cobalt catalysts was used to determine the number of reduced surface cobalt metal atoms. This is related to the overall activity of the catalysts during CO hydrogenation. Gas volumetric chemisorption at 100°C was performed using the method described by Reuel and Bartholomew. The experiment was performed in a Micromeritics ASAP 2010 using ASAP 2010C V3.00 software.

4.3. Reaction study in CO hydrogenation

4.3.1 Materials

The reactant gas used for the reaction study was the carbon monoxide in hydrogen feed stream as supplied by Thai Industrial Gas Limited (TIG). The gas mixture contained 9.73 vol % CO in H₂ (22 cc/min). The total flow rate was 30 ml/min with the H₂/CO ratio of 10/1. Ultra high purity hydrogen (50 cc/min) and high purity argon (8 cc/min) manufactured by Thai Industrial Gas Limited (TIG) were used for reduction and balance flow rate.

4.3.2 Apparatus

Flow diagram of CO hydrogenation system is shown in Figure 4.1. The system consists of a reactor, an automatic temperature controller, an electrical furnace and a gas controlling system.

4.3.2.1 Reactor

The reactor was made from a stainless steel tube (O.D. 3/8 "). Two sampling points were provided about and below the catalyst bed. Catalyst was placed between two quartz wool layers.

4.3.2.2 Automation Temperature Controller

This unit consisted of a magnetic switch connected to a variable voltage transformer and a solid state relay temperature controller model no.SS2425DZ connected to a thermocouple. Reactor temperature was measured at the bottom of the catalyst bed in the reactor. The temperature control set point is adjustable within the rang of 0-800 °C at the maximum voltage output of 220 volt.

4.3.2.3 Electrical Furnace

The furnace supplied heat to the reactor for CO hydrogenation. The reactor could be operated from temperature up to 800 °C at the maximum voltage of 220 volt.

4.3.2.4 Gas Controlling System

Reactant for the system was each equipped with a pressure regulator and an on-off valve and the gas flow rates were adjusted by using metering valves.

4.3.2.5 Gas Chromatograph

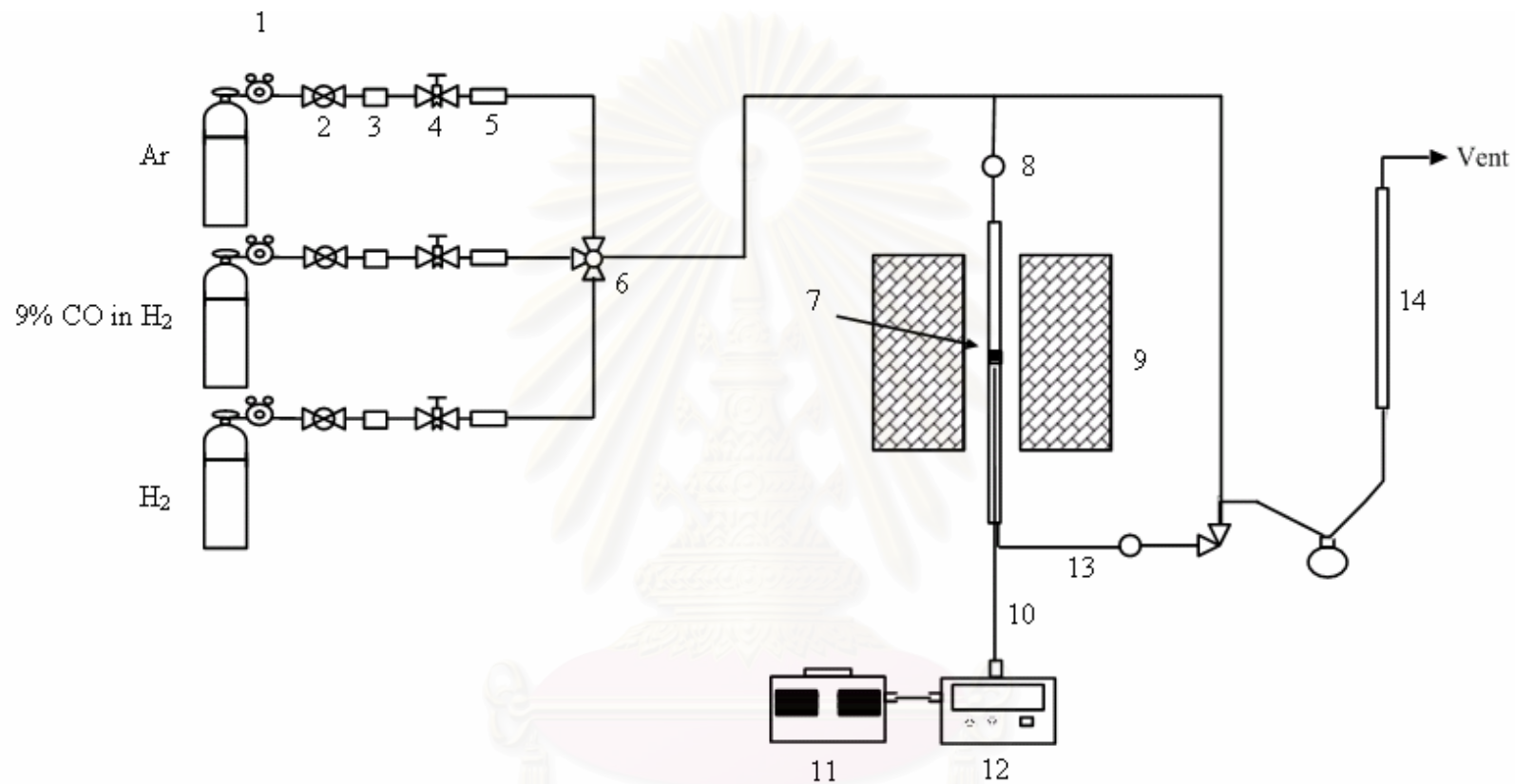
The composition of hydrocarbons in the product stream was analyzed by a Shimadzu GC-14B (VZ10) gas chromatograph equipped with a flame ionization detector. A Shimadzu GC-8A (molecular sieve 5A) gas chromatograph equipped with a thermal conductivity detector was used to analyze CO and H₂ in the feed and product streams. The operating conditions for each instrument are shown in the Table 4.2.

Table 4.2 Operating condition for gas chromatograph

Gas Chromatograph	SHIMADZU GC-8A	SHIMADZU GC-14B
Detector	TCD	FID
Column	Molecular sieve 5A	VZ 10
- Column material	SUS	-
- Length	2 m	-
- Outer diameter	4 mm	-
- Inner diameter	3 mm	-
- Mesh range	60/80	60/80
- Maximum temperature	350 °C	80°C
Carrier gas	He (99.999%)	N ₂ (99.999%)
Carrier gas flow	20 cc/min	-
Column gas	He (99.999%)	Air , H ₂
Column gas flow	20 cc/min	-
Column temperature		
- initial (°C)	60	70
- final (°C)	60	70
Injector temperature (°C)	100	100
Detector temperature (°C)	100	150
Current (mA)	80	-
Analysed gas	Ar, CO, H ₂	Hydrocarbon C ₁ -C ₄

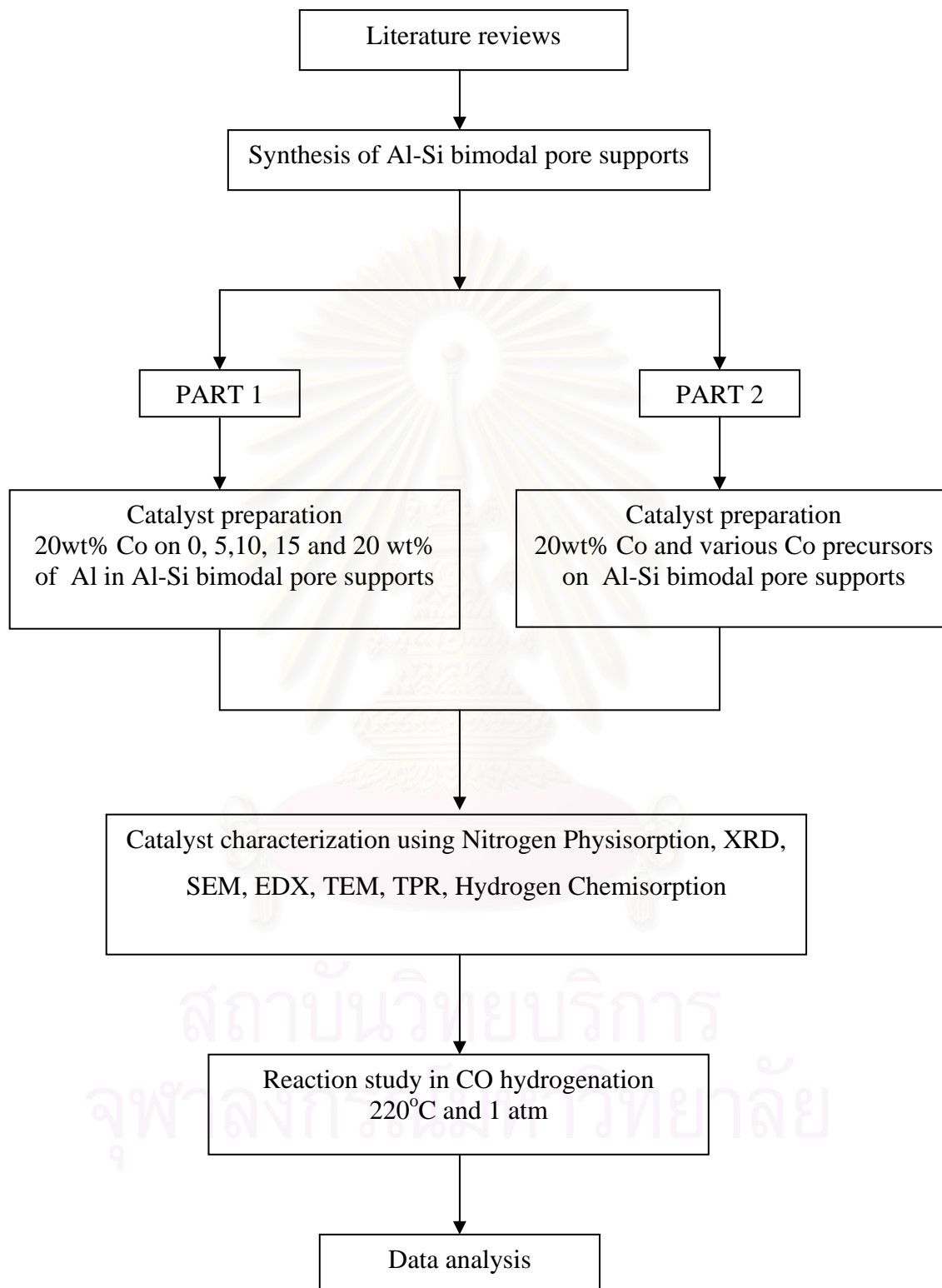
4.3.3 Procedures

1. Using 0.2 g of catalyst packed in the middle of the stainless steel microreactor, which is located in the electrical furnace.
2. A flow rate of Ar = 8 cc/min, 9% CO in H₂ = 22 cc/min and H₂ = 50 cc/min in a fixed-bed flow reactor. A relatively high H₂/CO ratio was used to minimize deactivation due to carbon deposition during reaction.
3. The catalyst sample was re-reduced *in situ* in flowing H₂ at 350°C for 3 h prior to CO hydrogenation.
4. CO hydrogenation was carried out at 220°C and 1 atm total pressure in flowing 9% CO in H₂.
5. The effluent was analyzed using gas chromatography technique [Thermal conductivity detector (TCD) was used for separation of carbon monoxide (CO) and methane (CH₄) and flame ionization detector (FID) were used for separation of light hydrocarbon such as methane (CH₄), ethane (C₂H₆), propane (C₃H₈), etc.] In all cases, steady-state was reached within 6 h.



- | | | | |
|-----------------------|-----------------------|----------------------------------|----------------------------|
| 1. Pressure Regulator | 2. On-Off Valve | 3. Gas Filter | 4. Metering Valve |
| 5. Back Pressure | 6. 3-way Valve | 7. Catalyst Bed | 8. Sampling point |
| 9. Furnace | 10. Thermocouple | 11. Variable Voltage Transformer | 12. Temperature Controller |
| 13. Heating Line | 14. Bubble Flow Meter | | |

Figure 4.1 Flow diagram of CO hydrogenation system

RESEARCH METHODOLOGY

CHAPTER V

RESULTS AND DISCUSSION

This chapter is divided into two sections. Section 5.1 described characteristics of 20 wt% cobalt (Co) dispersed on various amounts of alumina loading on alumina-silica bimodal pore support. Section 5.2 described characteristics and catalytic activity towards CO hydrogenation of various cobalt precursors on alumina-silica bimodal pore support.

5.1 Various alumina loading of 20 wt% cobalt on alumina-silica bimodal pore supported catalyst.

5.1.1 BET surface area

Table 5.1 BET surface area, average pore diameter and pore volume of various supports

Support	BET Surface area (m ² /g)	Average small pore diameter (nm)	Average large pore diameter (nm)	Pore volume (cm ³ /g)
Silica	72	-	46.1	0.255
5% Al-Si	111	3.2	54.4	0.367
10% Al-Si	127	3.1	40.8	0.419
15% Al-Si	151	3.0	51.8	0.373
20% Al-Si	189	3.0	40.0	0.379

The pore distribution of the obtained alumina-silica bimodal pore support exhibited the bimodal pore size distribution that shown in **Figure 5.1**. An increase in the amounts of alumina loading apparently resulted in an increase in the

portion of small pore. However, the average small and large pore diameter are almost the same size. Consequently, BET surface area increased with alumina loading from 72 m²/g of silica to 111, 127, 151, and 189 m²/g of 5% Al-Si, 10% Al-Si, 15% Al-Si, and 20% Al-Si, respectively, as shown in **Table 5.1**.

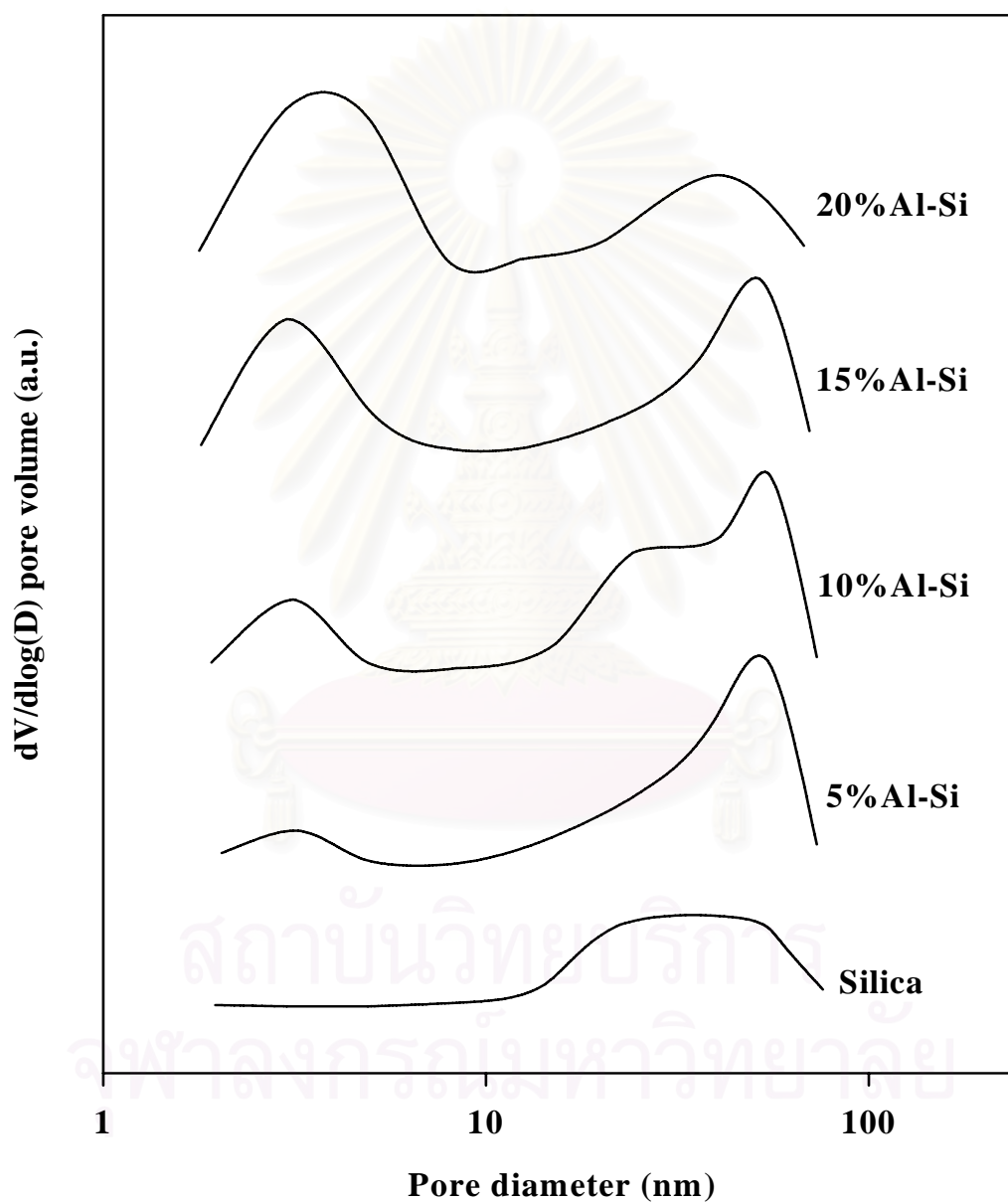


Figure 5.1 The pore distributions of various supports

Table 5.2 BET surface area, average pore diameter and pore volume of various catalysts

Catalyst	BET Surface area (m ² /g)	Average small pore diameter (nm)	Average large pore diameter (nm)	Pore volume (cm ³ /g)
Co/silica	54	-	48.1	0.249
Co/5% Al-Si	66	3.2	48.8	0.335
Co/10% Al-Si	69	2.9	28.2	0.320
Co/15% Al-Si	81	2.9	26.9	0.314
Co/20% Al-Si	90	3.1	24.6	0.265

It was found that the surface areas of the alumina-silica bimodal pore supported Co catalyst were 54-90 m²/g. In fact, the surface areas increased with amount of alumina loading.

5.1.2 X-ray diffraction (XRD)

XRD patterns of the silica support and alumina-silica bimodal pore supports before impregnation with the cobalt precursor are shown in **Figure 5.2**. It was observed that all supports exhibited only a broad XRD peak assigning to the conventional amorphous silica. After impregnation with the cobalt precursor, the catalyst samples were dried and calcined. The XRD patterns of the silica and alumina-silica bimodal pore supported Co catalyst are shown in **Figure 5.3**. Besides the observation of the characteristic peaks of the supports as shown in **Figure 5.2**, all calcined samples exhibited XRD peaks at 31° (weak), 37° (strong), 45° (weak), 60° (weak) and 65° (weak), which were assigned to the presence of Co₃O₄.

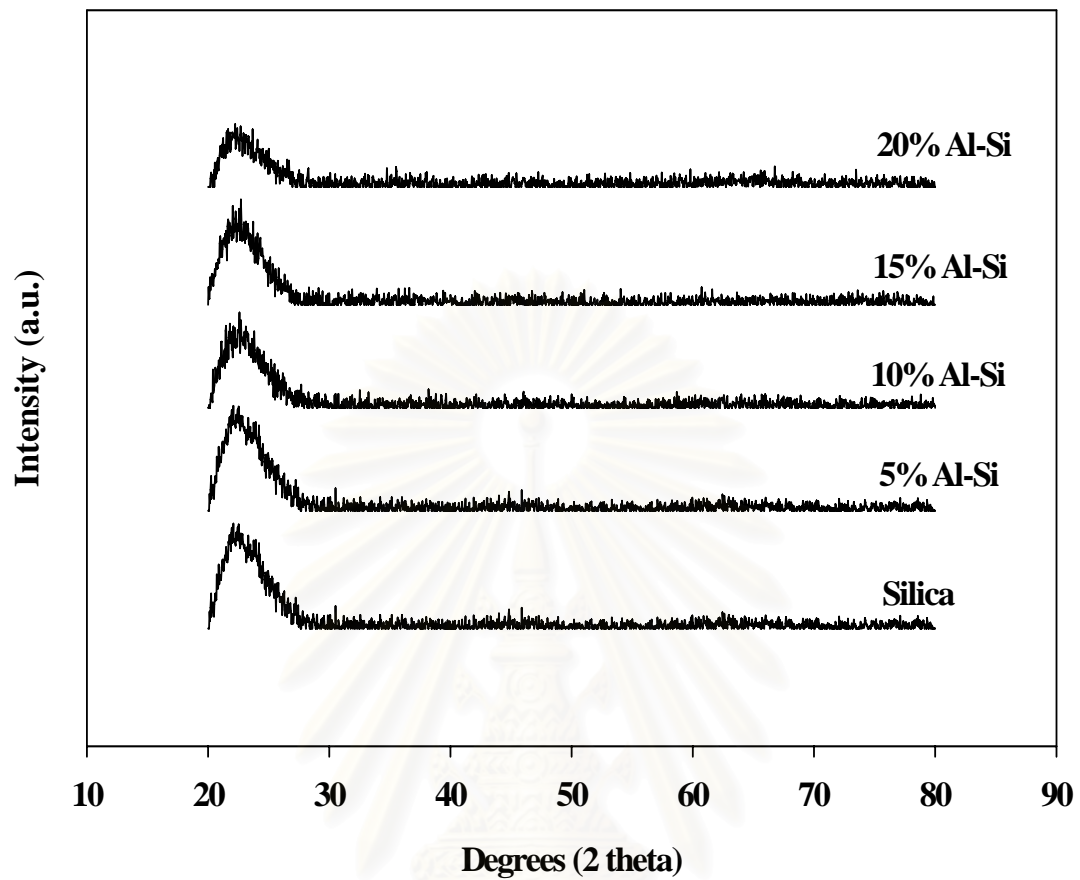


Figure 5.2 XRD pattern for various alumina loading of Al-Si bimodal pore supports.

สถาบันวิทยบริการ
จุฬาลงกรณ์มหาวิทยาลัย

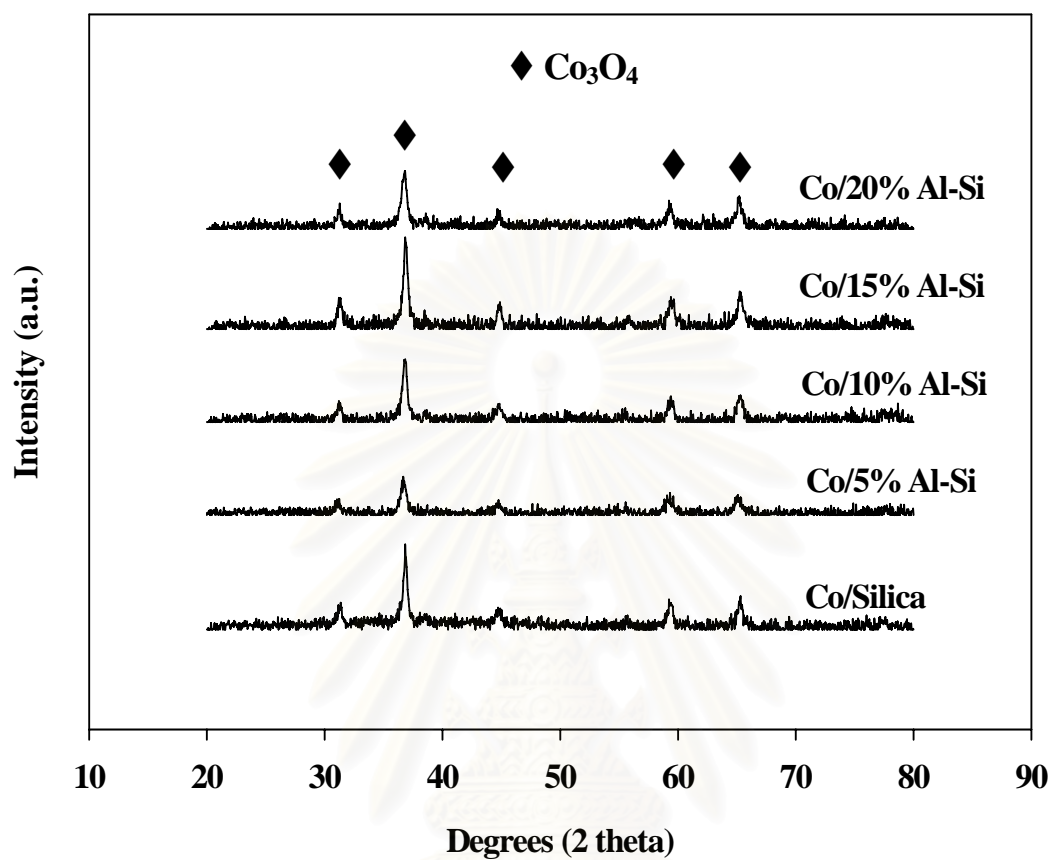


Figure 5.3 XRD pattern of cobalt based catalysts on various alumina loading of Al-Si bimodal pore supports.

สถาบันวิทยบริการ
จุฬาลงกรณ์มหาวิทยาลัย

5.1.3 Scanning electron microscopy (SEM) and Energy dispersive X-ray spectroscopy (EDX)

SEM and EDX were also conducted in order to study the morphologies and elemental distribution of the samples, respectively. The typical SEM micrograph and EDX mapping for silica and 15% Al-Si bimodal pore support are illustrated in **Figure 5.4-5.5** whereas silica and 15% Al-Si bimodal pore supported Co catalyst sample are shown in **Figure 5.6-5.7**. The external surface of catalyst granule is shown in all figures and the light or white patches on the catalyst granule surface represent high concentration of cobalt oxides species on the surface. It can be seen that the distribution of Co on the surface of the bimodal pore support was a slightly better than that of Co on the silica support.

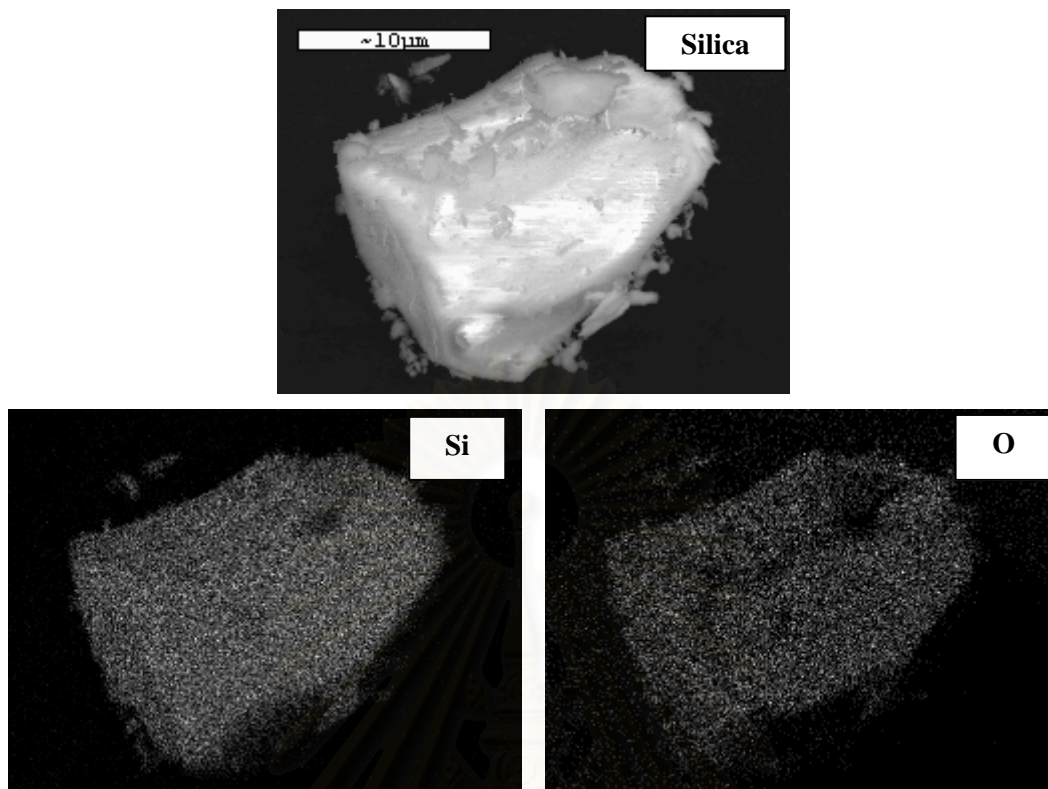


Figure 5.4 SEM micrograph and EDX mapping for silica (Q50) support granule.

สถาบันวิทยบริการ
จุฬาลงกรณ์มหาวิทยาลัย

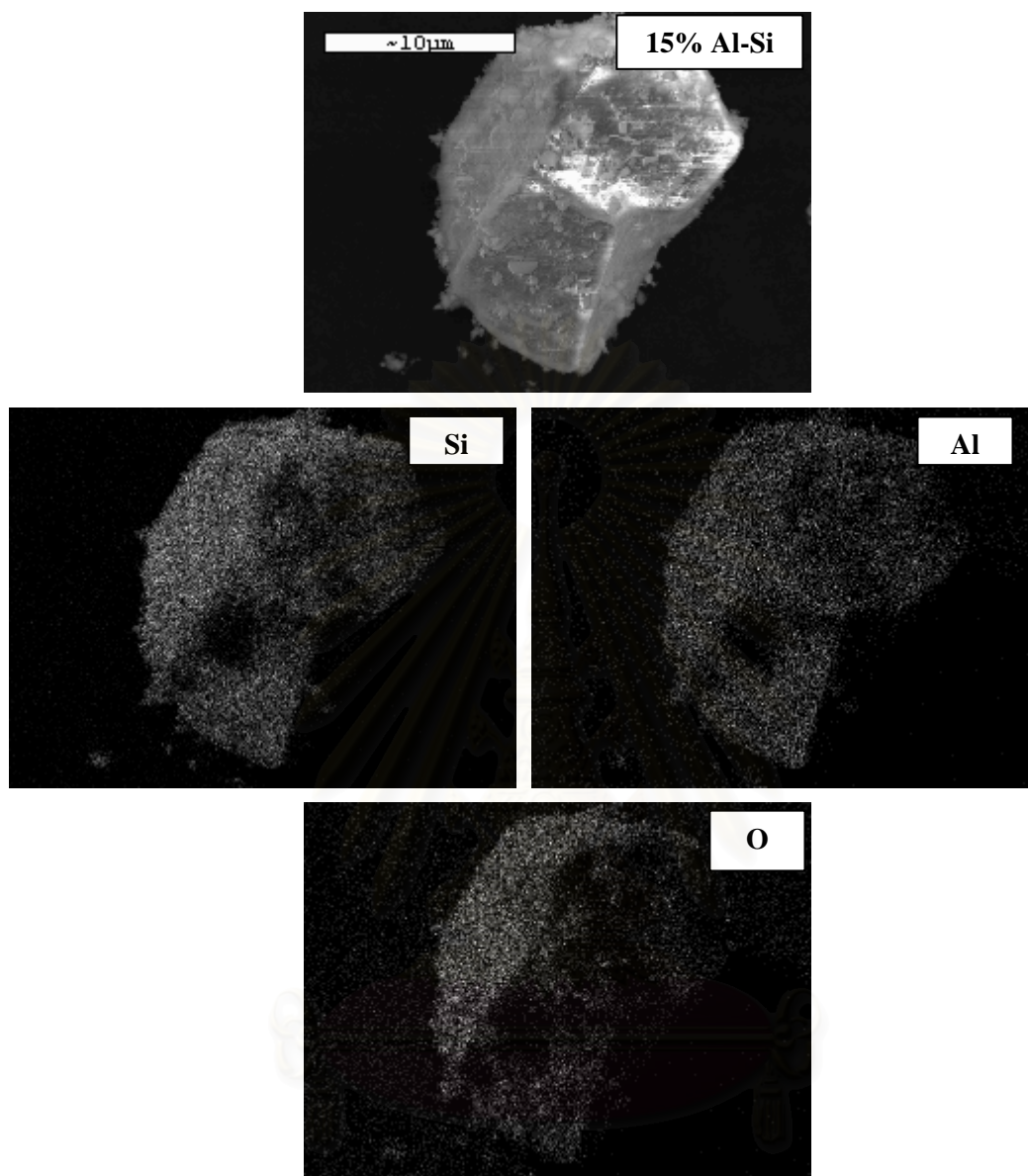


Figure 5.5 SEM micrograph and EDX mapping for 15% Al-Si bimodal pore support granule.

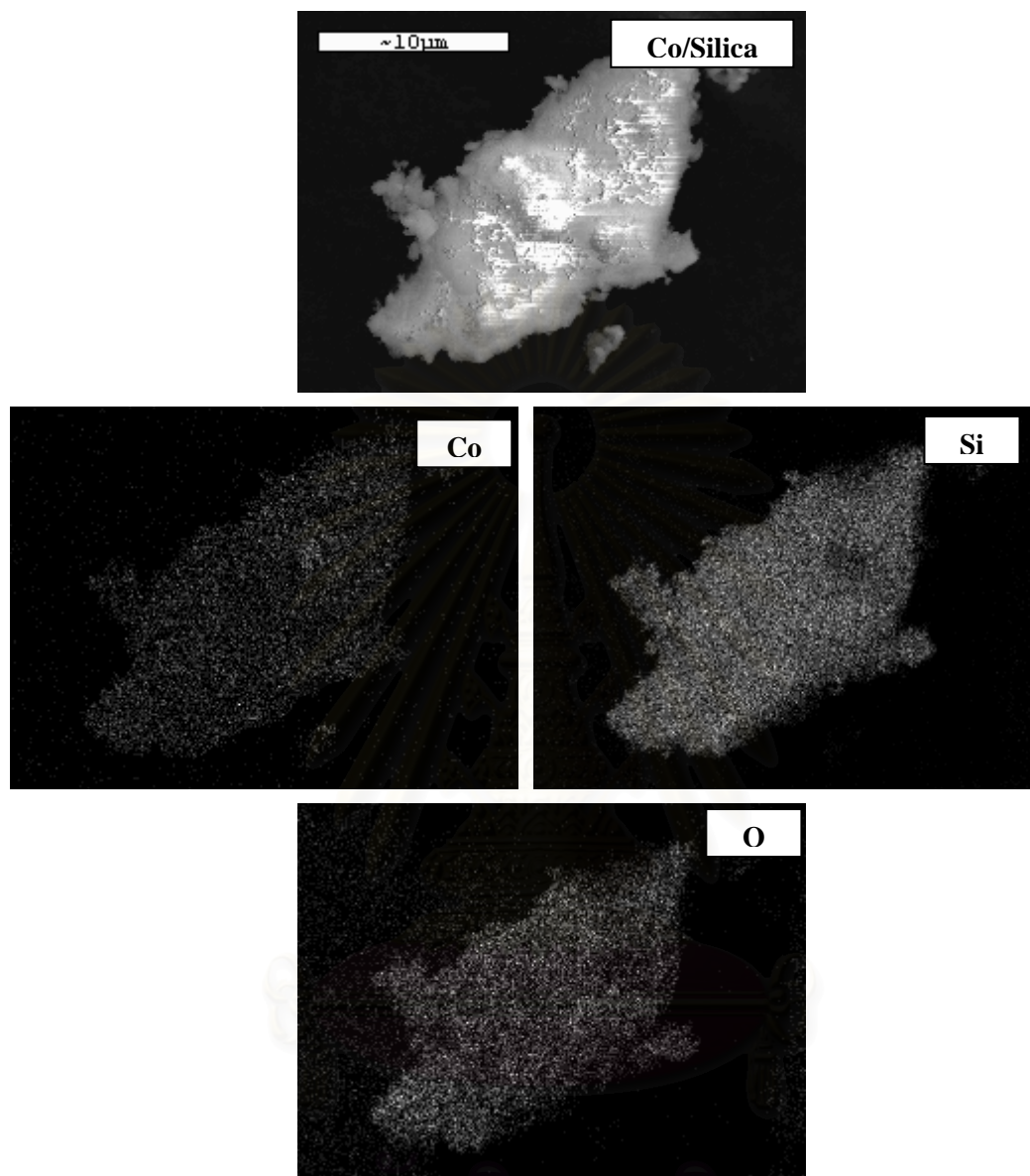


Figure 5.6 SEM micrograph and EDX mapping for Co/Silica catalyst granule.

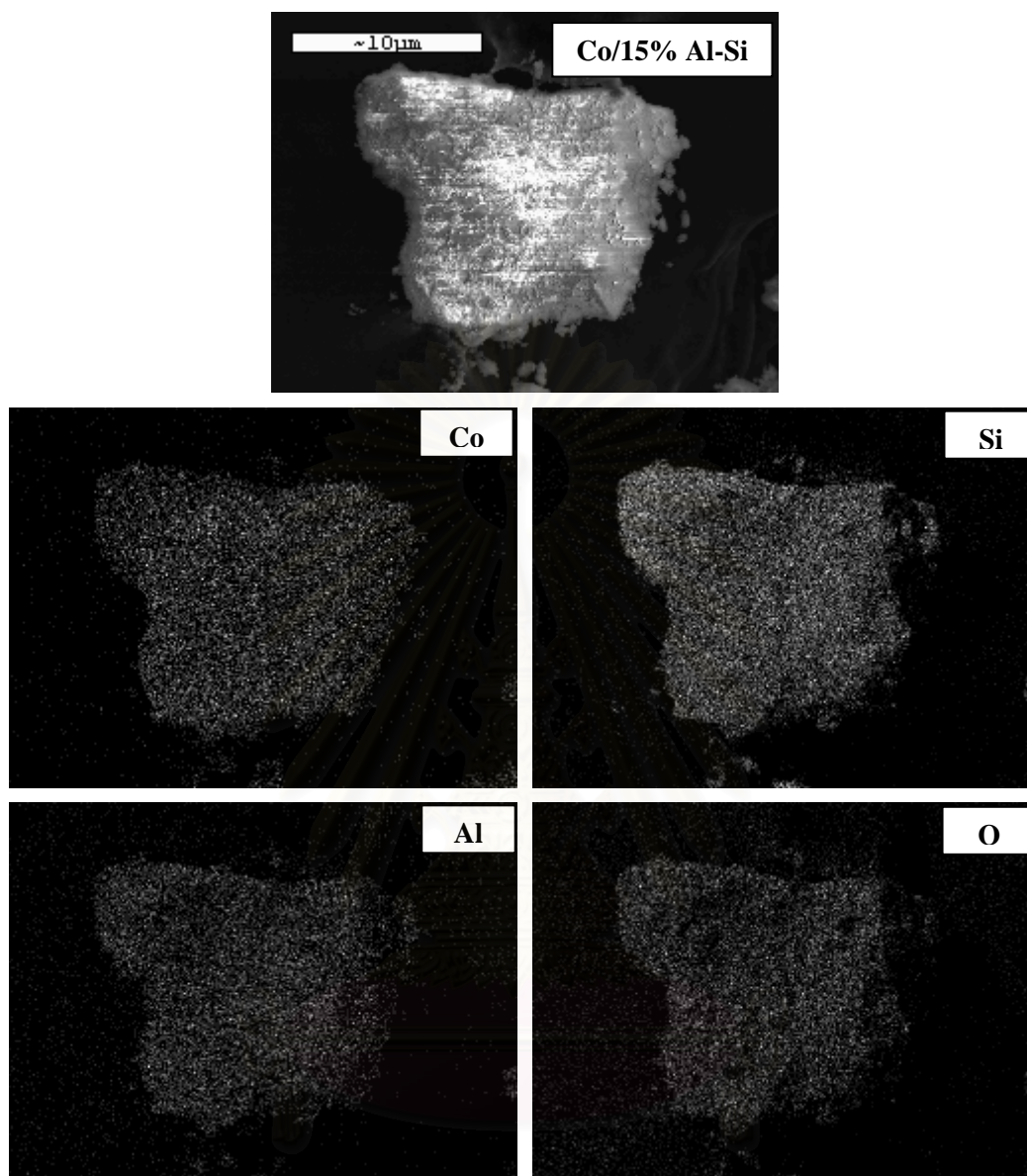


Figure 5.7 SEM micrograph and EDX mapping for Co/15%Al-Si catalyst granule.

สถาบันวิทยบริการ
จุฬาลงกรณ์มหาวิทยาลัย

5.1.4 Transmission Electron Microscopy (TEM)

In order to determine the dispersion and crystallite size of Co oxides species dispersed on the supports employed, the high resolution TEM was used. The TEM micrographs for silica and alumina-silica bimodal pore supports are shown in **Figure 5.8**. As seen in this figure, pore size of silica is 50 nm and pore sizes of all alumina silica bimodal pore support are smaller than the silica support. The TEM micrographs for Co oxides species dispersed on silica supports and alumina-silica bimodal pore supports are shown in **Figure 5.9-5.10**. Apparently, the crystallite size seemed to decrease with alumina loading. The Co oxide species on the bimodal pore supports were also well dispersed having the crystallite size of 18 to 22 nm. It can be seen that the crystallite size of Co oxide species on the bimodal pore supports was smaller than that on the silica supports indicating less agglomeration of Co oxide species.



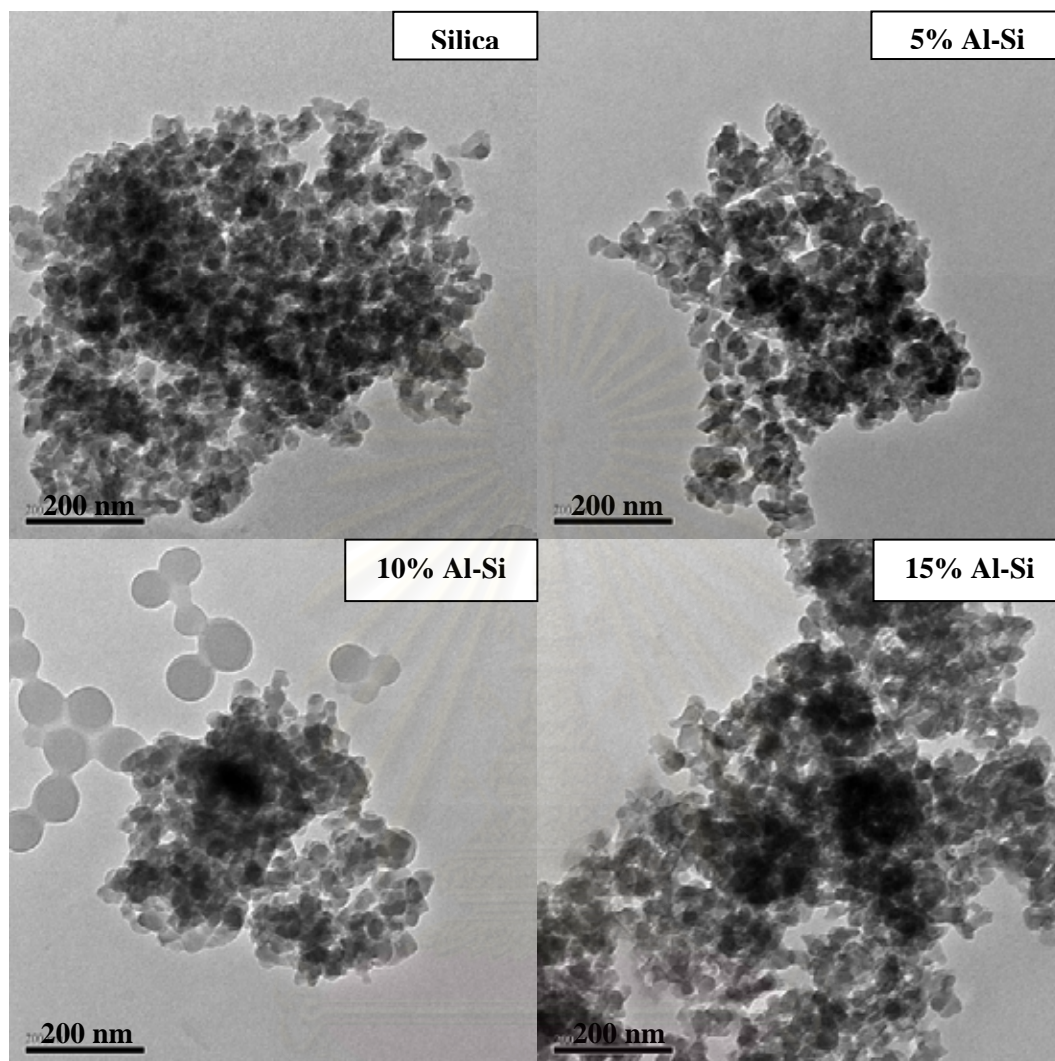


Figure 5.8 TEM micrographs of silica (Q-50), 5% Al-Si, 10% Al-Si and 15% Al-Si bimodal pore supports.

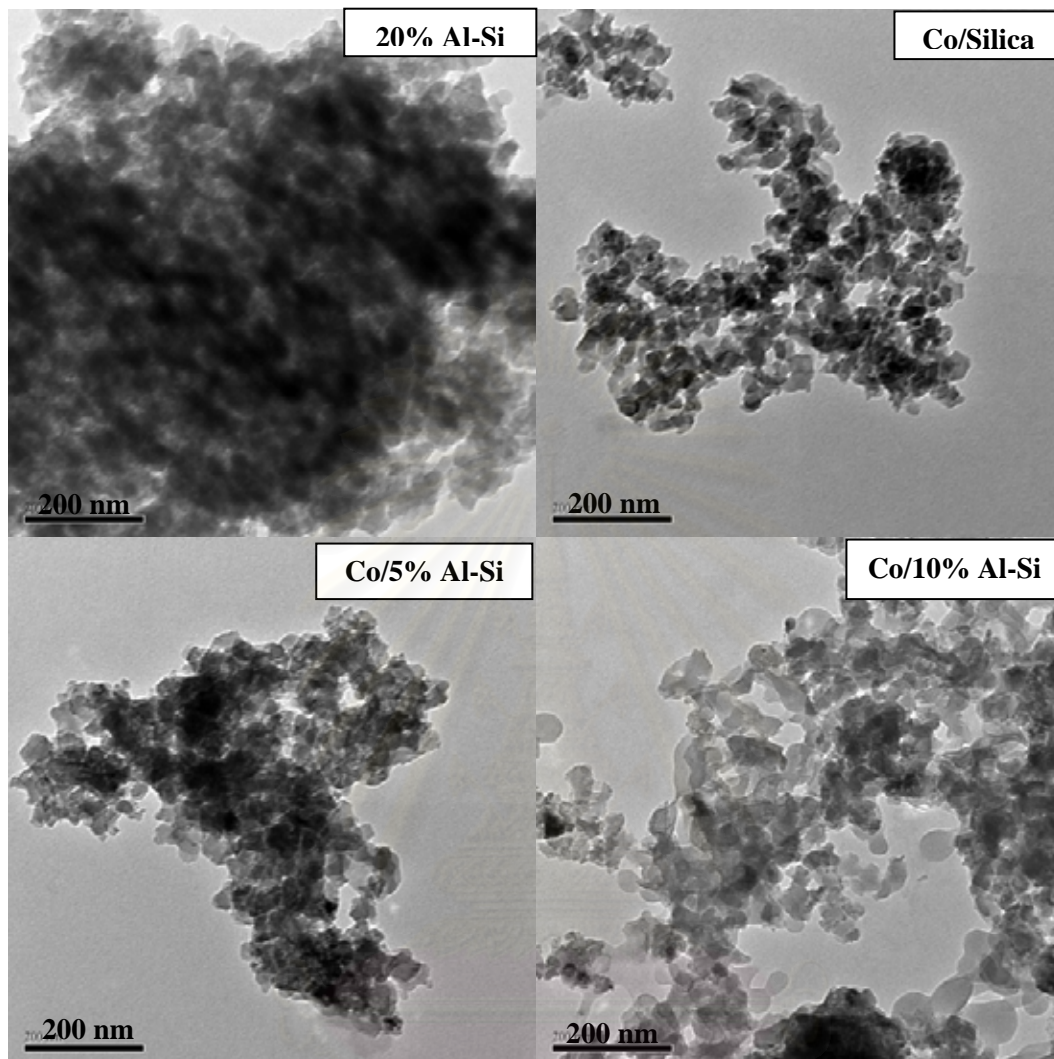


Figure 5.9 TEM micrographs of 20% Al-Si bimodal pore supports, silica supported Co catalyst, 5% Al-Si bimodal pore supported Co catalyst and 10% Al-Si bimodal pore supported Co catalyst structure.

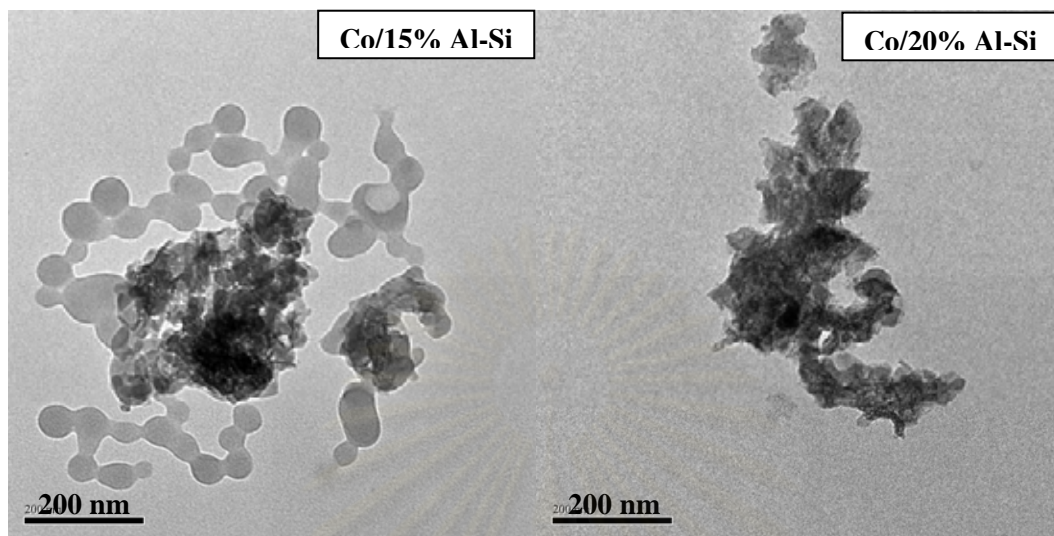


Figure 5.10 TEM micrographs of 15% Al-Si bimodal pore supported Co catalyst and 20% Al-Si bimodal pore supported Co catalyst structure.

สถาบันวิทยบริการ
จุฬาลงกรณ์มหาวิทยาลัย

5.1.5 Temperature programmed reduction (TPR)

As mentioned, TPR was performed in order to determine the reduction behaviors of Co oxides species on various samples. TPR profiles for Co catalysts with various alumina loading of Al-Si bimodal pore supports used are shown in **Figure 5.11**. Basically, only two reduction peaks can be observed. The peaks can be assigned to the two-step reduction of Co_3O_4 to CoO and then to Co^0 [25]. Upon the TPR conditions, the two reduction peaks based on two-step reduction may or may not be observed. For the Silica supported Co catalyst, a TPR peak located at 350-800°C. However, this reduction peak was dramatically shifted about 50-80°C lower for all alumina-silica bimodal pore supported Co catalysts. This suggests that presence of alumina in bimodal pore support can facilitate the reduction process of cobalt oxide species leading to reduction at a lower temperature.

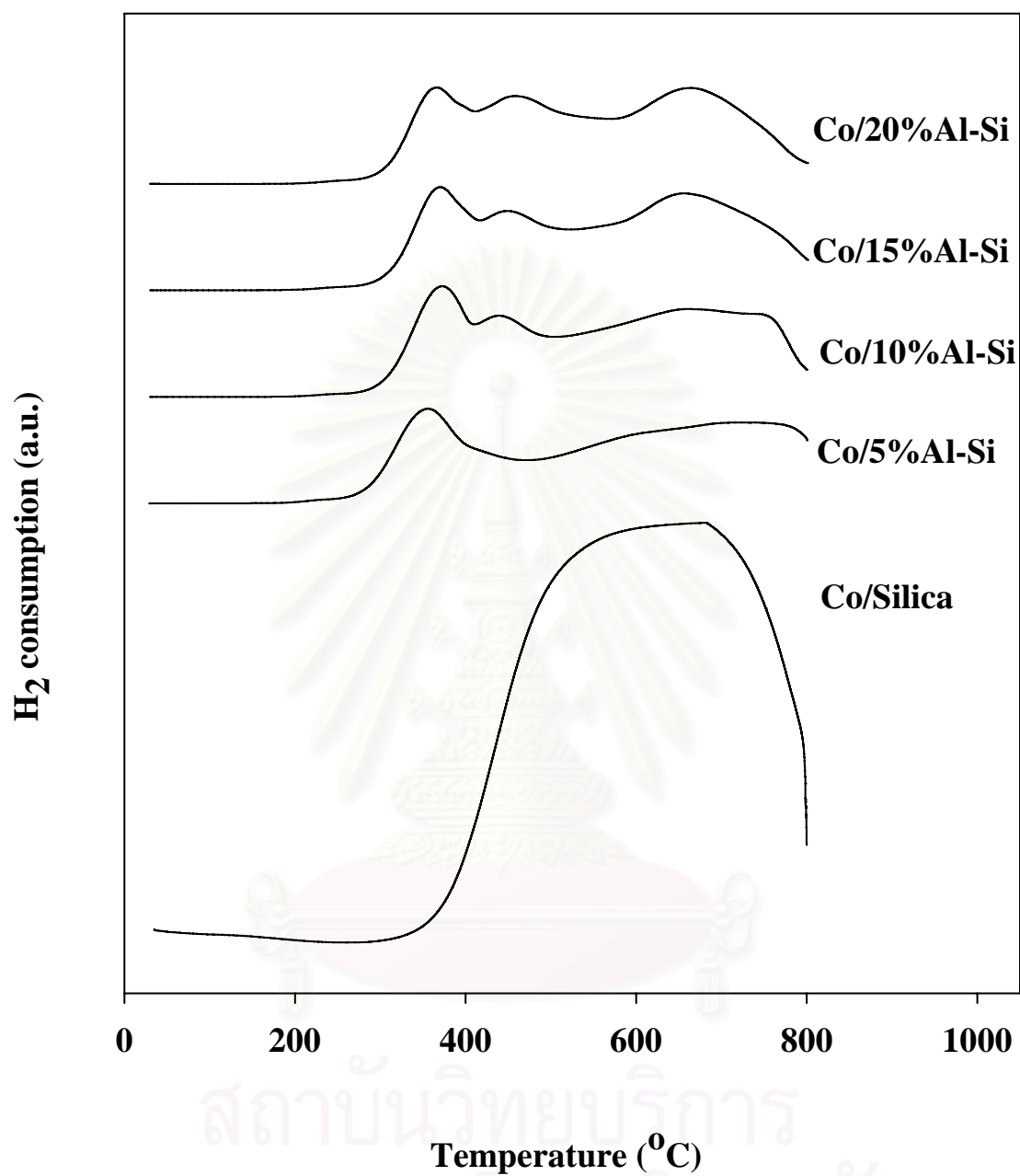


Figure 5.11 TPR profiles for Co catalysts with various alumina loading of Al-Si bimodal pore supports used.

5.1.6 H₂ chemisorption

The resulted H₂ chemisorption is illustrated in **Table 5.3**. The amounts of H₂ adsorbed on the catalytic phase were in the range of 0.44 - 3.19 $\mu\text{mol/g}$ of sample. The dispersion of Co was 2.58-18.81% upon increasing the amount of Al loading in the alumina-silica bimodal supports. The H₂ adsorbed increased with increasing the amounts of alumina loading. The silica supported Co catalyst shows the lowest amount of H₂ adsorbed, and the 20 wt% of alumina on alumina-silica supported Co catalyst shown the highest amount of H₂ adsorbed. It was found that the number of the reduced cobalt metal surface atoms was the largest for the cobalt dispersed on the 20 wt% of alumina on alumina-silica support (Co/20%Al-Si).

5.1.7 Reaction study in CO hydrogenation

The reaction study results are listed in **Table 5.3**. It can be seen that for the silica supported catalyst it exhibited the lowest activity among other catalysts. In fact, activities 3-5 times increased with increasing the amounts of alumina loading in the alumina-silica bimodal support. As known, upon the methanation, the majority of the product is methane. However, considering the selectivity, it can be observed that the selectivity to C₂-C₄ products apparently did not change with the alumina loading. The effect of alumina loading for the alumina-silica bimodal pore supports on the activities and selectivity is also listed in **Table 5.3**.

Table 5.3 Results of H₂ chemisorption, Cobalt dispersion, steady state rate and selectivity to products

Catalyst sample	Total H ₂ chemisorption (μmol/g cat)	Metal dispersion (%)	Steady state Rate (x10 ² gCH ₂ /gcat.h)		Selectivity to CH ₄ (%)	
			Initial ^a	Steady state ^b	Initial ^a	Steady state ^b
Co/silica	0.44	2.58	15.1	8.8	99.7	99.0
Co/5% Al-Si	0.78	4.60	27.3	24.4	99.9	99.9
Co/10% Al-Si	0.91	5.36	29.5	29.7	99.8	99.7
Co/15% Al-Si	1.35	7.97	29.5	32.5	99.6	99.7
Co/20% Al-Si	3.19	18.81	36.8	37.0	99.9	99.9

^a CO hydrogenation was carried out at 220°C, 1 atm and H₂/CO/Ar = 20/2/8.

The steady-state was reached after 5 min of reaction.

^b After 6 h of reaction.

5.2 Various Co precursors of silica and 15%Al-Si bimodal pore supported catalyst.

5.2.1 BET surface area

Table 5.4 BET surface area, average pore diameter and pore volume of various Co precursors

Sample	BET Surface area (m ² /g)	Average small pore diameter (nm)	Average large pore diameter (nm)	Pore volume (cm ³ /g)	Co Crystallize size (nm)
CoN/SiO ₂	54	-	48.1	0.249	28.9
CoAT/SiO ₂	56	-	52.0	0.233	24.8
CoAA/SiO ₂	64	-	50.0	0.301	22.8
CoCl/SiO ₂	44	-	50.3	0.212	84.5
CoN/15%Al-Si	81	2.9	26.9	0.314	18.9
CoAT/15%Al-Si	114	2.9	24.7	0.380	11.7
CoAA/15%Al-Si	97	4.9	53.7	0.301	15.7
CoCl/15%Al-Si	76	2.9	25.7	0.301	53.1

The BET surface areas for the catalyst samples are given in **Table 5.4**. The pure silica support before cobalt impregnation had the surface area of 72 m²/g. The surface areas of the cobalt catalysts prepared with different cobalt precursors were found to be in the range of 44-64 m²/g and in the order of CoAA/SiO₂ > CoAT/SiO₂ > CoN/SiO₂ > CoCl/SiO₂. The alumina-silica bimodal pore support had surface areas of 151 m²/g. After cobalt impregnation, the surface areas of the cobalt catalysts prepared with different cobalt precursors were found to be in the range of 76-114 m²/g and in the order of CoAT/15%Al-Si > CoAA/15%Al-Si > CoN/15%Al-

Si > CoCl/15%Al-Si. The significant decrease in surface areas of the original support materials was due to cobalt deposition in the pores of silica and alumina. However, all the Al-Si bimodal pore-supported Co catalysts exhibited higher surface areas than those of silica-supported Co catalysts prepared upon all cobalt precursors employed.

5.2.2 X-ray diffraction (XRD)

The XRD patterns of the silica and Al-Si bimodal pore supported Co catalyst of different Co precursors are shown in **Figure 5.12**, all calcined samples exhibited XRD peaks at 31° (weak), 37° (strong), 45° (weak), 60° (weak) and 65° (weak), which were assigned to the presence of Co_3O_4 . This indicated that the Co_3O_4 formed was highly dispersed on all catalyst samples. For CoAA/ SiO_2 , the average cobalt oxide crystallite sizes calculated using the Scherrer's equation was found to be 22.8 nm as shown in **Table 5.4**. Using CoAA resulted in the smallest cobalt particle size among other cobalt precursor for silica support. For CoAT/15%Al-Si and CoAA/15%Al-Si, the average cobalt oxide crystallite sizes were smallest among other catalysts similar to what has been suggested for Co/MCM-41 prepared from CoAA and CoAT (J. Panpranot *et al*, 2003)

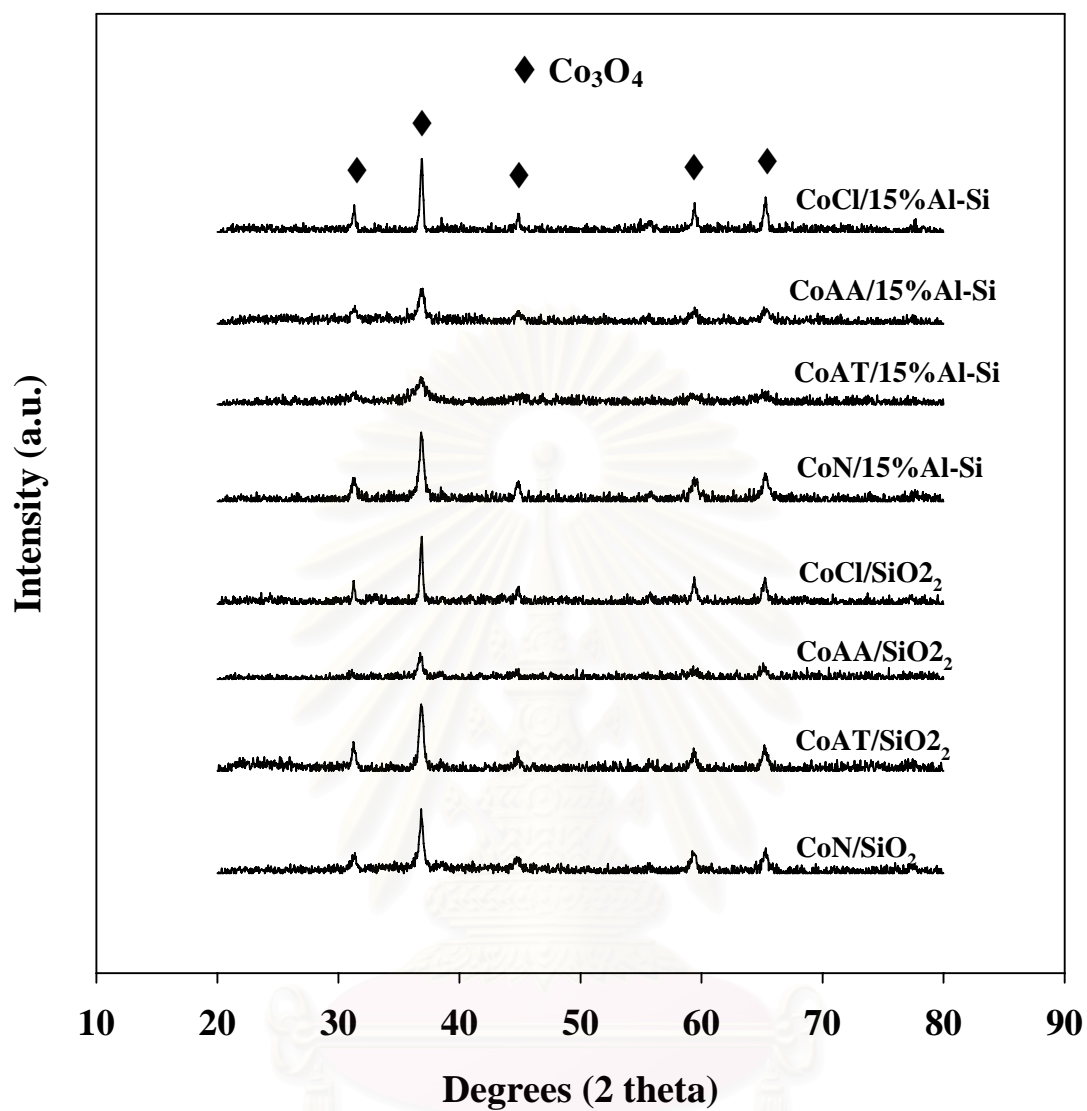


Figure 5.12 XRD pattern of cobalt based catalysts on various cobalt precursors

5.2.3 Scanning electron microscopy (SEM) and Energy dispersive X-ray spectroscopy (EDX)

SEM and EDX were also conducted in order to study the morphologies and elemental distribution of the samples, respectively. The typical SEM micrographs along with the EDX mapping (for Co, Si, and O) of the different Co precursors of silica-supported Co catalysts are illustrated in **Figures 5.13-5.16** for CoN/SiO₂, CoAT/SiO₂, CoAA/SiO₂, and CoCl/SiO₂ samples, respectively. It can be observed that Co oxide species obtained from CoN, CoAA and CoAT were well distributed all over the catalyst granule. However, it was obvious that the use of CoCl as the Co precursor resulted in very poor dispersion of Co oxide species on SiO₂ as seen in **Figure 5.16**. The typical SEM micrograph along with the EDX mapping (for Co, Si, Al and O) of the different Co precursors of 15% Al-Si bimodal pore-supported Co catalysts are illustrated in **Figures 5.17-5.20** for CoN/15% Al-Si, CoAT/15% Al-Si, CoAA/15% Al-Si, and CoCl/15% Al-Si samples, respectively, indicating the external surface of the sample granule. It can be seen that the Co oxide species obtained from all Co precursors were well distributed (shown on EDX mapping) all over the sample granule. It can be seen that the distribution of Co on the surface of the bimodal pore support were a slightly better than that of Co on the silica support for all different Co precursors.

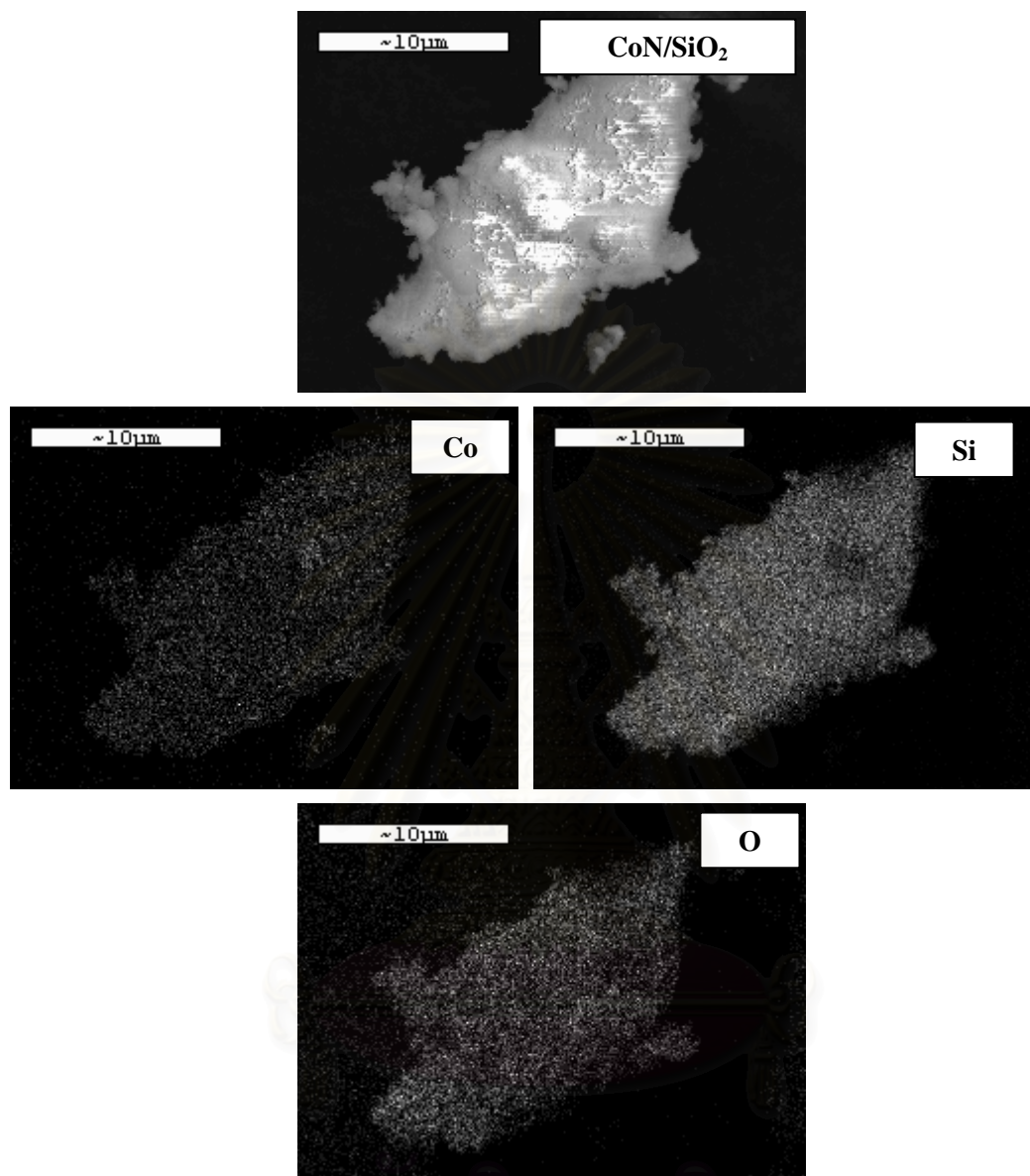


Figure 5.13 SEM micrograph and EDX mapping for CoN/SiO₂ catalyst granule.

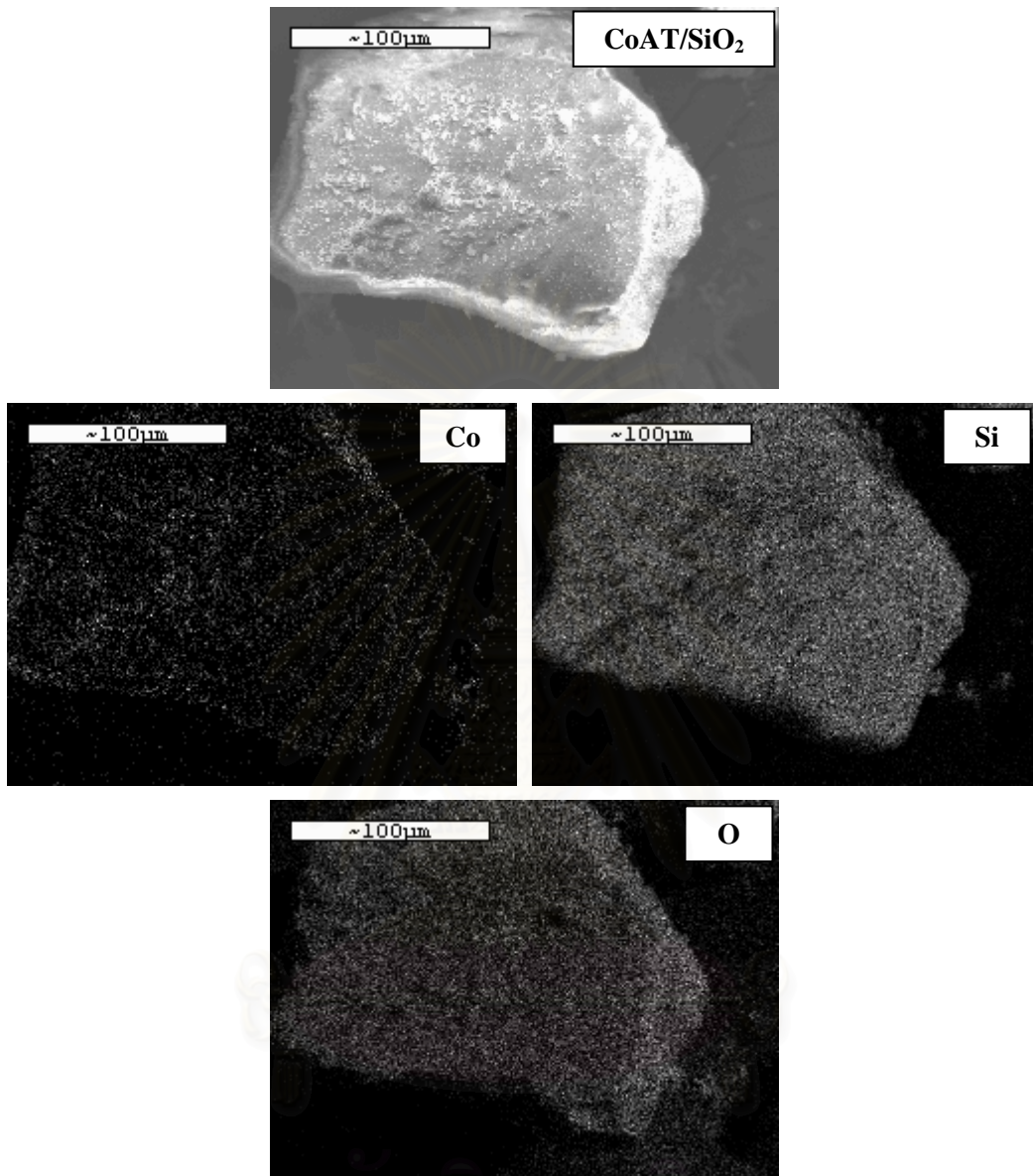


Figure 5.14 SEM micrograph and EDX mapping for CoAT/SiO₂ catalyst granule.

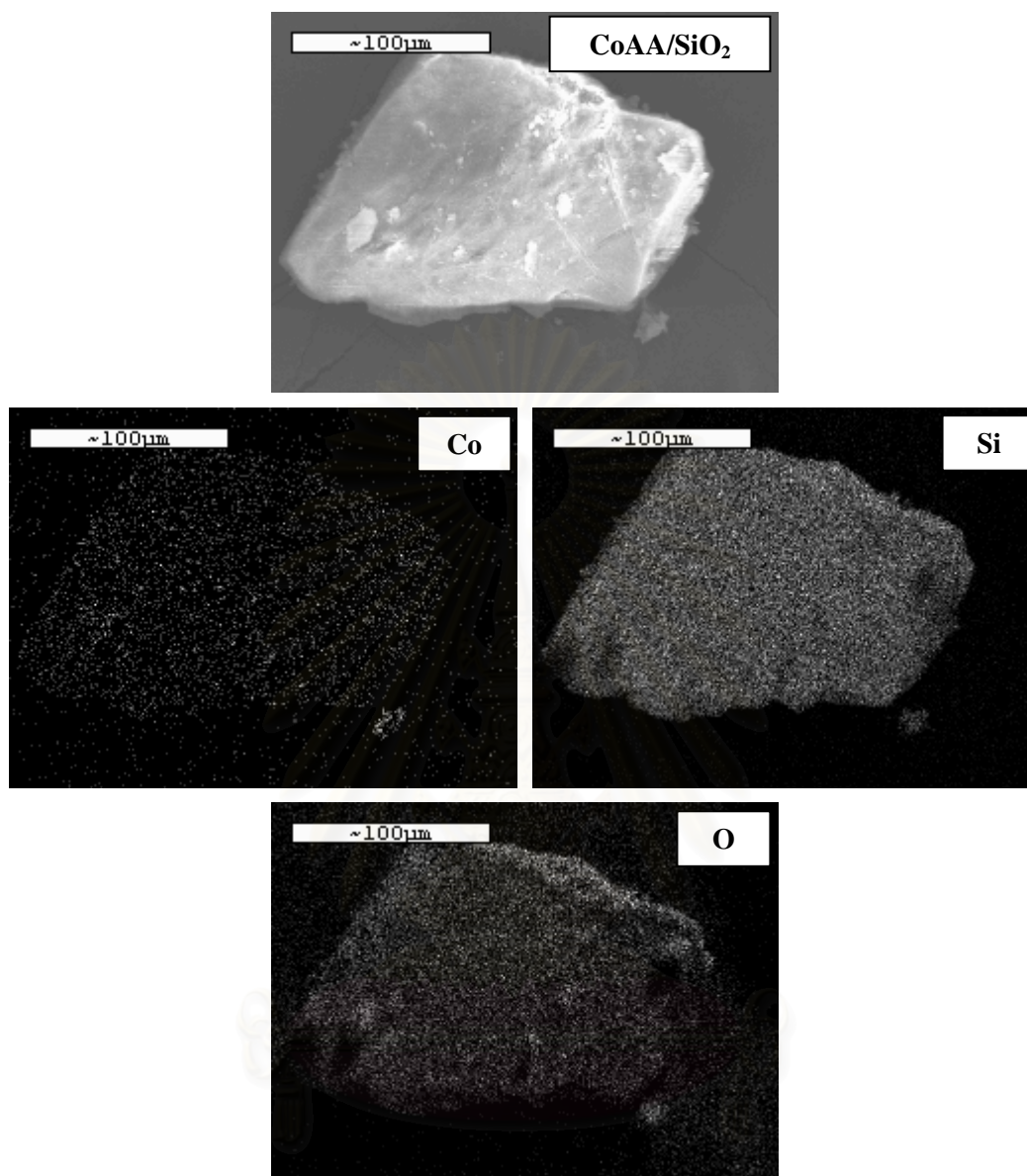


Figure 5.15 SEM micrograph and EDX mapping for CoAA/SiO₂ catalyst granule.

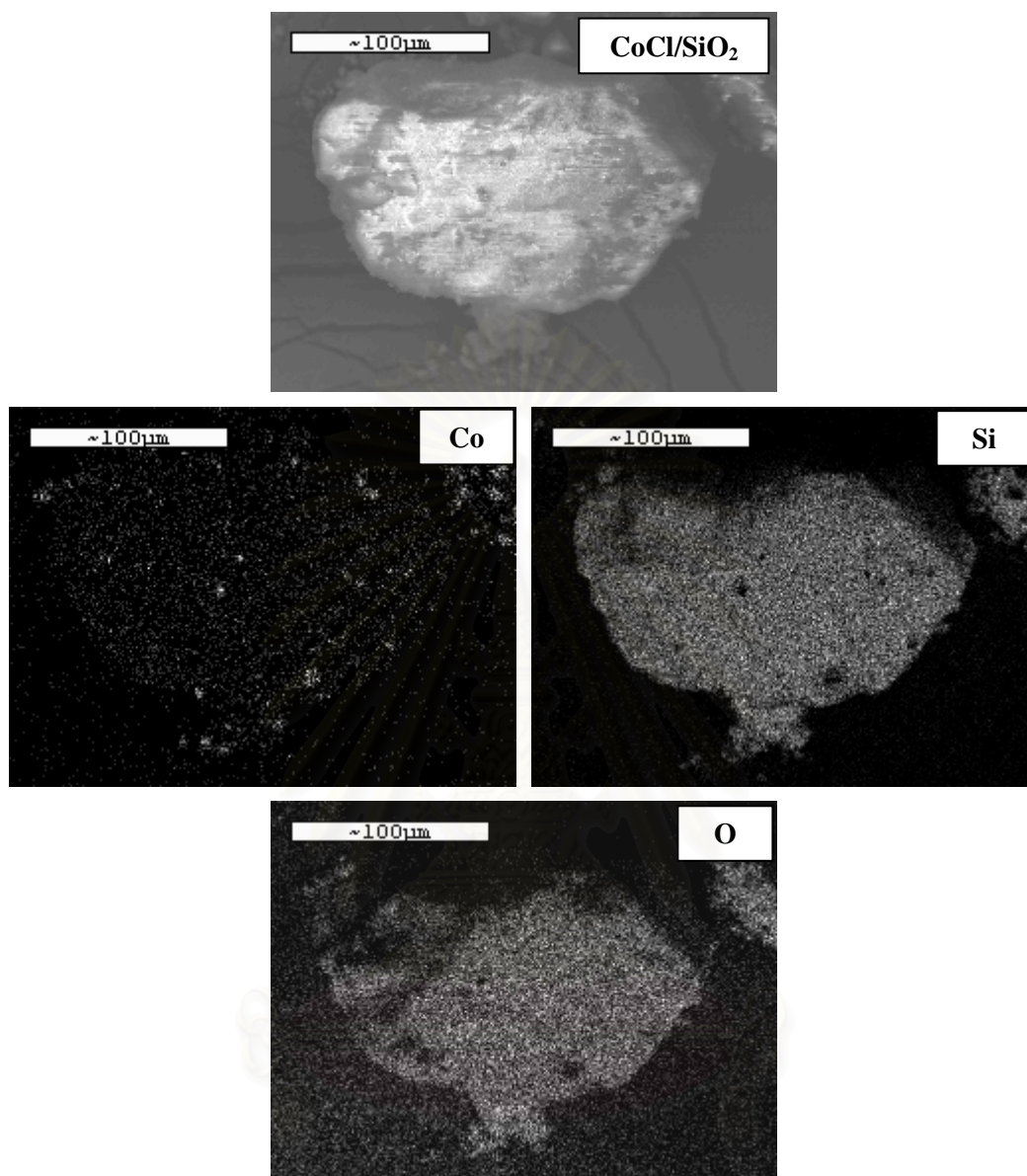


Figure 5.16 SEM micrograph and EDX mapping for CoCl/SiO₂ catalyst granule.

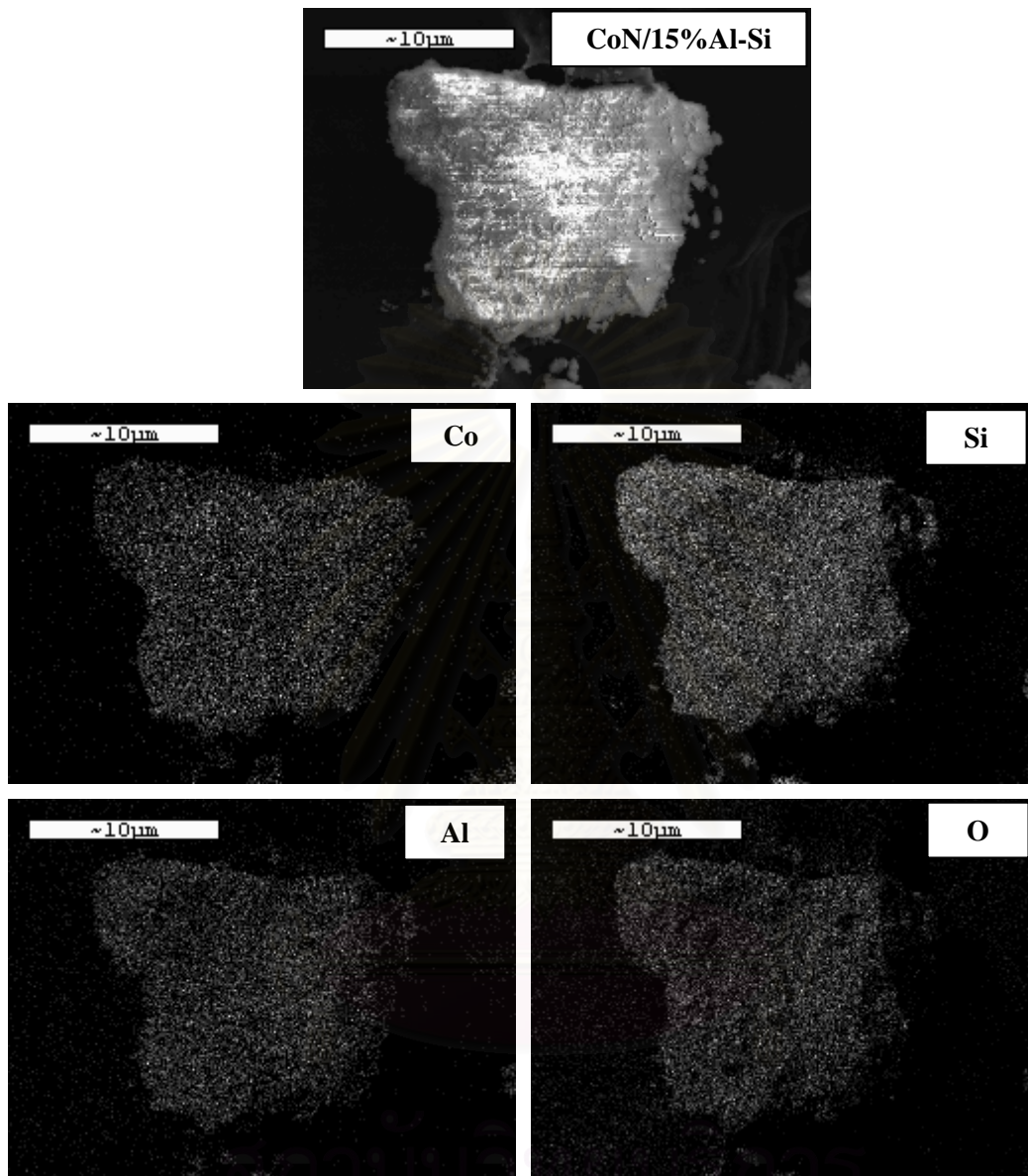


Figure 5.17 SEM micrograph and EDX mapping for CoN/15%Al-Si catalyst granule.

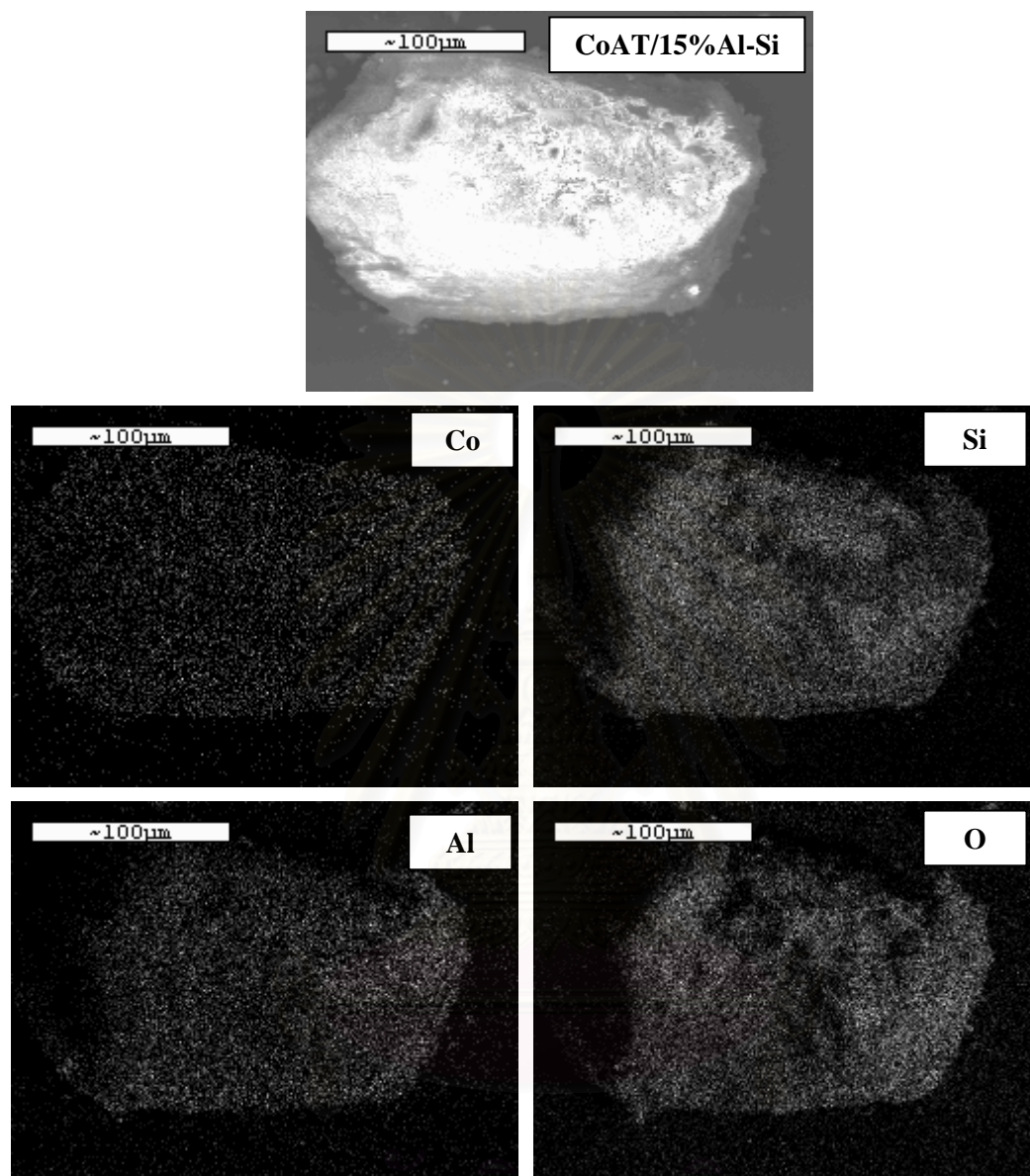
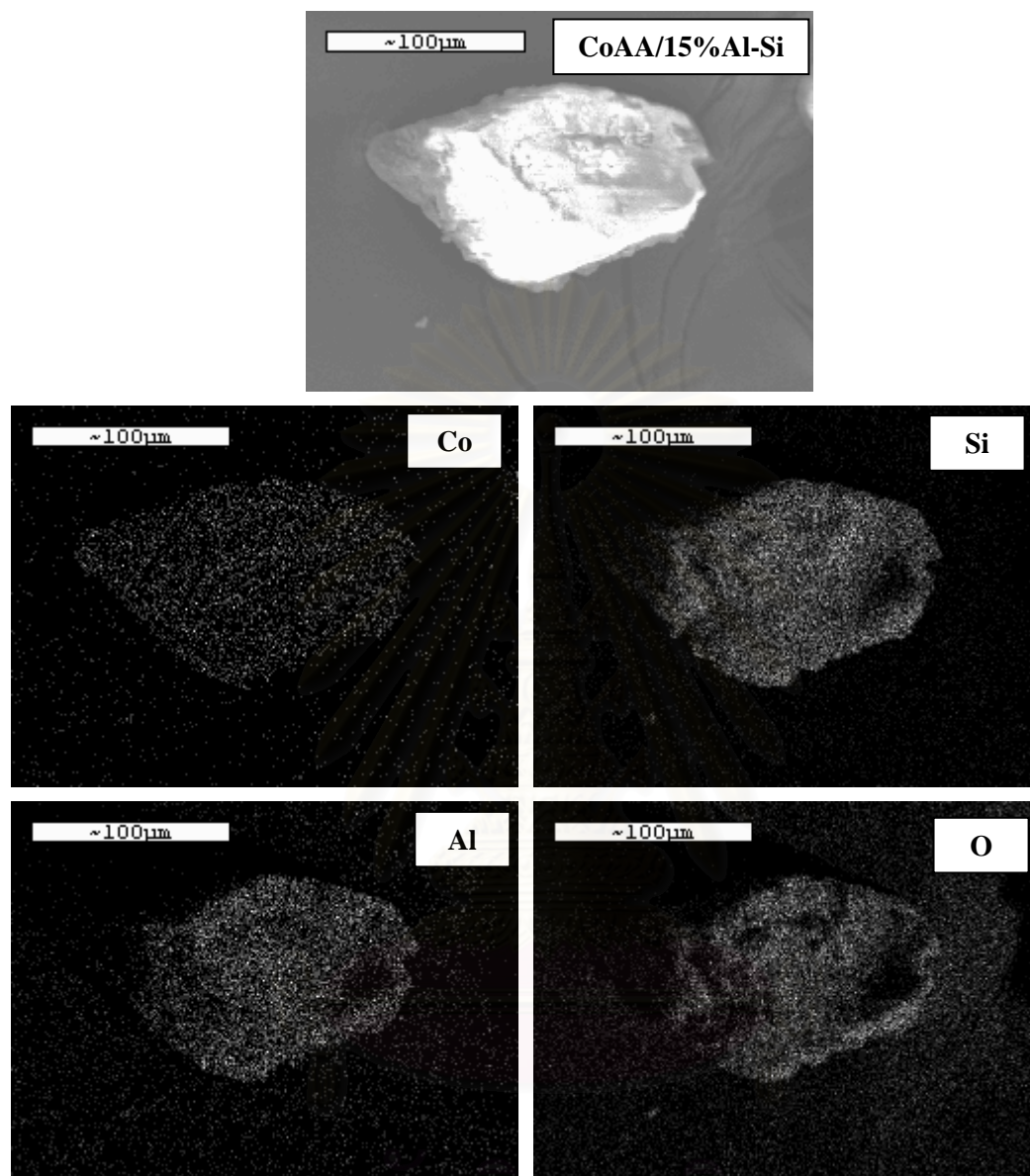


Figure 5.18 SEM micrograph and EDX mapping for CoAT/15%Al-Si catalyst granule.



สถาบันวิทยบริการ
จุฬาลงกรณ์มหาวิทยาลัย

Figure 5.19 SEM micrograph and EDX mapping for CoAA/15%Al-Si catalyst granule.

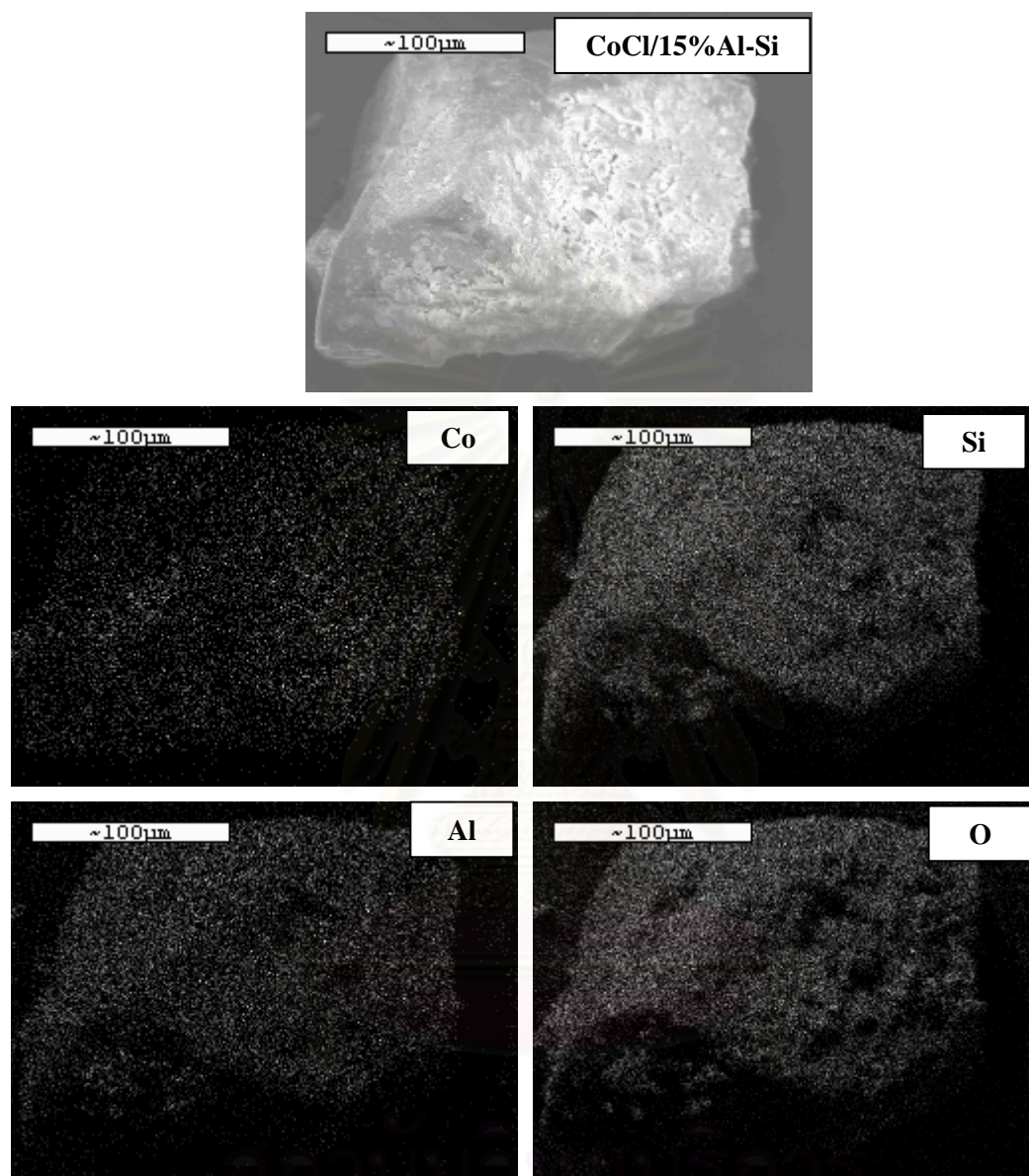


Figure 5.20 SEM micrograph and EDX mapping for CoCl/15%Al-Si catalyst granule.

5.2.4 Transmission Electron Microscopy (TEM)

TEM was conducted in order to identify the crystallite size and dispersion of Co oxide species for using different Co precursors on the various supports. The TEM micrographs for using different Co precursors for Co oxides species dispersed on silica supports are shown in **Figure 5.21** whereas those for 15% Al-Si bimodal pore supports are shown in **Figure 5.22**. Apparently, the crystallite size seemed to decrease with using bimodal pore support. The Co oxide species for using different Co precursors on the bimodal pore supports were also well dispersed having the crystallite size of 11 to 53 nm. The Co oxide on the silica supports have the crystallite size of 22 to 85 nm. It can be seen that the crystallite size of Co oxide species on the bimodal pore supports was smaller than that on the silica supports indicating less agglomeration of Co oxide species for all different Co precursors, especially, crystallite size of Co oxide species using cobalt chloride as Co precursor decreased from 84.5 nm to 53 nm.

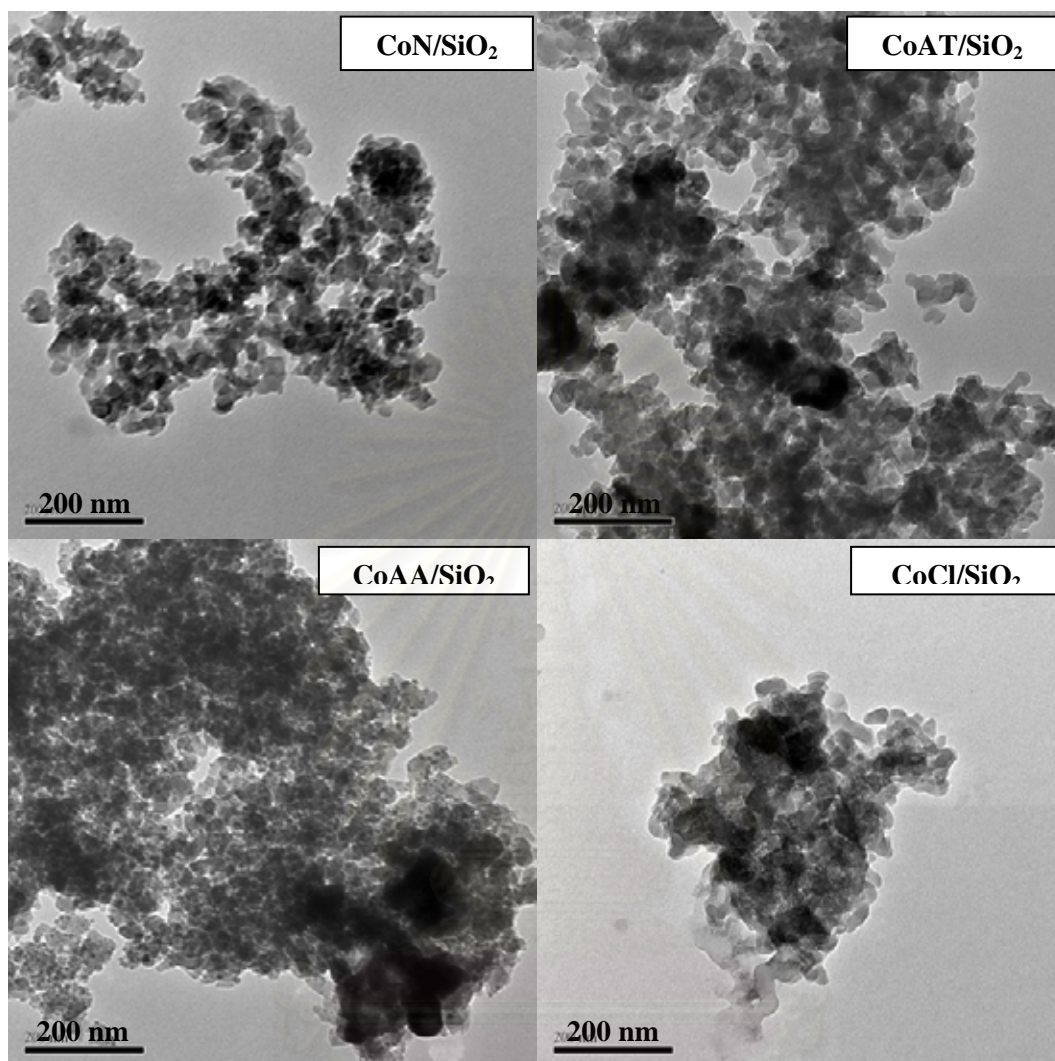


Figure 5.21 TEM micrographs of all cobalt dispersed on silica supports.

สถาบันวิทยบริการ
จุฬาลงกรณ์มหาวิทยาลัย

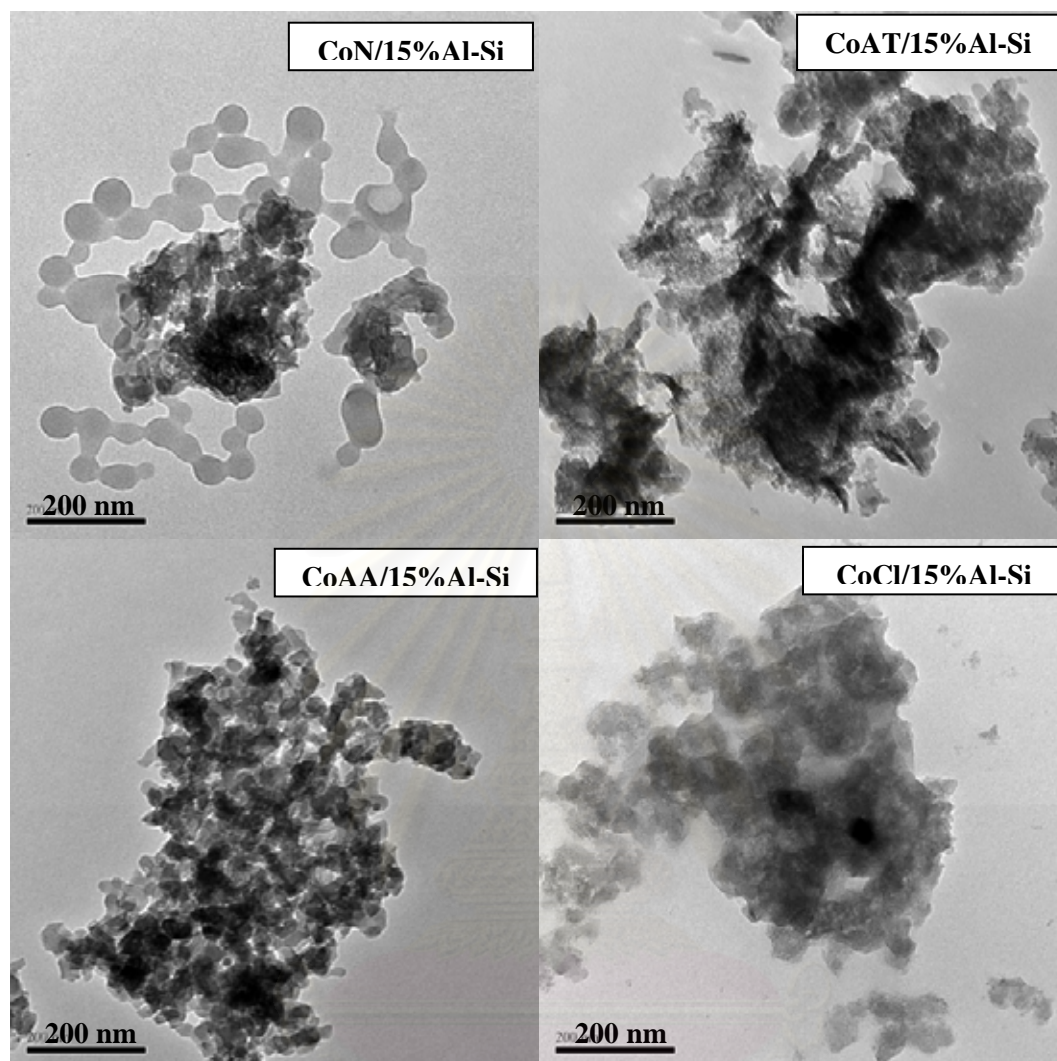


Figure 5.22 TEM micrographs of all cobalt dispersed on 15%Al-Si bimodal pore supports.

5.2.5 Temperature programmed reduction (TPR)

TPR was performed in order to determine the reduction behaviors of Co oxides species on various samples. The TPR profiles for Co catalysts with different Co precursors supported on silica and bimodal pore supports are shown in **Figure 5.23**. Basically, only two reduction peaks can be observed. The peaks can be assigned to the two-step reduction of Co_3O_4 to CoO and then to Co^0 (Y. Zhang *et al.*, 1999; D. Schanke *et al.*, 1995). Upon the TPR conditions, the two reduction peaks based on two-step reduction may or may not be observed. For silica supported cobalt catalysts, the use of CoCl as cobalt precursor has been found to give lowest degree of interaction between Co oxide species, the smaller cobalt particles (see CoAA/SiO_2) at silica surface were easier to be reduced. The use of CoN for silica supported Co catalysts has been found to give highest degree of interaction between Co oxide species, indicating that Co oxide could not be reduced at low temperature. For CoAA or CoAT as cobalt precursors for silica supported Co catalyst has been found to give higher degree of interaction between Co oxide species than that use of cobalt chloride as cobalt precursor.

For Al-Si bimodal pore support, the TPR profiles for use of CoCl as cobalt precursor, it exhibited the similar reduction degree due to cobalt particles size. For use of CoN , CoAA or CoAT as cobalt precursors for Al-Si bimodal pore supported cobalt catalysts exhibited the shift of reduction temperature being lower than that use of these cobalt precursors for silica supported cobalt catalysts.

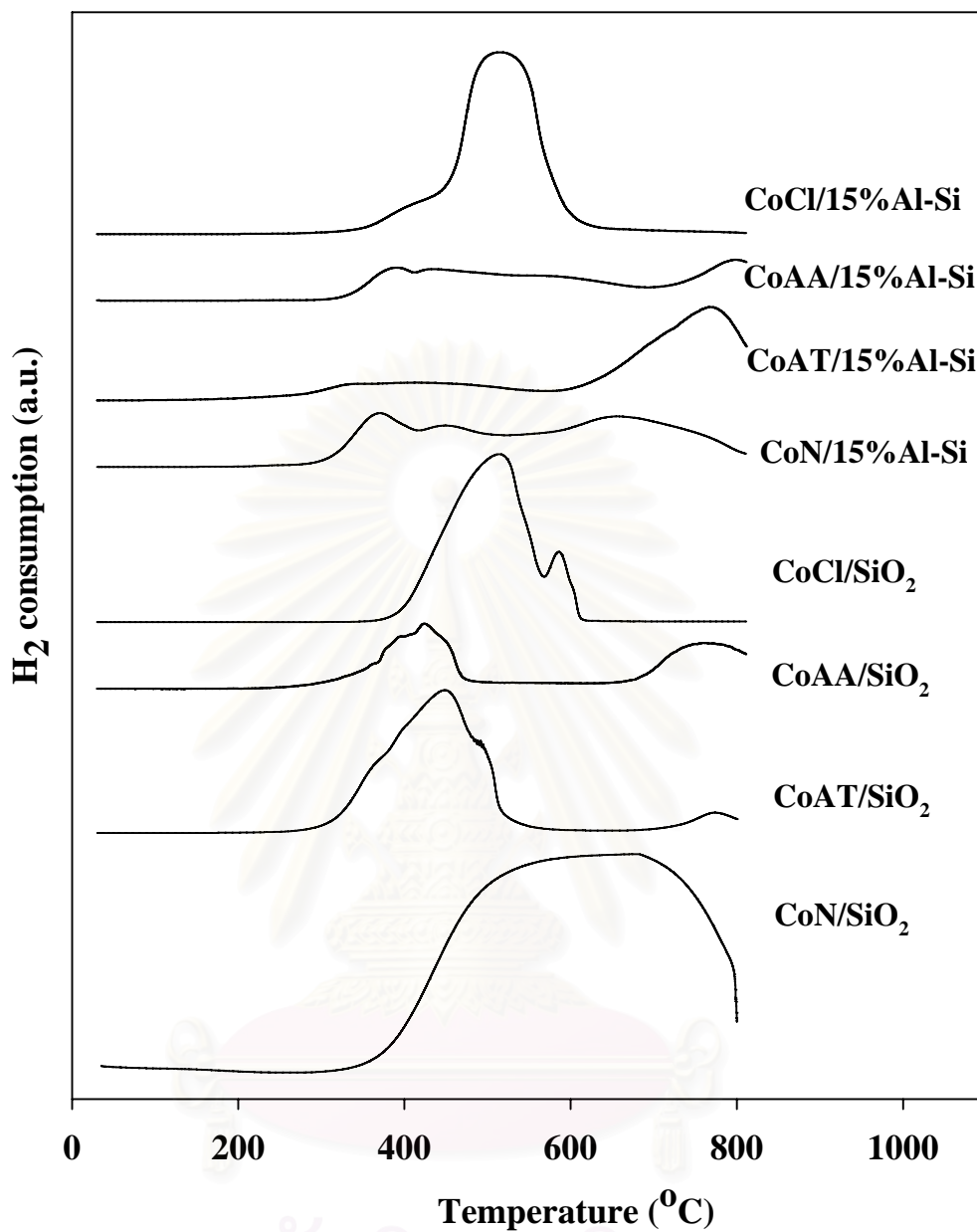


Figure 5.23 TPR profiles for Co catalysts with various Co precursors

5.2.6 Reaction study in CO hydrogenation

The reaction study under CO hydrogenation was also investigated in order to measure the activity and selectivity of catalysts. The reaction study results are listed in **Table 5.5**. It was found that at the reaction conditions used, the use of CoN as cobalt precursors for Al-Si bimodal pore supported cobalt catalysts (CoN/15%Al-Si) exhibited a much higher CO hydrogenation rate than all other catalysts in this study. The use of CoCl for silica and Al-Si bimodal pore supported cobalt catalysts exhibited the lowest activity among other catalysts. For use of CoAT for both types of supported cobalt catalysts resulted in lower activity than that of CoAA.

Table 5.5 Results of steady-state rate and selectivity to products

Catalyst sample	Steady state Rate ($\times 10^2 \text{gCH}_2/\text{gcat.h}$)		Selectivity to CH_4 (%)	
	Initial ^a	Steady state ^b	Initial ^a	Steady state ^b
CoN/SiO ₂	15.1	8.8	99.7	99.0
CoAT/SiO ₂	10.1	9.1	99.6	99.5
CoAA/SiO ₂	22.4	12.9	99.4	99.6
CoCl/SiO ₂	1.1	1.0	94.3	86.1
CoN/15%Al-Si	29.5	32.5	99.6	99.7
CoAT/15%Al-Si	17.7	17.3	98.9	98.9
CoAA/15%Al-Si	29.0	29.9	99.8	99.8
CoCl/15%Al-Si	6.5	5.5	91.1	94.3

^a CO hydrogenation was carried out at 220°C, 1 atm and $\text{H}_2/\text{CO}/\text{Ar} = 20/2/8$.

The steady-state was reached after 5 min of reaction.

^b After 6 h of reaction.

CHAPTER VI

CONCLUSIONS AND RECOMMENDATION

This chapter is focused upon the conclusions of the experimental details of cobalt (Co) catalysts dispersed on various alumina loading in alumina-silica bimodal pore support for carbon monoxide (CO) hydrogenation reaction, and compared with those on the cobalt (Co) catalysts on different cobalt precursors dispersed on alumina-silica bimodal pore support which were described in section 6.1. In addition, recommendations for further study are given in section 6.2.

6.1 Conclusions

6.1.1 Various alumina loading of 20 wt% cobalt on alumina-silica bimodal pore supported catalyst.

The present research showed a dependence of the characteristics and catalytic properties during CO hydrogenation on amounts of alumina loading in alumina-silica bimodal pore supports for Co catalysts. The study revealed that the presence of 20% alumina in bimodal pore support for Co catalyst (Co/20%Al-Si) exhibited the highest activity during CO hydrogenation. It appeared that the alumina-silica bimodal pore supports resulted in increased activities based on CO hydrogenation when increased the amount of alumina loading due to increase in Co dispersion. It indicated that the increased activities were caused by lower degree of interaction between the Co oxide species. However, it was found that the selectivity to C₂-C₄ products did not change at high alumina loading under methanation condition.

6.1.2 Various Co precursors of silica and 15%Al-Si bimodal pore supported catalyst.

The cobalt catalysts prepared by Al-Si bimodal pore support exhibited higher activity than those prepared by silica support with any change in product distribution upon methanation. Use of cobalt nitrate, cobalt acetate tetrahydrate or cobalt acetylacetonate as the cobalt precursors resulted in small cobalt particles distributed uniformly throughout the pore of supports. Pronouncedly large cobalt particles were evident on cobalt catalyst prepared from cobalt chloride. Thus, the lowest CO hydrogenation activity for using cobalt chloride as the cobalt precursor for both support types was observed. In this study, cobalt nitrate seemed to be the best cobalt precursor for preparing Al-Si bimodal pore-supported cobalt catalyst for CO hydrogenation, whereas using cobalt acetylacetonate resulted in the highest activity among other cobalt precursor for silica support.

6.2 Recommendations

1. In order investigation on different interactions, the amounts of Co loading should be varied to use in the alumina-silica bimodal pore supports.
2. Besides Co metal, other metals such as Ni, Pd, Fe and etc should be further investigated with alumina-silica bimodal pore supports.

REFERENCES

- Ali, S., Chen, B., and Goodwin, Jr., J.G. Zr promotion of Co/SiO₂ for Fisher-Tropsch Synthesis. J. Catal. 157 (1995): 35-41.
- Choi, J.G. Reduction of support cobalt catalysts by hydrogen. Catal Lett. 35 (1995): 291-296.
- Curtis, V., Nicolaidis, C.P., Coville, N.J., Hildebrandt, D., Glasser, D. The effect of sulfur on supported cobalt Fischer-Tropsch catalysts. Catal. Today 49 (1999): 33-40.
- Dalai, A.K., Das, T.K., Chaudhari, K.V., Jacobs, G., Davis, B.H. Fischer-Tropsch synthesis: Water effects on Co supported on narrow and wide-pore silica. Appl. Catal. A 289 (2005): 135-142.
- Farrauto, R.J. and Bartholomew, C.H. Fundamentals of industrial catalytic processes. 1st ed. London: Chapman & Hall, 1997.
- Feller, A., Claeys, M., and Steen, E.V. Cobalt cluster effects in zirconium promoted. Co/SiO₂ Fischer-Tropsch Catalysts. J. Catal. 185 (1995): 20-130.
- Girardon, J.S., Lermontov, A.S., Gengembre, L., Chernavskii, P.A., Constant, A.G., Khodakov, A.Y. Effect of cobalt precursor and pretreatment conditions on the structure and catalytic performance of cobalt silica-supported Fischer-Tropsch catalysts. J. Catal. 230 (2005): 339-352.
- Iglesia, E. Design, synthesis, and use of cobalt-based Fischer-Tropsch synthesis catalysts. Appl. Catal. A General. 161 (1997): 59-78.
- Iglesia, E., Reyes, S.C., Madon, R.J. Transport-enhanced α -olefin readsorption pathways in Ru-catalyzed hydrocarbon synthesis. J. Catal. 129 (1991): 238-256.
- Jacobs, G., Das, T., Zhang, Y.Q., Li, J.L., Racoillet, G., Davis, B.H. Fischer-Tropsch synthesis: support, loading, and promoter effects on the reducibility of cobalt catalysts. Appl. Catal. A. 233 (2002): 263-281.
- Jongsomjit, B., Sakdamnusun, C., Prasertdam, P. Dependence of crystalline phases in titania on catalytic properties during CO hydrogenation of Co/TiO₂ catalysts. Mater. Chem. Phys. 89 (2005): 395-401.
- Jongsomjit, B., and Goodwin, Jr., J.G. Co-support compound formation in Co/Al₂O₃ catalysts: effect of reduction gas containing CO. Catal. Today 77 (2002): 191-204.

- Jongsomjit, B., Panpranot, J., and Goodwin, Jr., J.G. Co-Support Compound Formation in Alumina-Supported Cobalt Catalysts. J. Catal. 204 (2001): 98-109.
- Jongsomjit, B., Panpranot, J., and Goodwin, Jr., J.G. Effect of zirconia-modified alumina on the properties of Co/ γ -Al₂O₃ catalysts. J. Catal. 215 (2003): 66-77.
- Jongsomjit, B., Sakdamnusun, C, and Goodwin, Jr., J.G.,and Praserthdam, P. Co-Support Compound Formation in Titania-Supported Cobalt Catalyst. Catal. Lett. 94 (2004): 209-215.
- Jongsomjit, B., Wongsalee, T., and Praserthdam, P. Characteristics and catalytic properties of Co/TiO₂ for various rutile: anatase ratios. Catal. Comm. 6 (2005): 705-710.
- Jongsomjit, B., Wongsalee, T., and Praserthdam, P. Study of cobalt dispersion on titania consisting various rutile: anatase ratios. Mater. Chem. Phys. 92 (2005): 572-577.
- Kogelbauer, A., Weber, J.C., and Goodwin, J.G., Jr. The formation of cobalt silicates on Co/SiO₂ under hydrothermal condition. Catal Lett. 34 (1995): 259-267.
- Kraum, M., and Baerns, M. Fischer-Tropsch synthesis: the influence of various cobalt compounds applied in the preparation of supported cobalt catalysts on their performance. Appl. Catal. A 186 (2002): 189-200.
- Martinez, A., Lopez, C., Marquez, F., Diaz, I. Fischer-Tropsch synthesis of hydrocarbons over mesoporous Co/SBA-15 catalysts: the influence of metal loading, cobalt precursor, and promoters. J. Catal. 220 (2003): 486-499.
- Moradi, G.R., Basir, M.M., Taeb, A., and Kiennemann, A. Promotion of Co/SiO₂ Fischer-Tropsch catalysts with zirconium. Catal. Comm. 4 (2003): 27-32.
- Nobuntu N., Neil, J.C. The effect of cobalt and zinc precursors on Co (10%)/Zn (x%)/TiO₂ (x = 0, 5) Fischer-Tropsch catalysts. J. of Molecular Catal. A: Chemical 225 (2005):137-142.
- O. Levenspiel, Chemical Reaction Engineering, 2nd ed., Wiley, New York, 1972, p. 496.
- Ohtsuka, Y., Takahashi, Y., Noguchi, M., i Arai, T., Takasaki, S., Tsubouchi, N., Wang1, Y. Novel utilization of mesoporous molecular sieves as supports of cobalt catalysts in Fischer-Tropsch synthesis. Catal. Today. 89 (2004): 419-429.

- Okabe, K., Li, X., Wei, M., Arakawa, H. Fischer–Tropsch synthesis over Co–SiO₂ catalysts prepared by the sol–gel method. Catal. Today 89(2004): 431-438.
- Othmer, K. Encyclopedia of chemical technology. Vol. 6. 4 th ed. New York: A Wiley Interscience Publication, John Wiley&Son, 1991.
- Oukaci, R., Singleton, A.H., Goodwin Jr., J.G. Comparison of patented Co F-T catalysts using fixed-bed and slurry bubble column reactors. Appl. Catal. A 186 (1999): 129-144.
- Panpranot, J., Kaewkun, S., Praserthdam, P., Goodwin, Jr., J.G. Effect of cobalt precursors on the dispersion of cobalt on MCM-41. Catal. Lett. 91 (2003): 95-102.
- Riva, R., Miessner, H., and Piero, G.D. Metal-support interaction in Co/SiO₂ and Ti/O₂. Appl. Catal. A 196 (2000): 111-123.
- Sales, L.S., Robles-Dutenhefner, P.A., Nunes, D.L., Mohallem, N.D.S., Gusevskaya, E.V., Sousa, E.M.B. Characterization and catalytic activity studies of sol-gel Co-SiO₂ nanocomposites. Mater. Char. 50 (2003): 95-99.
- Schanke, D., Vada, S., Blekkan, E.A., Hilmen, A., Hoff, A., Holmen, A. J. Catal. 156 (1995): 85.
- Shinoda, M.; Zhang, Y.; Yoneyama, Y.; Hasegawa, K.; Tsubaki, N. New bimodal pore catalyst for Fischer-Tropsch synthesis. Fuel Proc. Tech. 86(2004): 73-85.
- Sun, S., Fujimoto, K., Zhang, Y., and Tsubaki, N. A highly active and stable Fischer-Tropsch synthesis cobalt/silica catalyst with bimodal cobalt particle distribution. Catal. Comm. 4 (2003): 361-364.
- Sun, S.L., Tsubaki, N. and Fujimoto, K. The reaction performances and characterization of Fischer–Tropsch synthesis Co/SiO₂ catalysts prepared from mixed cobalt salts. Appl. Catal. A. 202 (2000): 121-131.
- Takahashi, R., Sato, S., Sodesawa, T., Yabuki, M. Silica–Alumina Catalyst with Bimodal Pore Structure Prepared by Phase Separation in Sol–Gel Process. J. Catal. 200 (2001):197-202.
- Tsubaki, N., Zhang, Y., Sun, S., Mori, H., Yoneyama, Y., Li, X., Fujimoto, K. A new method of bimodal support preparation and its application in Fischer-Tropsch synthesis. Catal. Comm. 2 (2001): 311-315.
- Vob, M., Borgmann, D., and Wedler, G. Characterization of alumina, silica, and titania supported cobalt catalysts, J. Catal. 212 (2002): 10-21.

- Young, R.S. COBALT: Its Chemistry, Metallurgy, and Uses. New York: Reinhold Publishing Corporation, 1960.
- Zhang , Y., Koike, M., Yang, R., Hinchiranan, S., Vitidsant, T., Tsubaki, N. Multi-functional alumina-silica bimodal pore catalyst and its application for Fischer-Tropsch synthesis. Appl. Catal. A: General. 292 (2005): 252-258.
- Zhang , Y., Shinoda, M.; Tsubaki, N. Development of bimodal cobalt catalyst for Fischer-Tropsch synthesis. Catal. Today. 93–95 (2004): 55-63.
- Zhang, Y., Wei, D., Hammache, S., Goodwin Jr., J.G. Effect of water vapor on the reduction of Ru-promoted Co/Al₂O₃. J. Catal. 188 (1999): 281-290.
- Zhang, Y.; Liu, Y.; Yang, G.; Sun, S.; Tsubaki, N. Effect of impregnation solvent on Co/SiO₂ catalyst for Fischer-Tropsch synthesis : highly active and stable catalyst with bimodal sized cobalt particles. Appl. Catal. A: General. 321 (2007): 79-85.



สถาบันวิทยบริการ
จุฬาลงกรณ์มหาวิทยาลัย



APPENDICES

สถาบันวิทยบริการ
จุฬาลงกรณ์มหาวิทยาลัย

APPENDIX A

CALCULATION FOR CATALYST PREPARATION

Preparation of alumina-silica bimodal pore supports by the incipient wetness impregnation method are shown as follows.

- Reagent:
- Polyethylene glycol (PEG)
Molecular weight = 200 g
 - Pure SiO₂ support (cariact Q-50)
 - Aluminium nitrate
Molecular weight = 375.14 g

Example calculation for the preparation of 5 wt% of alumina in alumina-silica bimodal pore support

Based on 100 g for support used, the composition of the support will be as follows:

$$\begin{aligned} \text{Alumina} &= 5 \text{ g} \\ \text{Silica} &= 100 - 5 = 95 \text{ g} \end{aligned}$$

For 5 g of support

$$\text{Alumina required} = 5 \times (5/95) = 0.263 \text{ g}$$

Alumina 0.263 g was prepared from aluminium nitrate in 0.3 mol/l polyethylene glycol aqueous solution and molecular weight of alumina is 27.

$$\begin{aligned} \text{Aluminium nitrate required} &= \frac{\text{MW of aluminium nitrate} \times \text{alumina required}}{\text{MW of Al}} \\ &= (375.14 \times 0.263) / 27 = 3.654 \text{ g} \end{aligned}$$

Since the pore volume of the pure silica support is 1.2 ml/g for silica. Thus, the total volume of impregnation solution which must be used is 6.0 ml for silica by the requirement of incipient wetness impregnation method, the 0.3 mol/l polyethylene glycol aqueous solution is added until equal pore volume for dissolve aluminium nitrate.

Preparation of Co/Al-Si catalysts by the incipient wetness impregnation method are shown as follows.

Reagent: - Cobalt (II) nitrate hexahydrate [$Co(NO_3)_2 \cdot 6H_2O$]

Molecular weight = 291.03 g

- Silica support
- Alumina-silica bimodal pore support

Example calculation for the preparation of Co/5%Al-Si

Based on 100 g for catalyst used, the composition of the catalyst will be as follows:

Cobalt = 20 g

Al-Si support = 100-20 = 80 g

For 5 g of catalyst

Cobalt required = $5 \times (20/80)$ = 1.0 g

Cobalt 1.0 g was prepared from $Co(NO_3)_2 \cdot 6H_2O$ and molecular weight of Co is 58.93

$$Co(NO_3)_2 \cdot 6H_2O \text{ required} = \frac{MW \text{ of } Co(NO_3)_2 \cdot 6H_2O \times \text{cobalt required}}{MW \text{ of } Co}$$

$$= (291.03/58.93) \times 1.0 = 4.94 \text{ g}$$

Since the pore volume of the Al-Si bimodal pore support is 0.373 ml/g. Thus, the total volume of impregnation solution which must be used is 1.87 ml for Al-Si bimodal pore by the requirement of incipient wetness impregnation method, the de-ionized water is added until equal pore volume for dissolve Cobalt (II) nitrate hexahydrate.

APPENDIX B

CALCULATION FOR TOTAL H₂ CHEMISSORPTION AND DISPERSION

Calculation of the total H₂ chemisorption and metal dispersion of the catalyst, a stoichiometry of H/Co = 1, measured by H₂ chemisorption is as follows:

Let the weight of catalyst used	=	W	g
Integral area of H ₂ peak after adsorption	=	A	unit
Integral area of 45 μl of standard H ₂ peak	=	B	unit
Amounts of H ₂ adsorbed on catalyst	=	B-A	unit
Concentration of Co (by AAS)	=	C	% wt
Volume of H ₂ adsorbed on catalyst	=	$45 \times [(B - A) / B]$	μl
Volume of 1 mole of H ₂ at 100°C	=	28.038	μl
Mole of H ₂ adsorbed on catalyst	=	$[(B - A) / B] \times [45 / 28.038]$	μmole
Total H ₂ chemisorption	=	$[(B - A) / B] \times [45 / 28.038] \times [1 / W]$	μmole/g of catalyst
	=	N	μmole/g of catalyst
Molecular weight of cobalt	=	58.93	
Metal dispersion (%)	=	$\frac{2 \times H_{2_{tot}} / g \text{ of catalyst} \times 100}{No \ \mu\text{mole } Co_{tot} / g \text{ of catalyst}}$	
	=	$\frac{2 \times N \times 100}{No \ \mu\text{mole } Co_{tot}}$	
	=	$\frac{2 \times N \times 58.93 \times 100}{C \times 10^6}$	
	=	$\frac{1.179 \times N}{C}$	

Table B.1 H₂ chemisorption results for various alumina-silica bimodal pore supported Co catalysts samples.

Sample	Total H ₂ chemisorption ($\mu\text{mol} / \text{g cat}$)	
	N	M
Co/Silica	0.44	2.58
Co/5% Al-Si	0.78	4.60
Co/10% Al-Si	0.91	5.36
Co/15% Al-Si	1.35	7.97
Co/20% Al-Si	3.19	18.81
CoAT/Silica	3.03	17.88
CoAA/Silica	1.67	9.82
CoCl/Silica	0.20	1.18
CoAT/15% Al-Si	3.14	18.48
CoAA/15% Al-Si	1.72	10.14
CoCl/15% Al-Si	0.22	1.28

APPENDIX C

CALIBRATION CURVES

This appendix showed the calibration curves for calculation of composition of reactant and products in CO hydrogenation reaction. The reactant is CO and the main product is methane. The other products are linear hydrocarbons of heavier molecular weight that are C₂-C₄ such as ethane, ethylene, propane, propylene and butane.

The thermal conductivity detector, gas chromatography Shimadzu model 8A was used to analyze the concentration of CO by using Molecular sieve 5A column.

The VZ10 column are used with a gas chromatography equipped with a flame ionization detector, Shimadzu model 14B, to analyze the concentration of products including of methane, ethane, ethylene, propane, propylene and butane. Conditions uses in both GC are illustrated in Table C.1.

Mole of reagent in y-axis and area reported by gas chromatography in x-axis are exhibited in the curves. The calibration curves of CO, methane, ethane, ethylene, propane, propylene and butane are illustrated in the following figures.

Table C.1 Conditions use in Shimadzu modal GC-8A and GC-14B.

Parameters	Condition	
	Shimadzu GC-8A	Shimadzu GC-14B
Width	5	5
Slope	50	50
Drift	0	0
Min. area	10	10
T.DBL	0	0
Stop time	50	60
Atten	0	0
Speed	2	2
Method	41	41
Format	1	1
SPL.WT	100	100
IS.WT	1	1

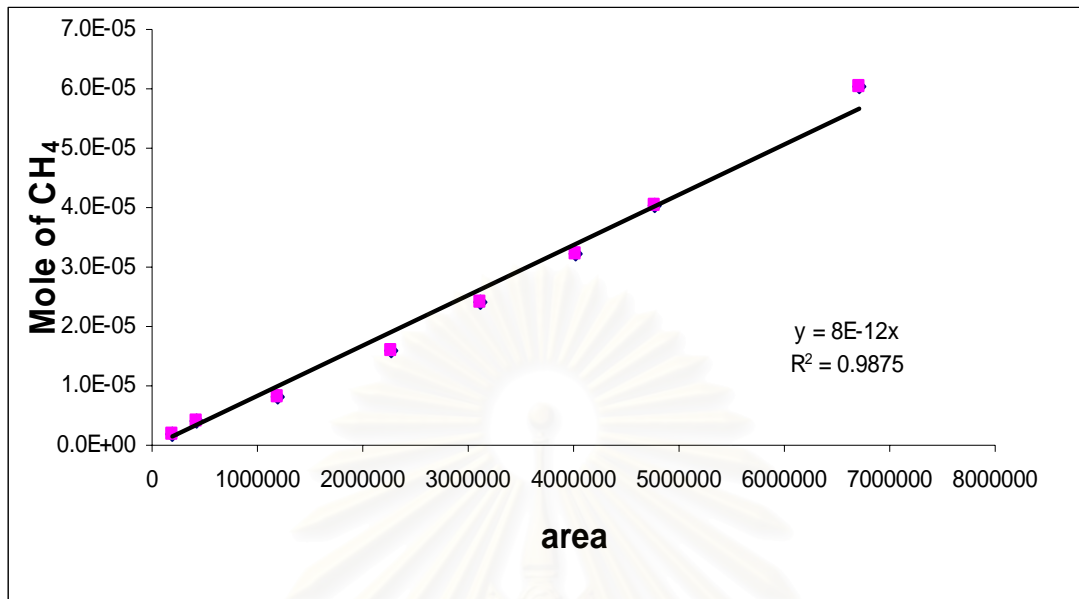


Figure C.1 The calibration curve of methane.

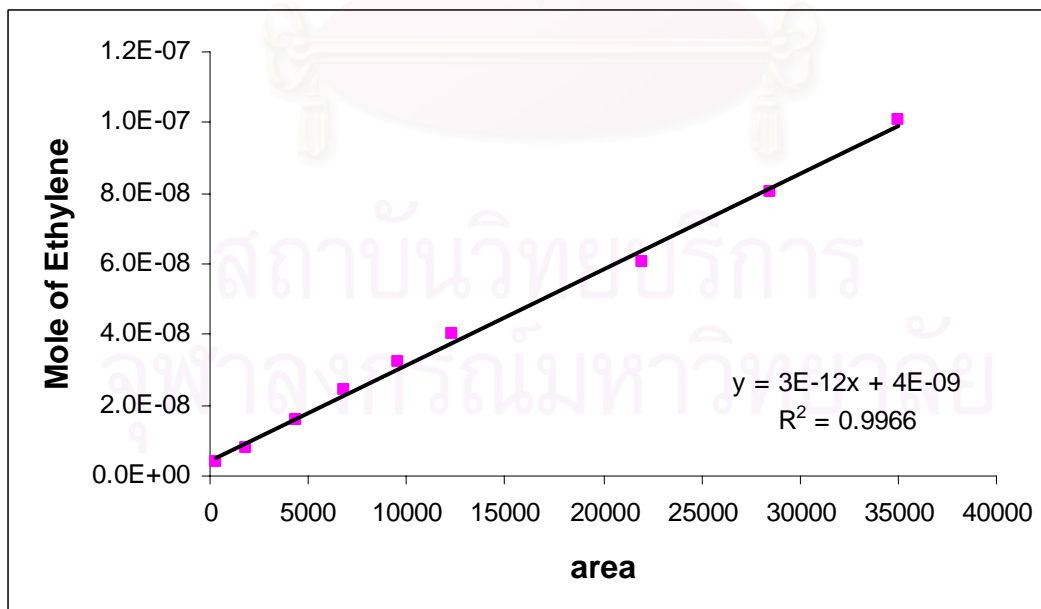


Figure C.2 The calibration curve of ethylene.

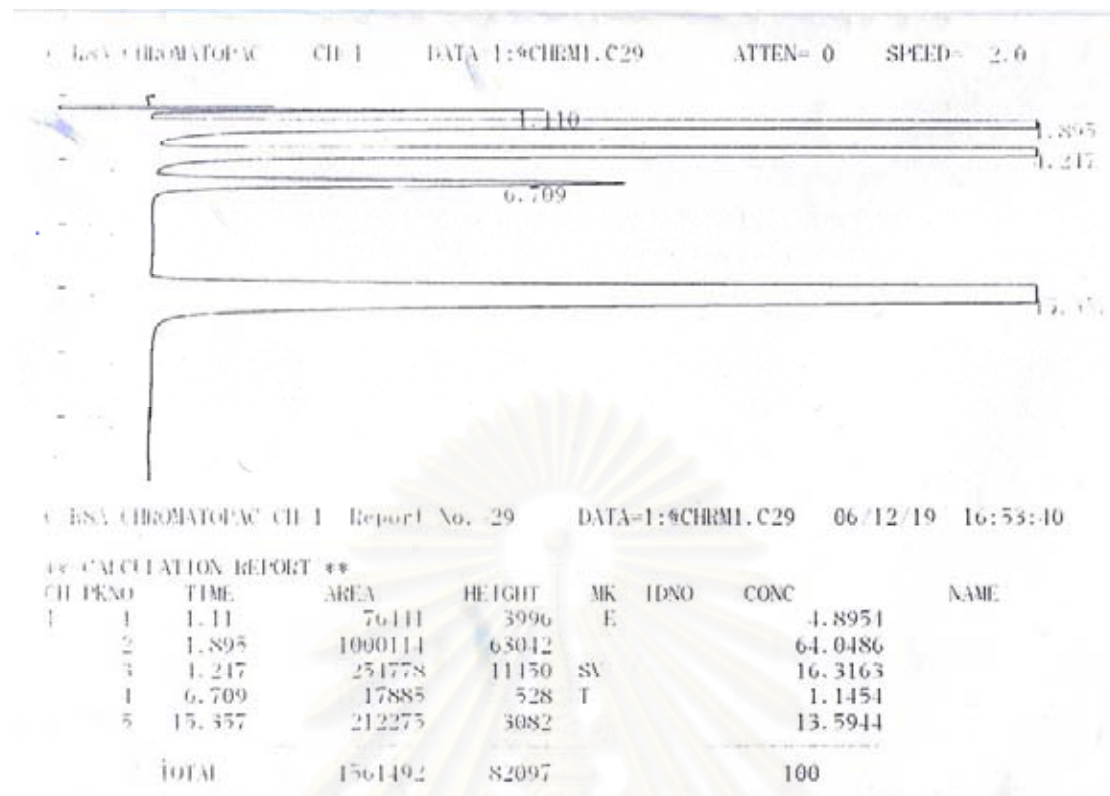


Figure C.3 The chromatograms of catalyst sample from thermal conductivity detector, gas chromatography Shimadzu model 8A (Molecular sieve 5A column).

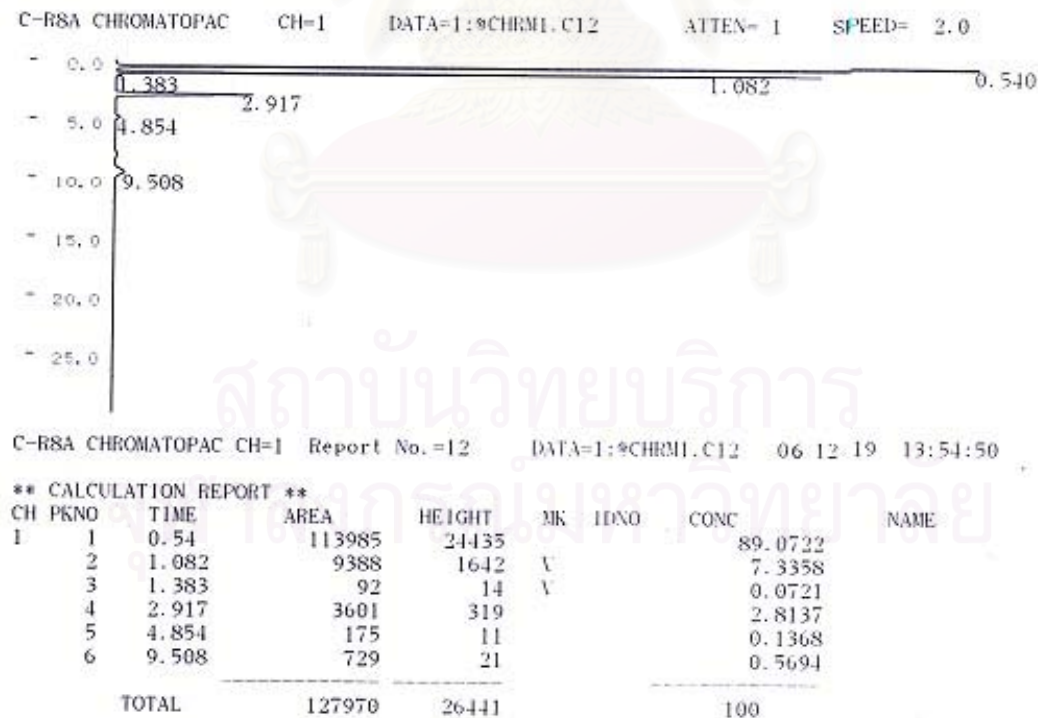


Figure C.4 The chromatograms of catalyst sample from flame ionization detector, gas chromatography Shimadzu model 14B (VZ10 column).

APPENDIX D

CALCULATION OF CO CONVERSION, REACTION RATE AND SELECTIVITY

The catalyst performance for the CO hydrogenation was evaluated in terms of activity for CO conversion rate and selectivity.

Activity of the catalyst performed in term of carbon monoxide conversion and reaction rate. Carbon monoxide conversion is defined as moles of CO converted with respect to CO in feed:

$$\text{CO conversion (\%)} = \frac{100 \times [\text{mole of CO in feed} - \text{mole of CO in product}]}{\text{mole of CO in feed}} \quad (\text{i})$$

Reaction rate was calculated from CO conversion that is as follows:

Let the weight of catalyst used	=	W	g
Flow rate of CO	=	2	cc/min
Reaction time	=	60	min
Weight of CH ₂	=	14	g
Volume of 1 mole of gas at 1 atm	=	22400	cc

$$\text{Reaction rate (g CH}_2\text{/g of catalyst)} = \frac{[\% \text{ conversion of CO} / 100] \times 60 \times 14 \times 2}{W \times 22400} \quad (\text{ii})$$

Selectivity of product is defined as mole of product (B) formed with respect to mole of CO converted:

$$\text{Selectivity of B (\%)} = 100 \times [\text{mole of B formed} / \text{mole of total products}] \quad (\text{iii})$$

Where B is product, mole of B can be measured employing the calibration curve of products such as methane, ethane, ethylene, propane, propylene and butane

$$\text{mole of CH}_4 = (\text{area of CH}_4 \text{ peak from integrator plot on GC} - 14B) \times 8 \times 10^{12} \quad (\text{iv})$$

APPENDIX E**LIST OF PUBLICATIONS**

1. Jutakorn Srisawat, Bunjerd Jongsomjit and Piyasan Prasertdam, “Characteristics and catalytic properties of alumina-silica bimodal pore supported cobalt catalyst for carbon monoxide hydrogenation”, Proceedings of the 17th Thailand Chemical Engineering and Applied Chemistry Conference, Changmai, Thailand, Oct., 2007.
2. Jutakorn Srisawat, Bunjerd Jongsomjit and Piyasan Prasertdam, “Characterization of cobalt dispersed on alumina-silica bimodal supports and its application towards CO hydrogenation ”, Submitted to Materials Chemistry and Physics, Aug., 2007.



สถาบันวิทยบริการ
จุฬาลงกรณ์มหาวิทยาลัย

VITA

Miss. Jutakorn Srisawat was born on August 19th, 1984 in Ratchaburi, Thailand. She finished high school from Saithamachan school, Ratchaburi in 2002, and received the Bachelor degree of Chemical Technology from Chulalongkorn University in March 2006. She continued her Master's study at the department of Chemical Engineering, Chulalongkorn University in 2007.



สถาบันวิทยบริการ
จุฬาลงกรณ์มหาวิทยาลัย